



UNIVERSITÀ
DI PAVIA

UNIVERSITÀ DEGLI STUDI DI PAVIA

Dipartimento di Scienze della Terra e dell'Ambiente

Dottorato di Ricerca in Scienze della Terra e dell'ambiente

**Modelling of Soil Hydrological Dynamics along the Ticino Valley
Irrigation Cascade in Lombardy**

Anno Accademico 2022-2023

Ciclo XXXVI

Alice Bernini

Coordinatore
Prof. Silvio Seno

Tutor
Prof. Michael Maerker

ABSTRACT.....	4
1 INTRODUCTION AND MOTIVATION.....	6
1.1 State of the art	6
1.2 Aims and objectives.....	8
2 STUDY AREA.....	10
2.1 Geological and geomorphological setting.....	12
2.2 Hydrological setting	13
3 MATERIAL AND METHODS.....	16
3.1 SWAT model characteristics.....	16
3.2 Input Data	19
3.2.1. Digital Elevation Model.....	20
3.2.2 Soil	21
3.2.3 Land use.....	29
3.2.4 Climate Data	31
3.2.5 Management.....	32
3.3 Soil water content sensors.....	33
3.4 Model Set-Up	34
3.5 Calibration and Validation of SWAT Model.....	36
3.5.1 MOD16 Data	40
3.6 Trend analysis	42
4 RESULTS.....	44
4.1 Input analysis.....	44
4.1.1 Topography.....	44
4.1.2 Soil.....	45
4.1.3 Landuse change.....	49
4.1.4 Weather data and climate change	50
4.2 Soil water content sensors.....	54
4.3 SWAT model	56
4.5 Calibration and validation.....	57
4.5.1 Sensitivity analysis.....	61
4.6 Output analysis.....	62
4.7 Trend analysis	65
5 DISCUSSION.....	66

6 CONCLUSION AND OUTLOOK 75
REFERENCES..... 78

APPENDIX

ACKNOWLEDGEMENTS

ABSTRACT

The doctoral research project explores the complex soil hydrological dynamics along the irrigation cascade in Lombardy's Ticino Valley, aiming to model hydrological processes within an agricultural landscape. This PhD thesis is part of the CE4WE project (Circular Economy for Water and Energy), funded by the Lombardy Region, dedicated to advancing sustainable water cycle management through the development of technologies, knowledge, and specific skills.

The application of SWAT (Soil Water Assessment Tool), a basin-scale, physically based model that simulates water dynamics in the soil, is a central focus of this project. SWAT was chosen because it allows to incorporate agricultural management practices such as irrigation, essential for the intensively used agricultural study area. SWAT's water balance calculations are based on various input data, including topography, land use, soil types, and climate data. The topographic analysis are based on a "hybrid" Digital Elevation Model (DEM). Moreover, land use and soil information from DUSAF 2018 and ERSAF pedologic maps have been used respectively, as well as meteorological data from ARPA Lombardia stations. Subsequently, sub-basins were defined for the SWAT model in the study area that are characterized by artificial drainage channels. The flat terrain emphasizes vertical connectivity, while the absence of natural watercourses and the dense network of irrigation channels pose unique challenges. Once the SWAT model was set-up, simulations were conducted from 2004 to 2022, on a monthly scale. SWAT was calibrated using satellite actual evapotranspiration data (MOD16) through SWAT-CUP software.

The model performance was assessed using Kling-Gupta Efficiency (KGE). A general KGE of 0.59 was obtained, implying its adeptness in simulating the intricate dynamics of the study area. However, for some HRUs we reach a KGE of more than 0.85. Besides the general good simulation results there it's important to note that both the uncalibrated and calibrated representations of actual evapotranspiration have a tendency to underestimation during winter periods. This discrepancy may be attributed to the resolution differences between Hydrological Response Units (HRUs) and MOD16 data, revealing a potential limitation in accurately representing seasonal variations.

After the validation phase, my analyses focused on climatic changes, over the past 18 years. I observed a significant increase in rainless days. Furthermore, the study explored variations in temperature (T) and actual evapotranspiration (AET) highlighting an increase,

and a consequential decrease in soil water content (SWC), impacting water resource availability and crop productivity. This also caused an increased water stress for crops and the ecosystem, highlighting the direct impact of adverse climate conditions on soil hydrology and agriculture. These results contribute significantly to the understanding of regional hydrological processes, as it specifically addresses recent droughts in the Lombardy lowlands, ensuring that the system's stability is maintained.

Furthermore, the project conducted an assessment of potential future scenarios involving climate change and sustainable agricultural management.

1 INTRODUCTION AND MOTIVATION

This thesis was conducted as part of the CE4WE project - Circular economy for Water and Energy, funded by Hub Research and Innovation of the Lombardy Region. The main purpose of the project is to develop innovative technologies, knowledge, and skills specifically addressing the sustainable management of the water cycle, identifying new analytical procedures, and creating new models for a capillary mapping of pollutants by applying the concept of circular economy to the entire water cycle. This PhD thesis contributes to the aims and objectives of CE4WE Project by providing a numeric assessment approach to quantify the hydrological dynamics of the soil-water-atmosphere interface considering the specific landuse pattern with intensive irrigation agriculture.

1.1 State of the art

The intricate relationship between soil and water forms the foundation of our ecosystems, influencing from agricultural productivity to the health of our natural landscapes. It is crucial to understand this relationship, particularly in regions where irrigation plays a significant role in maintaining the balance of these ecosystems. However, the increasing pressure on local, national, and regional water resources is observed, which are essential for irrigation, energy production, industrial, domestic, and environmental applications. In Europe, both the quality and quantity of water are degrading, with a reduction in the available water level, leading to adverse impacts on the environment. Additionally, climate changes introduce a new layer of uncertainty regarding water availability (Abbaspour et al., 2015). In particular, water is a prerequisite for agriculture, which is increasingly affected by climate change, a global phenomenon that affects the Earth system in various ways, including altering hydrological and hydraulic processes (Bian et al., 2021). Moreover, water resources are under increasing pressure, not only for climate change but are also by factors such as population growth (Maja and Ayano, 2021), industrialization, the need for increased food production (Pereira, 2017) and, as a consequence, land use changes (Cheng et al., 2022).

These challenges underscore the extreme need to have a conscious management of the water resource, that is analysing the impact of different land use, agriculture practices and climate change on the hydrological cycle (Nkwasa et al., 2022). The first step in this direction is the development of tools to understand and assess water dynamics. Hydrological models address this need by simulating various scenarios, past and future, becoming a crucial support in water

resource management. Indeed, to understand and predict the effects of climate change on the water cycle, hydrological models have been developed globally in recent years, playing a central role in studying hydrological processes simulating the quantity and the quality of the water resources and assessing the impact of climate change (Devi et al., 2015; Kour et al., 2016). Numerical hydrogeological models are now an indispensable tool in hydrogeological studies. Through modelling, it is possible to parameterize water circulation, as well as make predictions about the system's behaviour in response to natural and anthropogenic stresses. These models provide a quantitative understanding of the repercussions of climate change on hydrological regimes, addressing adverse consequences like water scarcity and drought (Kour et al., 2016). Among these models, SWAT (Soil and Water Assessment Tool) is the most widely used hydrological model in the world (Gassman et al., 2014), being applied for different purposes such as: i) the quantification of water resources or their appropriate management (Abbaspour et al., 2015; Karim C. Abbaspour et al., 2007; Cuceloglu et al., 2017; Jayakrishnan et al., 2005; Schuol et al., 2008), ii) the assessment of water quality (Abbaspour et al., 2015; Karim C. Abbaspour et al., 2007), or iii) analysis of impacts of land use and climate change on the hydrology (Abbaszadeh et al., 2023; Krysanova and Srinivasan, 2015; Narsimlu et al., 2013).

SWAT needs specific parameters such as topography, soil and land use maps and climate data and subdivides the basin into sub-basins, which in turn are split up into Hydrological Response Units (HRUs), representing areas with homogenous topography, soil and land use. The advancement in the field of hydrology was significantly marked by the conceptualization and implementation of Hydrological Response Units. This approach has provided a more understanding of soil characteristics and their three-dimensional spatial distribution. This has augmented ability to model and predict hydrological processes with increased accuracy and reliability (Flugel, 1995).

However, applying hydrological models, including SWAT, in lowland areas presents some challenges (Sun et al., 2020), such as availability and data quality and the complexity of urban landforms. Indeed, lowland areas cover a large part of the most densely populated regions in the world and, therefore, the appropriate hydrological dynamics in these areas are of great social and economic value (Brauer et al., 2013). The general characteristics of lowland areas are related to a flat topography and low hydraulic gradients (Lam et al., 2010). Moreover, these areas are often heavily modified in terms of the drainage systems due to human activity.

Therefore, it is quite difficult to derive first order watersheds (Donmez et al., 2020) and to assess their hydrological dynamics. Moreover, as stated by Becker et al. (2019) the calibration of a hydrological model in a flat, complex agricultural environment is a quite difficult task too.

Therefore, instead of the classical calibration using discharges, alternative procedures must be evaluated. Remote sensing technologies provide large-scale spatially distributed observations, giving new possibilities in calibrating and validating hydrologic models (Odusanya et al., 2019). As shown by (Parajuli et al., 2018) satellite based products were successful used to calibrate spatially distributed hydrological models, in particular, if human activities such as irrigation interfere with the natural system or if we have a general lack of observed information in terms of their spatio-temporal scales (Odusanya et al., 2019). This is the case of the unique region of the Ticino Lowland area in Lombardy. This area is a world-unique region characterized by springs (risorgive and fontanili) and a dense network of irrigation channel for agriculture. This cascade system has a profound impact on the region's hydrology, that it has been relatively understudied in terms of water dynamics. This area, indeed, with the Ticino River that is the only natural drainage, is characterized by a unique agricultural context with a tradition getting back to the 11th century and being an example of sustainable water use (Ticino Irrigation Cascade), has never been assessed in a quantitative way using a physically based hydrological model.

In this context, the conscious management of water resources and the efficient use of water in agriculture are key to addressing the challenges posed by climate change. Hydrological models, such as SWAT, play a significant role in the study of hydrological processes and in the analysis of the impact of climate change on the water cycle. Therefore, we need to develop innovative solutions to overcome these challenges and improve our ability to predict and manage the effects of climate change on water resources.

1.2 Aims and objectives

Considering the aforementioned factors, the focus of this doctoral thesis is to develop a hydrological model that accurately represents the soil hydrological dynamics of a micro-scale basin lowland area, in the Ticino Valley, within the Lombardy region of Italy. Subsequently the model is applied to assess the effects of climate change over the last decades.

In particular, the Ticino Valley, with its unique irrigation cascade, presents a complex and interesting case study for this research. Understanding the impacts of climate change requires before an in-depth study of the physical properties of the soil, the mechanics of the irrigation system, and the climatic conditions that influence both.

To achieve the thesis objectives, the Soil & Water Assessment Tool (SWAT) model software (J.G. Arnold et al., 1998), a physical hydrological model operating at basin scale (Neitsch et al., 2011), was applied.

Nevertheless, deriving the first-order watershed in a lowland area, which is intensively cultivated having an anthropogenic drainage system can be particularly challenging, as described above. Therefore, the initial project goal was to set up SWAT, primarily completed in the first year.

The second year focused on model calibration. The missing information on water resources used for irrigation and the general characteristic of the lowland area makes it difficult to calibrate and validate the model in a traditional way using discharge as calibration parameter. In the third year of my PhD, the focus shifted to validating the model, employing actual evapotranspiration data (MOD16) as in the calibration process. Once calibrated and validate, analyses were conducted on both the model's input climate data (precipitation and temperature) and some of its outputs (actual evapotranspiration and soil water content). This analysis aimed to examine how climate changes are influencing the hydrological properties of the study area.

This investigation aims to assess innovative approaches to manage water resources in future. The final goal, indeed, is to provide a tool that can help to establish sustainable irrigation practices in the Ticino Valley and similar regions around the world.

In the following chapters, the specifics of the research methodology, the findings, and discussion of their implications for the future of hydrology and irrigation management in Lombardy lowlands are presented.

2 STUDY AREA

The study area (Figure 1) covers approximately 50 km² and is located about 15 km southwest of the city of Milan in Lombardy region, close to the boarder with the Piedmont region. The area covers parts of the left side the Ticino River Valley with elevation ranging between 76 m a.s.l. in the south-western part of the Ticino River to 127 m a.s.l. around the town of Abbiategrasso (Figure 2).

The Ticino River, a tributary of the Po River, holds significant importance, acknowledged through its designation as a regional park in Italy and protected status by UNESCO. The lower floodplain is marked by intense agricultural practices and considerable anthropogenic influence. Despite this, numerous semi-natural areas persist in the region (Sconfietti et al., 2018).

The region is characterized by a humid subtropical climate (Cfa), following the Köppen climate classification (Kottek et al., 2006) with warm summers and cold winters and a mean temperature of 13°/year. The mean annual rainfall amount to 814 mm/year, measured at Vigevano SS494 Arpa Lombardia station (Figure 2), which is located close to Ticino River, in the middle part of the study area at an elevation of 94 m a.s.l.

In particular, the study area is a sub-basin delimited by the “Naviglio di Bereguardo” to the east, “Fosso Morto” to the southeast, and the “Canale Scolmatore di Nord Ovest” to the northwest.

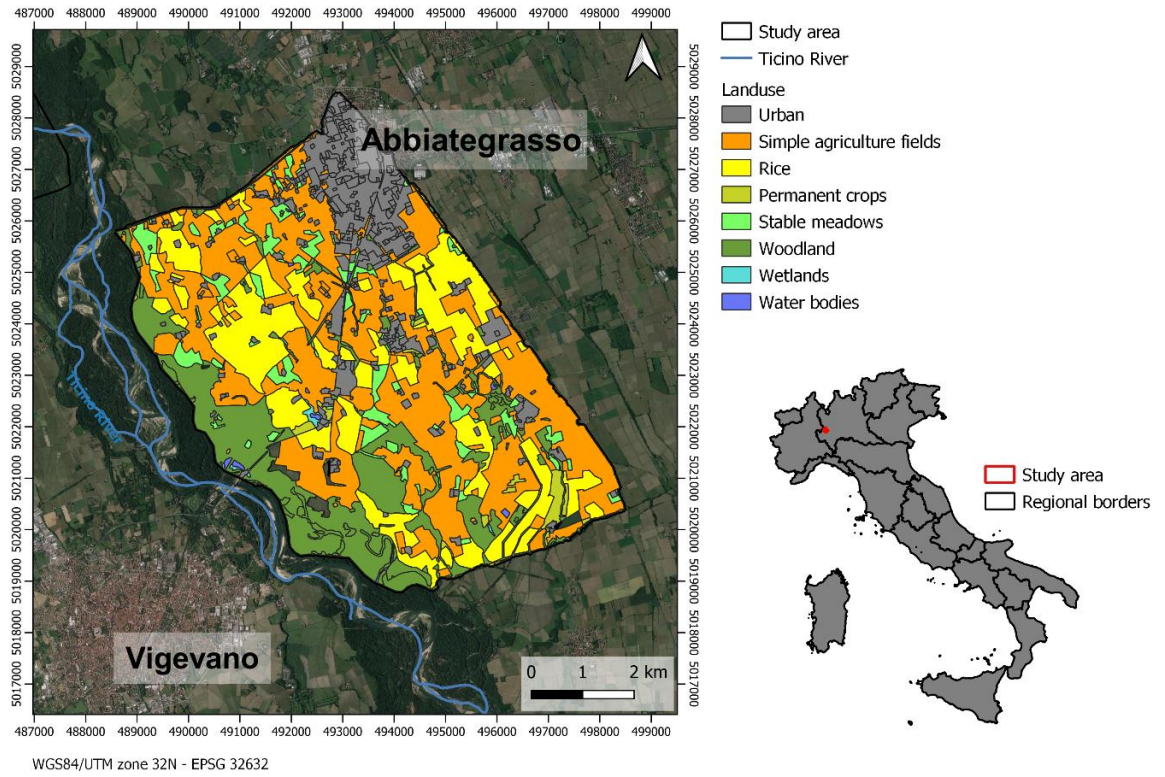


Figure 1: right site: location of the study area in Italy. Left: overview of study area, with its dominant land-use classes.

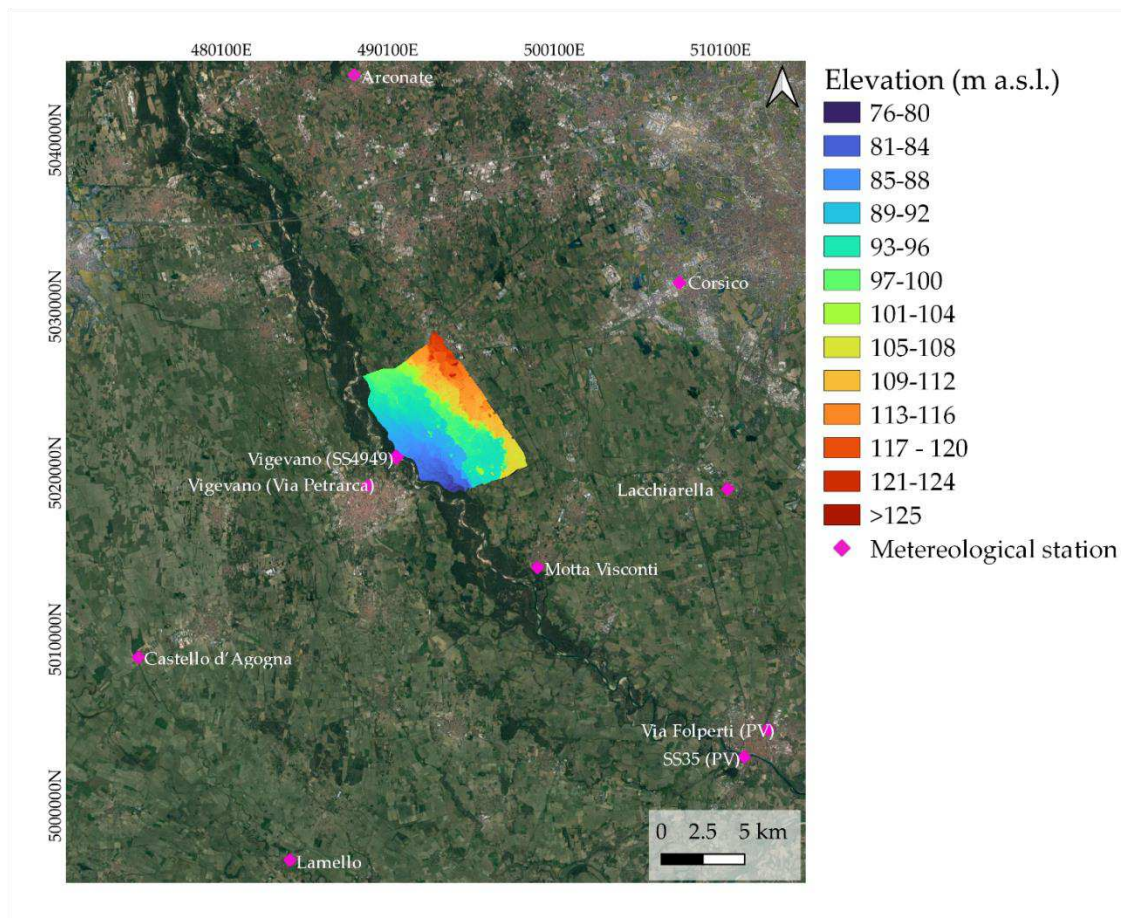


Figure 2: elevation of the study area and spatial distribution of the meteorological stations

2.1 Geological and geomorphological setting

The Ticino River is the only natural drainage of the area flowing towards the southeast. The area, in fact, is characterized by an artificial agricultural landscape, shaped by human activity, and constantly evolving.

From a geomorphological point of view the study area is mainly flat, except for the river terraces, because of the erosive activity of the Ticino River. The area is defined as “low irrigated plain,” characterized by abundant surface water and springs (fontanili), widely utilized for agricultural purposes.

Particularly, the area can be subdivided into three main terrace levels oriented in a parallel way to the Ticino River in the orographic left, while on the orographic right the terraces are less developed, and we find only one order.

The Ticino River, which flows through the Po Valley, has over time created these series of river terraces, which consist of a flat surface and a terrace slope. These fluvial terraces are due

to phases of erosion and deposition that have alternated, leading to the genesis of alluvial terraces. The terrace escarpments are characterized by springs at their base.

The study area falls within three CARG 1:100,000 maps, specifically in “Foglio 44 Novara”, “Foglio 45 Milano” and “Foglio 58 Mortara”. Generally, the area lies in an upper level, the “Livello fondamentale della Pianura” characterized by Pleistocene (würm) fluvioglacial deposits with sandy gravels. These deposits, with coarse grain sizes enable water to infiltrate and constitute a significant recharge zone for the aquifer. An intermediate level, characterized by terraced Holocene deposits, predominantly sandy-gravelly with a slight silty component. Finally, the recent and current fluvial deposits represent the youngest layer (Upper Holocene) in the Ticino valley, featuring predominantly sandy-gravelly composition with a minor silty content and modest thickness.

Above these fluvial and fluvioglacial deposits soil developed with different depth according to the age of the terrace level, ranging from regosols in the lower part to luvisol and umbrisols in the upper part, according to World reference base for soil resources (1998), with predominantly sandy-loam texture.

2.2 Hydrological setting

From the hydrogeological point of view the area is dominated by a groundwater flow directed towards the Ticino River (Figure 3).

This area represents the groundwater recharge zone corresponding to Holocene floodplains and Pleistocene fluvioglacial sediments, where the aquifer is uninterrupted by less permeable layers. These are the areas where infiltration from rainfall, snowmelt, and irrigation allows for the recharge of the shallow aquifer, which can then reach the deeper aquifers.

As already mentioned, this part of the Ticino Valley is characterized by the presence of springs, classified as “*risorgive*” and “*fontanili*.” “*Risorgive*” are forming by groundwater naturally emerging due to changes in topography and permeability of sediments at the base of the terrace escarpments. Instead “*fontanili*”, refers to springs of lowland areas modified by human intervention (Baker et al., 2022; De Luca et al., 2013).

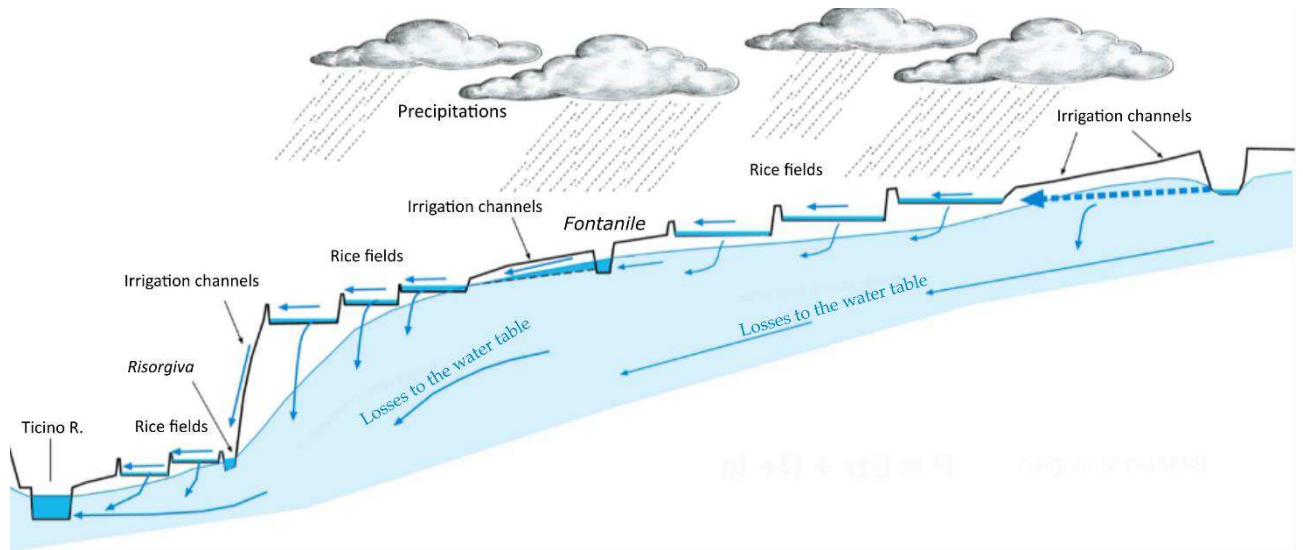


Figure 3: schematic representation of the geohydrological settings of the study area. The figure represents the different orders of terraces with the respective springs at their basis, and the drainage action of the Ticino River.

Fontanili and *risorgive* are fed by groundwater: much of the rainwater, in fact, infiltrates into the permeable soils, while the rest of the precipitation is removed from system by evapotranspiration or superficial runoff. However, since the study area is mainly flat the contribution of the surface runoff is almost nil (Baker et al., 2022). In fact, the variation of the springs discharge is mainly due to the infiltration of water after periods of rain or irrigation (Balestrini et al., 2021).

During the spring-summer period, actually, large quantities of water are distributed through a complex channel network to irrigate fields. So, water distributed for irrigation use is not only important for agriculture, but also contributes decisively to the recharge of the water table, which in turn helps to feed the springs of the different terrace base levels (see Figure 3). Moreover, the region is characterized by particular land use and land management practices dating back to eleventh century with the construction of irrigation channels (De Luca et al., 2013) and the reuse of water along the fluvial terrace cascade of the Ticino River. Thus, representing for centuries, a sustainable and effective reuse of irrigation water.

Nowadays, the main crops, based on the DUSAF 6.0 land use map (Regione Lombardia, 2019) are maize and rice. Maize (with other simple agriculture fields such as wheat, sorghum, and barley) covers about 32% of the area, while rice makes up to 21% of the area. Moreover, about

the 18% of the study area is cover by woodland mainly concentrating on the lowermost terrace level.

Both maize and rice require a high amount of irrigation water (Balestrini et al., 2021; Perego et al., 2014). The irrigation season of maize is from June to September (Lasagna et al., 2020), and is conducted typically as flow irrigation, while the rice fields, in general, are flooded from mid-April to early May and remain flooded until the end of August or September (Baker et al., 2022; Balestrini et al., 2021; Lasagna et al., 2020). In 2022 one of the hottest years of the century in the study area, the rice fields were flooded in late May until late August, with intermittent flooding. The large quantities of water used for rice cropping are affecting the recharge of the water table (Bove, 2021). In rice paddy areas, indeed, it was observed by Lasagna et al. (2020) that the main factor in changing the water level is the agricultural technique of rice cultivation.

However, in recent years, climate change is strongly affecting water availability increasingly, in the study area. It is therefore necessary to progressively adopt specific plans for water scarcity situations, to prevent and mitigate the effects of any severe reduction in water resource availability and to protect agricultural production as much as possible.

3 MATERIAL AND METHODS

3.1 SWAT model characteristics

In this study the Soil and Water Assessment tool (SWAT) model software, developed by Arnold et al., 1998 was applied. This decision was made after conducting a comprehensive bibliographic review on various hydrological models. The SWAT model was chosen due to its ability to incorporate various management practice (e.g., irrigation and crop rotation) into its simulation, crucial for intensively used agricultural and irrigated areas.

SWAT is an open-source hydrological model developed for the USDA Agricultural Research Services. SWAT model is a physically based, semi-distributed, and continuous-time hydrological model (Neitsch et al., 2011). It has been widely utilized in various hydrologic and environmental conditions worldwide (Donmez et al., 2020). The model operates at basin scale and was developed to assess and predict the impacts of land use/cover changes, climate variability and land management practices on watershed hydrology, sediment and chemical yields in a complex basin with variations of soil landuse and management conditions over a long period of time (Jeffrey G. Arnold et al., 1998; Neitsch et al., 2011). One of the advantages of the SWAT model is its ability to simulate human activity and agriculture practices, making it adaptable to new situations (Janjić and Tadić, 2023). Catchment areas lacking adequate soil data, rainfall, temperature, and runoff information pose challenges for the utilization of the SWAT model. Nevertheless, the model can estimate the relative effects of different management scenarios on water quality, sediment, and agricultural characteristics in the ungauged catchments (Janjić and Tadić, 2023).

In the context of the intensively used agricultural and irrigated study area, the SWAT model proves to be particularly helpful.

Specific input is required for the application of the SWAT model and the water balance calculous: i) the DEM for the delineation of the hydrographic network and sub-basins; ii) the land use map and soil map for delineating Hydrological Response Units (HRU); and finally, iii) daily climatic data (precipitation, maximum and minimum temperatures, average solar radiation, average wind speed, and average relative humidity) required for model creation and water balance (Douglas-Mankin et al., 2010).

The hydrological cycle delineates the continuous exchange of water within the hydrosphere, involving the atmosphere, soil, surface waters, deep waters, and living organisms (Figure 4).

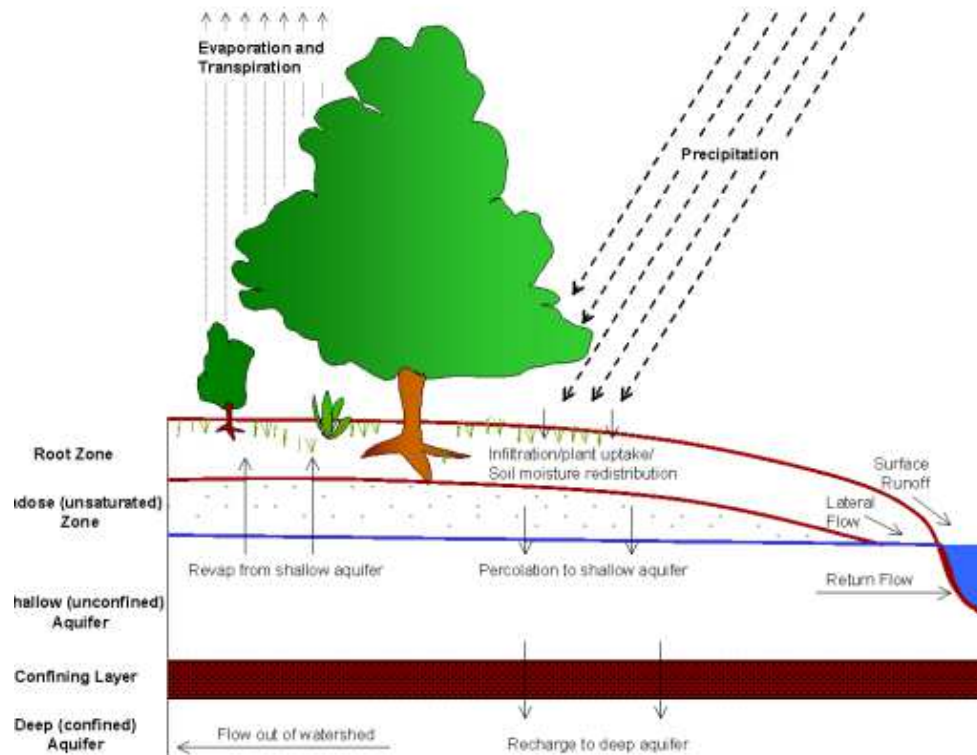


Figure 4: water balance, as working in SWAT (figure obtained from Neitsch et al., 2011).

The hydrologic cycle simulated by SWAT is based on water balance equation (1), calculated for each HRU:

$$SW_t = SW_0 + \sum(R_{day} - Q_{surf} - E_a - W_{seep} - Q_{gw})$$

Equation 1: Water balance used in SWAT

where SW_t is the final soil water content (mm H_2O), SW_0 is the initial soil water content on day i (mm H_2O), t is the time (days), R_{day} is the amount of precipitation on day i (mm H_2O), Q_{surf} is the amount of surface runoff on day i (mm H_2O), E_a is the amount of evapotranspiration on day i (mm H_2O), w_{seep} is the amount of water entering the vadose zone from the soil

profile on day i (mm H₂O), and Q_{gw} is the amount of return flow on day i (mm H₂O) (Neitsch et al., 2011).

In this way, SWAT simulated hydrological process include surface runoff, infiltration, and canopy storage. Soil process include lateral flow from soil, return flow from shallow aquifer and tile drainage, capillary rise from the surface aquifer to the root zone, redistribution of moisture in the soil profile and evapotranspiration and finally, deep aquifer recharge that removes water from the system (Abbaspour et al., 2015).

In this study, in particular, was chosen to use the SWAT model as it is able to include detailed management strategies (e.g. plan the irrigation) and to take into account spatially distributed land use and management changes and their effects on individual components of the water balance, such as actual evapotranspiration (AET) (Becker et al., 2019), which is used as a variable in the calibration procedure. In SWAT, evapotranspiration plays a crucial role. Following the calculation of potential evapotranspiration (PET), the model proceeds to calculate the actual evapotranspiration. (Ferreira et al., 2021; Ritchie, 1972). To calculate the actual evapotranspiration, SWAT first evaporates any rain intercepted by plant canopy. Next, SWAT calculates the maximum amount of transpiration and the maximum amount of sublimation/ evaporation of the soil using an approach similar to that of (Ritchie, 1972). The actual amount of sublimation and evaporation from the soil is then calculated (Neitsch et al., 2011). SWAT utilize Potential Evapotranspiration (PET), coupled with soil properties and land use characteristics, to estimate actual evapotranspiration and it provides the possibility to utilize various methods for calculation potential evapotranspiration, including: Penman-Monteith, Hargreaves, and Priestly-Taylor.

In this study, the Penman-Monteith method was used for the calculation of evapotranspiration with the SWAT model. The Penman-Monteith method requires solar radiation, air temperature, relative humidity and wind speed. The Penman-Monteith equation combines components that represent the energy needed to sustain evaporation, the strength of the mechanism required to remove water vapor, and the terms of aerodynamic and surface resistance (Neitsch et al., 2011). The Penman-Monteith equation is:

$$\lambda E = (\Delta * (H_{(net)} - G) + \rho_{air} * C_p * [e_z^o - e_z] / r_a) / (\Delta + \gamma * (1 + r_c / r_a))$$

Equation 2: Penman.Monteith equation

where λE is the latent heat flux density ($\text{MJ m}^{-2} \text{d}^{-1}$), E is the depth rate evaporation (mm d^{-1}), Δ is the gradient of the vapor saturation pressure-temperature curve, de/dT ($\text{kPa } ^\circ\text{C}^{-1}$), H_{net} is the net radiation ($\text{MJ m}^{-2} \text{d}^{-1}$), G is the heat flux ground density ($\text{MJ m}^{-2} \text{d}^{-1}$), ρ_{air} is the density of air (kg m^{-3}), c_p is the specific constant pressure heat ($\text{MJ kg}^{-1} \text{ } ^\circ\text{C}^{-1}$), e_{z0} is the air saturation vapor pressure at height z (kPa), e_z is the water vapour pressure of the air at height z (kPa), γ is the psychrometric constant ($\text{kPa } ^\circ\text{C}^{-1}$), r_c is the plant canopy resistance (s m^{-1}), and r_a is the diffusion resistance of the air layer (aerodynamic resistance) (s m^{-1}).

In a flat and intensively irrigated area the tradition method to subdivide watershed in subbasin based on the stream network is not enough to represent the reality, for this reason, the subbasins were delineated in GIS environment to create a more realistic representation, based on geomorphological units (river terrace levels). These non-traditional boundaries of the subbasin were made because only vertical connectivity of the area was considered, assuming negligible horizontal surface and underground flows, considering the completely flat nature of our study area with limited surface runoff.

In this study, the SWAT model was performed on a monthly basis in order to have the same time resolution as the observed data and then a monthly AET time series was generated for each HRU.

3.2 Input Data

The first and crucial step in the research process was to collect and processed the SWAT input data, ensuring respective data quality. The goodness of input data is not only fundamental for the reliability of the SWAT model, but also for the exploration of hydrological dynamics within the study area.

Sources, temporal, and spatial resolution for each data set used in this study are documented in Table 1.

Table 1: sources and description of input data utilized to setup SWAT model.

DATA TYPE	SOURCES	RESOLUTION and DESCRIPTION
TOPOGRAPHY	Deutsches Zentrum für Luft- und Raumfahrt (DLR) and Ministero dell’Ambiente: Geoportale Nazionale, 2019	10 m “Hybrid” Digital Elevation Model
SOIL	Geoportale della Lombardia	1:50.000, Soil information bases
LANDUSE	Geoportale della Lombardia	1:10.000, Land Use and Land Cover 2018 (DUSAF 6.0)
WEATHER	Arpa Lombardia	Daily, ARPA Lombardia hydro-nivo-meteorological data.

3. 2.1. Digital Elevation Model

Topography is a key element in the SWAT hydrological model and contributes significantly to its ability to accurately simulate hydrological process, even if the area is flat like the one analyzed.

In this study, the 12 m resolution Digital Elevation Model (DEM) sourced from TanDEM-X, provided by Deutsches Zentrum für Luft- und Raumfahrt (DLR) was used. To improve his accuracy, the DEM was corrected through the creation of a mask incorporating vegetation and urbanization, effectively minimizing noise. To do this, to urban and forest vegetation land uses were coded with “no data” value. This is followed by the conversion of land use data from shape format to grid format. The last step involves the use of a grid calculator to multiply the Digital Elevation Model (DEM) with the reclassified land use data. This process ensures the effective removal of vegetated and urban areas.

Subsequently, this refined DEM was integrated in SAGA GIS with 1 m resolution Digital Terrain Model (DTM) derived from Lidar measurements conducted along the Ticino River,

derived from PCN-PST. The 1 m resolution DTM was imported in SAGA GIS as ASCII file using the ESRI/INFO grid format. The values were exported as points, using the grid to XYZ export format and then importing a point shape from the XYZ data. Finally, we used a thin plate spline method for spatial data smoothing and interpolation.

The process of interpolating the DEM at 12 m resolution with the DTM was referred to as "mosaicking" and the interpolation with the nearest neighbor algorithm (Voronoi) was conducted to close the sinks of the new DEM combined with the DTM.

The final DEM was reprojected with a resolution of 10 meters and the projection system used for the digital elevation model is the WGS 84/ UTM ZONE 32 N, then adopted for all other data utilized. This "hybrid" DEM was utilized in this study to conduct a comprehensive characterization fo the study area, emplying SAGA GIS version 7.8.0 for detailed terrain analysis.

3.2.2 Soil

The relationship between soil and water is complex and multifaceted, influencing everything from the health of ecosystems to agricultural productivity. Indeed, SWAT requires various soil characteristics. These characteristics, such as soil texture, structure, depth, and organic matter content, play a crucial role in determining how water moves through the soil. They affect the rate of infiltration, percolation, runoff, and evapotranspiration, all of which are key processes modelled in SWAT. By accurately representing these soil characteristics, SWAT can provide more reliable predictions of water flow and nutrient transport, which are essential for effective water resource management and sustainable agricultural practices. Understanding and accurately interpreting the intricate relationship between soil and water is a crucial aspect of environmental and agricultural research.

Initially, soil data was extracted from a FAO-UNESCO soil map at a scale of 1: 5,000,000 sourced from FAO (<https://data.apps.fao.org/?lang=en>), to facilitate the initial model runs. Subsequently, for a more deep analysis, the shapefile of 1:50,000 scale ERSAF soil map was downloaded from ('Regione Lombardia, 2013. Basi informative dei suoli. Geoportale della Lombardia.', <https://www.geoportale.regione.lombardia.it/>) moreover ERSAF provided 37 soil profiles in the study area.

The pedological map of ERSAF, at a scale of 1:50,000, categorizes soils according to the USDA Soil Taxonomy classification. In the study area, seven types of soil are identified, which are subsequently incorporated into the SWAT model:

- UDORTHENTS: soils with a significant horizon of accumulation of silica, and "Ud" indicates that the soil has a udic moisture regime, meaning it has sufficient moisture throughout the year.
- HAPLUSTALFS: belongs to the Alfisols soil order according to the USDA Soil Taxonomy. soils with a horizon of accumulation of clay and "Hap" suggests that they have a horizon of illuviation (accumulation of material leached from above). Haplustalfs are commonly in areas of relatively recent erosional surfaces or deposits, most of them late Pleistocene in age.
- HAPLUDALFS: the term "Hapludalfs" originates from "Hapl," signifying minimal horizon, and "udalfs," denoting the suborder of Alfisols, similar to Haplustalfs but have a udic moisture regime. These soils formed principally in late-Pleistocene deposits or on a surface of comparable age.
- DYSTRUDEPTS: "Dystr" indicates a lack of specific soil features associated with other orders, and "udepts," representing the suborder of Inceptisols characterized by a udic moisture regime. Soils with a horizon of illuviation. They developed mostly in late-Pleistocene or Holocene deposits. Most of the Dystrudepts that formed in alluvium are now cultivated, and many of the other Dystrudepts are used as pasture.
- EUTRUDEPTS: the term "Eutrudepts" originates from "Eut" suggests they are well-drained, and "udepts," representing the suborder of Inceptisols characterized by a udic moisture regime soil with a horizon of illuviation Many developed in Holocene or late-Pleistocene deposits. The vegetation was mostly deciduous hardwoods, but the gently sloping soils are now cultivated and many of the steeply sloping soils are used as pasture.
- USTIPSAMMENTS: the term "Ustipsamments" is formed from "Usti," denoting an ustic moisture regime, and "psamments," representing the suborder of Entisols primarily composed of unconsolidated sand deposits.
- USTORTHENTS soils with a horizon of accumulation of silica and have an ustic moisture regime. The "orthents" are primarily Entisols on recent erosional surface.

However, both ERSAF map and soil profiles lacked the specific soil characteristics outlined in Table 2, essential for SWAT modelling. The ERSAF profiles, indeed, describe only specific

soil properties such as soil pH in water, soil organic carbon (SOC%), texture (sand, silt, clay content in %) and topsoil depth (cm), and the soil input file (.sol) specifies the physical properties for every layer within the soil. The physical properties of the soil play a key role in regulating the movement of water and air throughout the soil profile, significantly influencing the water cycling within HRU.

To address this gap, the compilation of the “usersoil” table in the SWAT database was conducted. The usersoil table in SWAT serves as a user-defined soil database. This table is provided in the project database, allowing users to adapt their soil properties. This flexibility becomes valuable when default soil databases are not accurate in representing the soils within the area of interest. Creating a usersoil table involves preparing a CSV file with specific columns, each representing different soil properties. The file should be comma-separated, with essential columns such as SNAM, NLAYERS, SOL_Z, CLAY, SILT, SAND, SOL_CBN for each available soil layer (with a minimum of 1 layer).

Table 2: soil characteristics required by SWAT.

Variable name	Definition	Measurement unit
HYDGRP	Soil hydrologic group (A, B, C, or D). Required only for the SWAT ArcView interface. The U.S. Natural Resource Conservation Service (NRCS) classifies soils into four hydrologic groups based on infiltration characteristics of the soils.	
SOL_ZMX	Maximum rooting depth of soil profile	mm
ANION_EXCL	Fraction of porosity from which anions are excluded.	
SOL_CRK	Potential or maximum crack volume of the soil profile expressed as a fraction of the total soil volume.	
SOL_Z	Depth from soil surface to bottom of layer	mm
SOL_BD	Moist Bulk Density	Mg/m ³ or g/cm ³
SOL_AWC	Available water capacity of the soil layer	mm H ₂ O/mm soil
SOL_K	Saturated hydraulic conductivity	mm/hr
SOL_CBN	Organic carbon content	% Soil weight
SOL_CLAY	Clay content	% Soil weight
SOL_SILT	Silt content	% Soil weight

SOL_SAND	Sand content	% Soil weight
SOL_ROCK	Rock fragment content	% Total weight
SOL_ALB (top layer)	Moist soil albedo	
USLE_K (top layer)	USLE equation soil erodibility (K) factor	0.013 (ton m ² h)/ (m ³ ton cm)

This table was filled with soil properties using SPAW software (Saxton, n.d.), which utilizes pedotransfer functions. The SPAW (Soil-Plant-Atmosphere-Water) model incorporates a program known as "Soil Water Characteristics," designed for calculating soil water characteristics. This program emulates available water, saturated hydraulic conductivity, and Bulk density, utilizing soil texture as a basis. Additionally, it adjusts factors such as gravel content, compaction, salinity, and organic matter.

For each soil type identified on the pedological map, a specific ERSAF profile was chosen to input accurate information into the SPAW software, and the calculations of soil properties were systematically performed. For what concern soil hydrologic groups were determined according to Arnold et al. (2012) and following the directives of USDA Soil Survey (National Resources Conservation Service, 2007). The fraction of anions exclusion was set to 0.5 according to the SWAT Input Data (J. G. Arnold et al., 2012). The potential or maximum crack volume of the soil profile expressed as a fraction of the total soil volume was set to zero as there was no information available to evaluate this parameter, nevertheless considering the soil texture in the study area, is plausible that this value is 0.

These calculated values were subsequently validated through on-site fieldwork, where soil analysis covered different terrace levels (identified using SAGA GIS) and included different land-use and soil types (Figure 5). Based on the already available data, using soil profiles previously dug and provided by ERSAF, sampling areas were identified along a south section of the study area designated for hydrological model development, because the profiles supplied by ERSAF were found to be lower in the southern part compared to the northern part. The purpose of the investigations was to define the characteristics of the soil substrates in the study area, aiming to provide a general characterization of the soils and it was possible to validate the input data for the SWAT hydrological model.

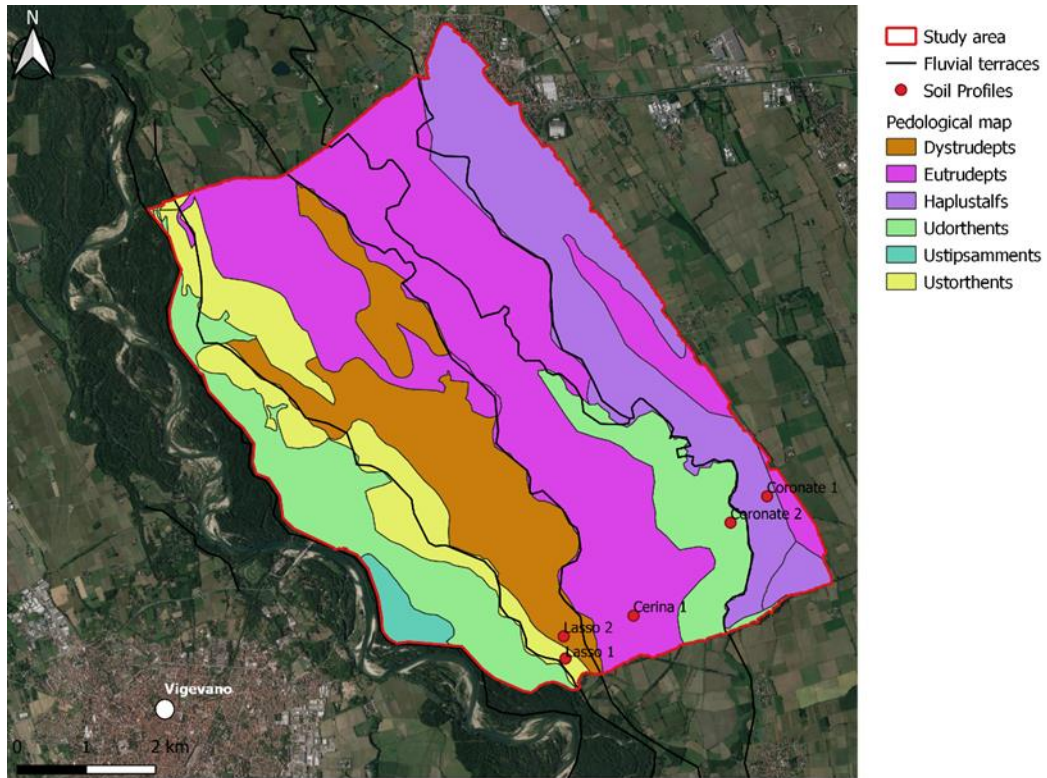


Figure 5: location of soil profiles

The field work involved the digging of five soil profiles, with subsequent measurement of saturated hydraulic conductivity utilizing a constant head permeameter (Amoozometer).

Pedological profiles typically exhibit a series of layers parallel to the surface, referred to as horizons. These horizons can be distinguished by unique characteristics resulting from pedogenetic processes. Describing the pedological profile essentially involves detailing its horizons to derive information about the manifesting processes and the soil properties observable or measurable in situ (Certini and Ugolini, 2021; Cremaschi and Rodolfi, 1991). The information collected during field surveys includes data related to specific soil features (depth, colour, texture, reaction to hydrochloric acid, pH, % gravel, concretions, presence of roots, etc.) as well as station data (location, elevation, brief description of the landscape or vegetation surrounding the survey point). Soil characteristics were, of course, recorded separately for each horizon within the same profile. All pedological observations were georeferenced using a GPS tool (Garmin GPSMap 65Ss).

Additionally, soil samples were collected for each of the horizons affected by pedogenesis and subjected to comprehensive laboratory analysis.

Laboratory analyses characterize the soil from both chemical and physical perspectives. Various analyses were conducted on the sampled soils, across different soil horizons, to determine their characteristics. The following analyses were performed:

- Particle size (sand, silt, clay): following the regulations (D.M. 13/09/1999 SO n° 185 GU n° 248 21/10/1999 - Met II.6), soil particle size was determined through wet sieving using a hydrometer. The principle is based on using the hydrometer to measure the mass density of the soil-water suspension after a predetermined sedimentation time, subsequently deducing the distribution of elementary particles of different sizes.
- pH: following the regulations (D.M. 13/09/1999 SO n° 185 GU n° 248 21/10/1999 - Met III.1), pH was determined potentiometrically on a soil-water suspension.
- Active limestone: following the regulations (D.M. 13/09/1999 SO n° 185 GU n° 248 21/10/1999 - Met V.2), the active limestone content is determined by reacting a fine soil sample with an excess of ammonium oxalate solution under cold conditions.
- Cation exchange capacity (C.E.C): following the regulations (D.M. 13/09/1999 SO n° 185 GU n° 248 21/10/1999 - Met XIII.2), the exchange between the cations present on the soil exchange sites and the ammonium ion in the ammonium acetate exchange solution is first carried out by shaking and then by leaching. The excess ammonium acetate solution is removed through repeated washes with ethanol. Subsequently, the adsorbed ammonium is determined by distillation according to Kjeldahl, either directly on the sample or on an aliquot of the solution obtained by leaching the NH_4^+ -soil with a sodium chloride solution.
- Exchangeable potassium, calcium, magnesium, and sodium: Following the regulations (D.M. 13/09/1999 SO n° 185 GU n° 248 21/10/1999 - Met XIII.5), the content of calcium, magnesium, potassium, and sodium ions, removed from exchange sites with a pH 8.2-buffered barium chloride solution, is determined by flame atomic absorption spectrophotometry (FAAS).

As already mentions, K_{sat} was measured in the field in two different depth 10 and 30 cm using a constant-head permeameter (Amoozegar, 1989) (Figure 6). K_{sat} was calculated in mm/h following the Glover solution proposed by Zangar (1953) and adopted by Amoozegar (1989). K_{sat} is used as a proxy for infiltration.



Figure 6: amoozemeter during fieldwork

3.2.3 Land use

Land-use is a fundamental element in the SWAT model, or in hydrological models in general, because it can greatly affect hydrological process (Lin et al., 2007). For example, in an urbanized area infiltration will be low relative to a wooded area, or the various agricultural crops may vary evapotranspiration and soil water content.

For this input data, the shapefile of a land-use map (DUSAF 2018) at a scale of 1:10,000 from the Geoportale della Lombardia (ERSAF “Ente Regionale per i Servizi alla Agricoltura e alle Foreste - Regione Lombardia, 2019) was used. The DUSAF’s legend is structured in five hierarchical levels of which the first three are the classes of the project Corine Land Cover. The first level includes five general classes that cover the main types of coverage (anthropized areas, agricultural areas, wooded territories and semi-natural environments, wetlands water bodies), which are increasingly differentiated in the following levels. However, SWAT requires specific codes for different landuse. It was therefore necessary to associate the different classes of the DUSAF map with the corresponding codes found in the tables “crop” and “urban” in the SWAT reference database (see Table 3).

Additionally, analysis of land-use maps from 2007, 2012, 2015 and 2018 provided insights into the land-use changes across the past 19 years. Land use changes were calculated with percentages of area occupied by polygons on the DUSAF maps. Initially, the 1999 map was also considered, but was later excluded as it lacked detail compared to the others. Furthermore, the selected years align better with the run of SWAT model.

Table 3: land use classes of DUSAF and SWAT code required.

DUSAF LANDUSE	SWAT CODE
1112 - Continuous, moderately dense residential fabric	URMD
1121 - Discontinuous residential fabric	URBN
1122 - Sparse residential fabric	URLD
1123 - Scattered residential fabric	URLD
11231 Farmhouses	URBN
12111 - Industrial, artisanal, commercial settlements	UIDU
12112 - Agricultural productive settlements	UIDU
12122 - Public and private service facilities	UIDU

12123 - Technological facilities	UIDU
12124 - Cemeteries	URBN
122 – Road and railway networks	UTRN
1221 - Road networks and accessory spaces	UTRN
133 Construction sites	UIDU
134 - Degraded, unused, and non-vegetated areas	UIDU
1411 - Parks and gardens	URBN
1412 - Uncultivated green areas	URBN
1421 - Sports facilities	URBN
2111 – Simple agricultural fields	AGRL
2112 - Tree-covered arable land	AGRL
21131 - Open-field horticultural crops	ORCD
21141 - Open-field floriculture crops	ORCD
2115 - Family gardens	ORCD
213 - Rice fields	RICE
2241 - Poplar groves	POPL
2242 - Other agrarian woody plants	AGRL
2311 - Permanent meadows without tree and shrub species	RNGE
2312 - Permanent meadows with scattered tree and shrub species	MIGS
31111 - Broad-leaved forests of medium and high density managed by coppicing	FRSD
31121 - Low-density broad-leaved forests managed by coppicing	FRSD
3113 - Riparian formations	FRSD
3222 - Riparian vegetation	FRSD
3241 - Thickets with significant presence of tall shrub and tree species	RNGB
3242 - Thickets in abandoned agricultural areas	RNGB
411 - Vegetation of internal wetlands and peat bogs	WETF
511 - Riverbeds and artificial watercourses	WATR
5121 - Natural water basins	WATR
5122 - Artificial water basins	WATR

The shapefiles of soil and land use maps were converted in raster format in a GIS environment to be read by SWAT. The conversion of shapefiles into raster format is a crucial step in the SWAT modelling process because SWAT uses a raster-based approach for its spatial analysis. Moreover, the Lookup Table for both soil and land use was created. This table should classify each of the raster values with one of SWAT's soil and land cover/land use types.

3.2.4 Climate Data

SWAT's water cycle simulation is based on climate conditions, requiring precise daily-scale input data. This data, inclusive of daily cumulative precipitation (mm), maximum and minimum daily temperature (°C), daily average relative humidity (fraction), global solar radiation (Mj/m²), and daily average wind speed (m/s), can be incorporated if climate stations are available. Alternatively, the WHEATHER GENERATOR in SWAT can generate data or simulate missing days in time series from existing climate stations. In particular, the WGEN_CFSR_World, a weather database, was utilized to simulate the missing values of weather data. This database, which is an input into SWAT, contains long-term monthly weather statistics that cover the entire globe. It was developed using the Climate Forecast System Reanalysis (CFSR) global dataset from the National Centres for Environmental Prediction (NCEP).

Climate data covering 19 years (2004 to 2022) from 10 ARPA Lombardia climate stations (Table 4) were downloaded from the ARPA Lombardia website ('FORM RICHIESTA DATI', <https://www.arpalombardia.it/temi-ambientali/meteo-e-clima/form-richiesta-dati/>).

Table 4: Climate stations used in the SWAT model.

NAME	COORDINATES	ELEVATION
Arconate	45.32, 8.5	182
Castello d'Agogna	45.13, 8.4	106
Corsico	45.26, 9.5	119
Lacchiarella	45.19, 9.8	97
Motta Visconti	45.16, 8.59	100
Via Folperti (PV)	45.11, 9.9	77
SS35 (PV)	45.1, 9.8	71

Vigevano (SS4949)	45.2, 8.52	94
Vigevano (Via Petrarca)	45.19, 8.51	107

The meteorological data downloaded from ARPA Lombardia from 2004 to 2022 reveal various gaps attributable to data absence. To identify the gaps in the measured weather data, a Gantt diagram was created in Excel.

Following this analysis, the climate data was converted into text files, facilitating readability by SWAT. SWAT requires the weather data in a specific format. Each weather parameter is stored in a separate file with a specific extension (e.g. “pcp” for precipitation and “tmp” for temperature etc.). The data in these files should be arranged in a column format with each row representing a day. The first day should be the initial day of the year from which the simulation originates. If weather records contain missing data, they are indicated with “-99”.

The precision of weather data can markedly influence the accuracy of SWAT model outputs. Therefore, it is crucial to verify that weather data is both accurate and as complete as possible.

3.2.5 Management

A bibliographical analysis was conducted (e.g. Azar et al., 2016; Bux et al., 2022) to establish crop rotation models and defining specific sowing and harvesting schedules for each main crop type, moreover on-site inspections were carried out and some farmers in the area were interviewed.

It was discovered that corn and rice are the most common summer crops. Maize is sown between mid-April and early May, develops in mid-June and is harvested in late September. Rice is sown later than corn, between mid-April and late May and develops from early June to September / mid-October when it is harvested. Double cultivation often takes place: maize and sorghum are sown as a second crop in May after the harvesting of fodder crops (e.g., ryegrass) or winter cereals (e.g., barley or wheat). Other crops grown in the area consist mainly of herbaceous legumes (e.g., alfalfa and clover), which are mowed and harvested three to four times, almost monthly, during the period May-August (Table 5).

Table 5: typical calendar of the main crops in the study area. Green represents the sowing of crops, yellow the emergency/development, orange the harvest and blue the resting.

Ryegrass	Yellow	Yellow	Yellow	Yellow	Orange	Orange	White	White	White	Green	Green	Yellow
Maize	White	White	White	Green	Green	Yellow	Yellow	Yellow	Orange	Orange	White	White
Barley	Yellow	Yellow	Yellow	Yellow	Yellow	Orange	White	White	White	Green	Green	Yellow
Wheat	Yellow	Yellow	Yellow	Yellow	Yellow	Orange	White	White	White	Green	Green	Yellow
Rice	Blue	Blue	Blue	Green	Yellow	Yellow	Yellow	Yellow	Yellow	Orange	Blue	Blue
Sorghum	White	White	White	Green	Green	Yellow	Yellow	Yellow	Yellow	Orange	White	White

Due to the difficulty in locating precise information on each field and for each year, it was considered the most common crop rotation (ryegrass-corn rotation) in the study area and defining the sowing, irrigation, and harvesting times.

As regards irrigation, farmers were interviewed and field investigations were conducted, but no detailed information was obtained. Irrigation of each field, in fact, depends on the actual crop, the water availability of that moment and the management of the field. In addition, we would like to remember that the area is characterized by a dense network of irrigation channels that are managed by different consortia.

For irrigation scheduling, SWAT provides flexibility with both manual and automatic approaches. In manual scheduling, irrigation follows a predetermined scheme, while in automatic scheduling, the model autonomously decides the timing and quantity of irrigation based on the specific water needs of the crops (Maier and Dietrich, 2016). Due to the problem that there is not a clear picture of the irrigation schemes it was decided to apply the auto-irrigation module in SWAT. Hence, whenever the actual growth of plants falls below a threshold fraction due to water stress, the model automatically applies water. If enough water is available from the irrigation source, the model will add water to the soil until it is at field capacity (J. G. Arnold et al., 2012).

3.3 Soil water content sensors

Three soil moisture sensors TEROS12 were installed in different areas. TEROS 12 are high-quality soil moisture sensors designed for research purposes. It is designed to provide precise measurements, incorporating the assessment of soil water content, temperature, and electrical conductivity. The three areas where the sensors are installed are located in the same sites as

the soil profiles, indicating arable land (corn-ryegrass field), a wooded (forest) area and a rice field. Sensors were installed at depths of 10 cm and 35 cm; (ii) rice cultivation, with sensor depths of 10 cm and 30 cm; (iii) a forested area in which sensors were placed at depths of 10 cm, 30 cm, and 65 cm.

These in-situ measurements of soil water content will contribute to understanding the moment where irrigation occurs and can be compared with the SWAT output to comprehend the dynamic of the area.

3.4 Model Set-Up

To set-up and calibrate and validate SWAT, the subsequent steps were followed (Figure 7).

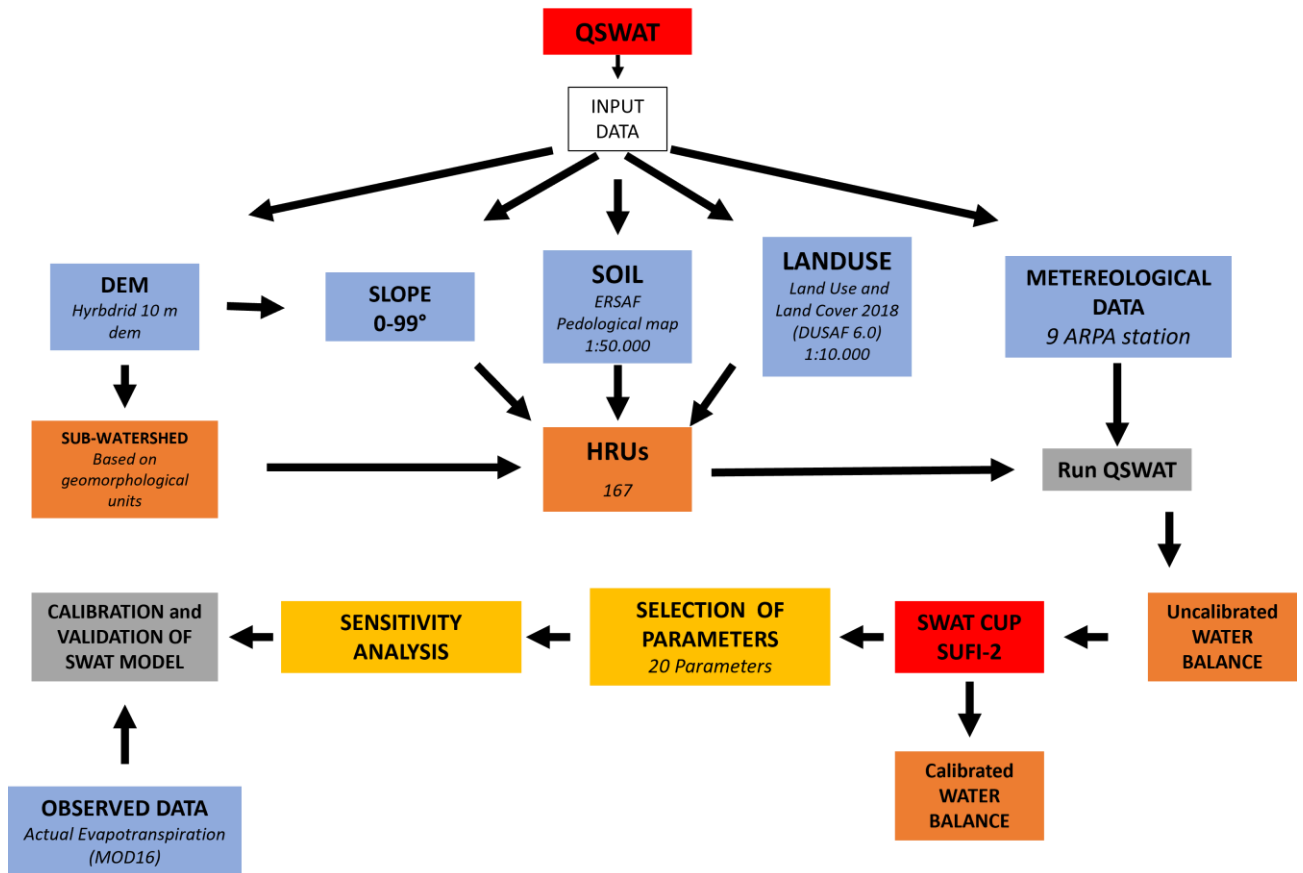


Figure 7: SWAT flowchart with calibration and validation procedure

In this study, the QSWAT (QSWAT3 version: 1.5.2) model in QGIS was utilized. QSWAT is the SWAT model plugin for QGIS (Quantum GIS) platform. QSWAT enabled the integration of the Soil and Water Assessment Tool into the QGIS environment, supporting seamless geospatial analysis and modelling of watershed processes.

After the collection of the input data, QSWAT was configured and parameterized, to perform hydrological modelling of the study area.

The primary objective was to explore alternative approaches for utilizing the model in a lowland area without a natural channel network. In delineating sub-basins within the SWAT, three distinct approaches were considered at the beginning of this project. i) the first approach implicated configuring the model conventionally, assuming natural drainage conditions and establishing stream and watershed delineation base on the topography, but this conventional delineation of sub-basins and, notably, watercourses was found to diverge significantly from the actual landscape, proved to be less representative of the true hydrological features of the study area; ii) the second method utilized a shapefile of artificial channels; however, it was observed that this dataset lacked crucial information for SWAT, particularly the flow rates. Since these channels are man-made and managed by humans, the absence of key parameters such as flow rates limited the completeness of the dataset; iii) the third and most fitting approach utilized a delineated sub-basin based on geomorphological units (river terrace levels) using QGIS (version 3.16) proving to be the most appropriate method for this study. This manual delineation allowed for a refined and accurate representation of the sub-basins, ensuring that the hydrological modelling process in SWAT depicted the complexities of the study area with greater reliability.

These units were individually defined and subsequently integrated into the SWAT model, which subdivided them into 167 HRUs.

Their extension in the study area varies from approximately 100 m² to 4,7 km², with an average extension of approximately 0.308 km². The size of HRUs depends on soil homogeneity and land use characteristics, with larger sizes for homogeneous areas and smaller for heterogeneous areas (Becker et al., 2019). The different dimensions of the HRUs allowed for a more accurate representation of the landscape, capturing the heterogeneity of land characteristics, and facilitating a more precise simulation of hydrological processes across the study area. This approach ensured a comprehensive and detailed analysis, considering the intricacies of the hydrological response at a finer spatial scale.

During the model set-up initial testing was conducted also on input data to ensure the robustness and reliability of the modelling process. These preliminary assessments included the input datasets to identify any deficiencies, inaccuracies, or potential challenges.

Initially, the modelling process used generalized data, incorporating the FAO soil map (with just one soil type covering the study area) and data from a single climate station. This approach facilitated an easier identification of critical points within the model, laying the foundation for subsequent refinement and optimization. After that, the model was parameterized using more detailed input data such as spatially distributed soil and climate data as well as a more complete landuse / landcover information.

Moreover, the initial area was bigger, but after different run, was decided to apply the model excluding the area adjacent to the Ticino River (current riverbed) to focus only on the region characterized by artificial drainage network, ensuring a more homogeneous area for realistic results.

Finally, in order to represent the hydrological process more accurately, several key modifications were made in the last run the model. As previously mentioned, one of those modifications was the incorporation of an auto-irrigation editing the “sub-basin input” in the model. This system was designed to automatically adjust the water supply based on the needs of the crops; in that way it ensures optimal irrigation. In addition to this, a more typical crops rotation was introduced. This rotation, which includes corn and ryegrass, was chosen due to its prevalence in region being modelled. The use of this rotation allowed for a more realistic representation of the agricultural practices in the area, and thus a more accurate prediction of the hydrological process.

The SWAT model was run for a period of 19 years, from 2004 to 2022. However, it is important to note that the first three years of this period were used as a warm-up. This warm-up period is crucial in hydrological modelling as it allows the model to stabilize and reach a state that is representative of the real-world conditions.

3.5 Calibration and Validation of SWAT Model

The term “calibration” refers to a procedure where the difference between model simulation and observation are minimized. Through this procedure, it is hoped that the model correctly simulates true processes in the physical system (Abbaspour et al., 2017).

Building the model using QSWAT a comparison between the model results and observational data was made. It is essential that the model's performance correspond with observed data to ensure the efficacy of the calibration process; significant disparities could render the calibration less effective. Subsequently, the model was calibrated. However, the conventional

runoff discharge could not be used for calibration due to the difficult nature of the area and substantial anthropogenic alterations to the natural drainage system.

In this study, actual evapotranspiration (AET) was considered as variable for the calibration procedure. The monthly evapotranspiration data was used, provided by Moderate Resolution Imaging Spectroradiometer (MODIS), downloaded (with resolution of 1 km) from 2007 to 2013, focused on 149 HRUs, as is possible learn in the next chapter.

In the initial stages of this study, the period from 2007 to 2013 was used entirely for calibration of the SWAT model. However, during the subsequent validation procedures various problems challenges was encountered.

Validation is the process of confirming that the calibrated model can accurately predict the response of the system under different conditions. In particular, it involves comparing the model's predictions with observed data that was not used during the calibration process. Given the issues encountered during validation, it was decided to subdivide the original calibration and validation periods. The new calibration period was from 2007 to 2010, while the validation period was from 2011 to 2013.

The model has been calibrated and validated with SWAT-CUP module (Calibration and Uncertainty Procedures) version 5.1.6.2. (Abbaspour et al., 2015; K. C. Abbaspour et al., 2007), a standalone program developed for SWAT calibration. Following the protocol established by (Abbaspour et al., 2017), the calibration process involved pre-calibration of input data, improvement of the model structure, identification of parameters to be optimized, identification of other sensitive parameters, model runs, post-processing and modifying new parameters.

The SWAT-CUP program contains five different calibration procedures: the Generalized Likelihood Uncertainty Estimation (GLUE) (Beven and Binley, 1992), Sequential Uncertainty Fitting (SUFI2) (Abbaspour et al., 2004; Abbaspour et al., 2007), Parameter Solution (parasol) (Van Griensven and Meixner, 2006), Markov chain Monte Carlo (MCMC) (e.g., Kuczera and Parent, 1998; Marshall et al., 2004; Vrugt et al., 2003), and Particle Swarm Optimization (PSO) (Kennedy and Eberhart, 1995).

SWAT-CUP enables sensitivity analysis, validation, and uncertainty analysis of SWAT model (Abbaspour et al., 2015).

In the current work the Sequential Uncertainty Fitting (SUFI-2) program (K. C. Abbaspour et al., 2007) was utilized for model calibration and uncertainty analysis. The SUFI-2 algorithm,

used for model calibration and sensitivity analysis, is a "stochastic" calibration, also performing an analysis of modelling uncertainty. This algorithm, in fact, maps all the uncertainties, which can be relative to the parameters used, the conceptual model, the input data etc. SWAT-CUP tries to capture most of the measured data within the 95% prediction uncertainty (95PPU) of the model in an iterative process (Abbaspour et al., 2015). 95PPU is calculated at the levels of 2.5% and 97.5% of the cumulative distribution of an output variable, generated by the propagation of the uncertainty of a parameter through the Latin Hypercube sampling technique (Abbaspour, 2019). In this way there is not a simple signal that represents the output but an envelope of acceptable solutions, expressed by 95PPU. What is wanted is that the 9PPU envelopes most of the observed data. To quantify the goodness of adaptation between simulated results, expressed with a band (the 95PPU) and the measured data (plus any errors in the measurement) expressed with a single signal, the algorithm SUFI-2 provides two indices called "P-factor " and " R-factor " (Abbaspour et al., 2004; Karim C. Abbaspour et al., 2007). P factor are the observed data within the 95th percentile. It is considered perfect (ideally) when this value approaches 1. R factor is the ratio between the average distance within the 95th percentile and the standard deviation of the measured data. The goal is for it to approach 0.

As said, the SUFI-2 algorithm was utilized for model calibration and uncertainty analysis in this study. SUFI-2's capability to accommodate ten distinct objective functions. An objective function is a mathematical formulation assessing the disparity between observed and simulated data, which play a crucial role in guiding the optimization process during model calibration, supporting in the identification of the parameter set that best represents the system under consideration.

By offering the option to use ten different objective functions, SUFI-2 enables to the calibration process to fit the unique requirements of the study, thereby enhancing the accuracy and reliability of model predictions. This flexibility stands as a notable advantage of SUFI-2, contributing to its widespread adoption in hydrological modelling.

In this study, the Kling-Gupta efficiency (KGE) was selected as the objective function to assess model performance. The Kling-Gupta Efficiency is a widely used goodness of fit indicator in hydrological sciences for comparing simulations to observations. The KGE index ranges from -infinity to 1, where a value closer to 1 indicates a better match between the model

and the observed data. Anyway, the goal is not just to maximize KGE but to build a model that accurately represents the system of interest.

Twenty calibration parameters (Table 6) were made selected on the most commonly chosen SWAT calibration parameters used in previous SWAT calibration studies (Abbaspour et al., 2015; Becker et al., 2019; Lam et al., 2010), as well as parameters, which were found to be more sensitive than changes in AET. Parameter ranges have been defined based on the minimum and maximum values suggested by SWAT. After parameterizing the model and assigning the ranges, the program was run 500 times. After that, we moved on to post-processing and SWAT-CUP calculates the objective function and the 95PPU for all observed variables. New parameter ranges are suggested by the program for another iteration, which modifies the previous ranges focusing on the best parameter set of the current iteration.

To understand the more sensitive parameter, in the SWAT-CUP, the “P-Value” and “t-Stat” are particularly important: t-Stat represents the sensitivity of the parameter. A larger absolute value indicates that the parameter is more sensitive in a certain area; the P-Value represents the confidence level of the parameter sensitivity. The closer the value of p is to zero, the more significant and sensitive the parameter is. A model parameter is identified as sensitive when the value of P-Values is less than or equal to 0.05.

These two values are fundamental to determine which parameters most influence the model results.

After the calibration, model validation was conducted using SWAT-CUP, as well. As already stated, validation is used to enhance the accuracy of the calibrated parameters. These are indeed the same parameters that were calibrated, after the best run, without any further changes and the iteration must be with the same number of simulations used for calibration.

Table 6: 20 parameters selected for the calibration and range of the corrections.

Parameter Name in SWAT-CUP	Min_value	Max_value	Description
1:R_HRU_SLP.hru	0	0.2	Average slope steepness for overland flow
2:V_ESCO.hru	0.6	1	Soil evaporation compensation factor
3:R_CN2.mgt	-0.2	0.2	SCS runoff curve number for moisture conditions
4:V_ALPHA_BF.gw	0.07076	0.109757	Baseflow recession coefficient

5:V__GW_DELAY.gw	0	20.28156	Groundwater delay
6:V__GWQMN.gw	0	500	Threshold depth of water in the shallow aquifer required for return flow to occur
7:V__GW_REVAP.gw	0.1	0.2	Groundwater 'revap' coefficient
8:V__REVAPMN.gw	143.0484	342.7209	Threshold depth for water in the shallow aquifer for revap or percolation to occur
9:V__EPCO.hru	0	1	Plant evaporation compensation factor
10:V__RCHRG_DP.gw	0.009108	0.336392	Deep aquifer percolation fraction
11:V__CANMX.hru	9.93414	29.80586	Maximum canopy storage
12:R__SOL_BD(..).sol	0.190512	1.571738	Moist bulk density
13:R__SOL_AWC(..).sol	-0.5	0.95	Available water capacity of the soil layer
14:R__SOL_K(..).sol	-0.8	0.8	Saturated hydraulic conductivity
15:R__SOL_ALB(..).sol	-0.03	0.2	Moist soil albedo
16:R__SOL_ZMX.sol	24.9602	141.6598	Maximum rooting depth of soil profile
17:V__SLSOIL.hru	0	150	Slope length for lateral subsurface flow
18:R__SOL_Z(..).sol	-0.03	0.2	Depth from the soil surface to the bottom of the layer
19:R__SOL_CBN(..).sol	0.041925	0.185805	Organic carbon content
20:V__FFCB.bsn	0	1	Initial soil water storage

3.5.1 MOD16 Data

In this study, the monthly evapotranspiration data provided by Moderate Resolution Imaging Spectroradiometer (MODIS) was used, in particular, MOD16's AET was utilized for SWAT calibration (2007-2010) and validation (2011-2013).

MOD16 global evapotranspiration data is based on a 1 km² grid of AET surface that was developed with an energy balance model using satellite data as input (Mu et al., 2011).

Before using MOD16 data, other databases were also considered. One of the datasets analyzed is the Global Land Evaporation Amsterdam Model (GLEAM) data. (GLEAM; <http://www.gleam.eu>, last access: 27 December 2023). GLEAM supplies daily data for actual evapotranspiration (ET), root zone soil moisture, and surface soil moisture. Nevertheless, the

spatial resolution of GLEAM data, approximately 25 km², proves to be excessively coarse for the the study area of limited size.

To achieve a finer spatial resolution, the SMAP/Sentinel data (SMAP, https://nsidc.org/data/spl2smap_s/versions/1, last accessed on December 27, 2023) was also explored. This dataset offers soil moisture estimates at a more detailed 3 km grid.

Given the various evapotranspiration databases available, the MOD16 data was chosen for its 1 km resolution, considering the limited size of the study area. This higher resolution data can provide more detailed information, especially useful in heterogeneous landscapes.

Specifically, “MOD16” refers to the MODIS Evapotranspiration project, which is part of NASA’s Earth Observing System (EOS). This project estimates global terrestrial evapotranspiration from earth land surface using satellite remote sensing data (Nasa, n.d.). The MOD16 global evapotranspiration product can be used to calculate regional water and energy balance, soil water status, and provides key information for water resource management.

The MOD16 algorithm (Mu et al., 2011, 2007) calculates evapotraspuration based on the the Penman–Monteith equation. This equation, to estimates evapotranspiration, includes a variety of inputs, these include for Moderate Resolution Images Spectroradiomete (MODIS) remotely sensed data such as soil cover, albedo, LAI, an improved vegetation index (EVI) and a daily meteorological analysis data set from NASA’s Global Modelling and Assimilation Office (GMAO) (Mu et al., 2011; Odusanya et al., 2019). This algorithm operates, calculating the daily evapotranspiration as the combined total of ET during the daytime and nighttime.

ET vertically is sum of the water vapor fluxes arising from soil evaporation, wet canopy evaporation, and plant transpiration on the dry canopy surface. Terrestrial ET incorporates evaporation from both wet and moist soil, rainwater intercepted by the canopy, and transpiration through stomata on plant leaves and stems. To calculate canopy conductance for plant transpiration, the algorithm employs the Leaf Area Index (LAI) to scale stomatal conductance up to the canopy level. During growing seasons, many plant species exhibit stomatal conductance control influenced by vapor pressure deficit (VPD) and daily minimum air temperature (T_{min}). Elevated temperatures often coincide with high VPDs, resulting in the partial or complete closure of stomata.

For a specific biome type, the Biome-Property-Look-Up-Table (BPLUT) contains two threshold values for T_{min} and VPD, for stomatal conductance control (Running, S.W. et al., 2019).

The MOD16 products cover a range of temporal resolutions, providing 8-day, monthly, and annual data on key parameters: evapotranspiration (ET); latent heat flux (LE); potential ET (PET); potential latent heat flux (PLE); and 8-day and annual quality control (ET_QC).

The MOD16 AET dataset is a raster in Geotiff format. Since the primary objective was to compare the value of the AET pixels with the monthly AET values simulated by SWAT for each HRU, the average evapotranspiration of each HRUs was extrapolated in R programming language (Figure 8). This method allowed for a detailed comparison between observed AET from MOD16 dataset and the simulated AET from the SWAT model on a monthly basis.

The SWAT model was calibrated and validated for 149 HRUs. These HRUs were selected out of a total of 167, with those falling in urbanized areas excluded from the calibration. The exclusion of urban areas was done because MOD16 does not calculate AET for these areas, moreover, the anthropogenic factors can influence the evapotranspiration process.

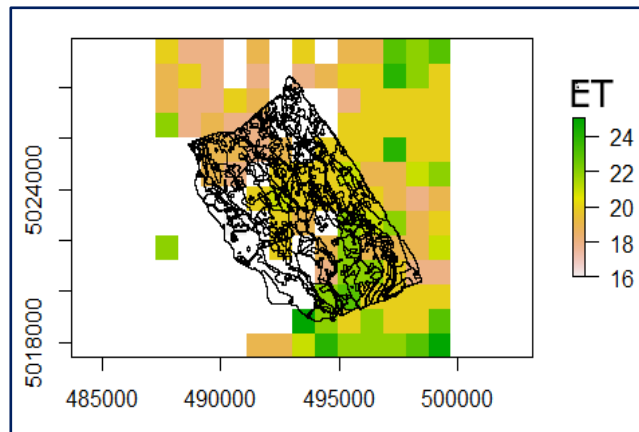


Figure 8: AET of MODIS over the study area subdivide in 167 HRU

3.6 Trend analysis

Following the calibration and validation of the model, a trend analysis of both input climate data, as well as output data, was conducted, using the Mann-Kendall test (Henry, 1945; Kendall, 1955). This nonparametric statistical method is frequently used in environmental studies to detect trends in time series data (Aboelnour et al., 2020). The test specifically evaluates the presence of an increasing or decreasing trend over time by examining the rank

correlation of data points. The Mann-Kendall test was applied to climate data, including temperature, no-rain days, as well as for hydrological process, with actual evapotranspiration and soil water content. For each data set, the Kendall coefficient (τ) was calculated to quantify the strength and direction of observed trend, concurrently, the p-values was determined to have statistical significance of the identified trends, a p-value below a predetermined significance level (e.g., 0.05) indicates a statistically significant trend, the Mann-Kendall test was performed using "MannKendall" function in the "Kendall" package in R (McLeod, 2005).

4 RESULTS

In the following paragraphs, I will explain the results derived from the analysis conducted during this doctoral research. Specifically, I will describe the results obtained through the utilization of input data. Subsequently, I will detail the findings arising from the calibration and validation processes. Finally, I will present and analyse the output data.

It is important to highlight that a substantial portion of the findings presented here has been previously documented in the article (Bernini et al., 2023).

4.1 Input analysis

As outlined in the preceding sections, the input data for the Soil and Water Assessment Tool comprehend elements such as topography, soil, land use, and climatic data. Beyond their fundamental role for running the model, these datasets have been subjected to in-depth analyses. This doctoral study recognizes the significance of not only employing these inputs for the model's execution, but also investigating and examining them independently. The subsequent paragraphs will elaborate on the detailed analyses performed on these key input parameters. These analyses contribute to a comprehensive understanding of the study area. By examining the individual characteristics of the topography, soil, land use, and climatic conditions, I identified the complex interplay of factors influencing the hydrological processes within the designated area.

4.1.1 Topography

One of first results of my doctoral thesis, was the mosaicking of TanDemX and Lidar to create a "hybrid" Digital Elevation Model (with 10 m resolution), allowing an evaluation of the landscape. The most important thing of this results revealed a distinctive feature that defines the area—the presence of fluvial terraces. Particularly, this is evident in the Vertical Distance to Channel Network (Figure 9), showing three distinct orders of terraces originating from the river Ticino. These results permit to understand the topography, contributing to understand the unique landscape of the study area.

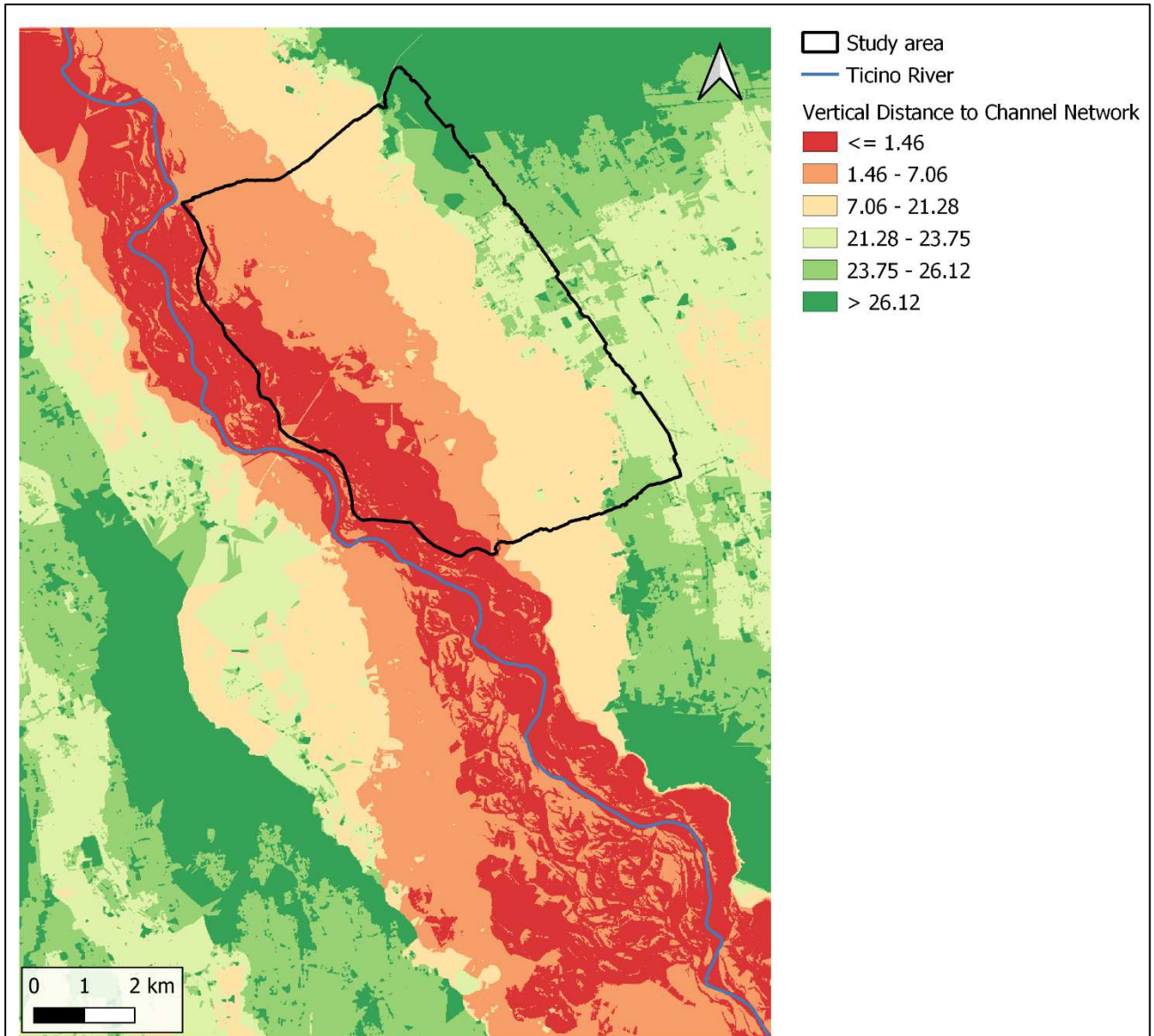


Figure 9: vertical distance to channel network representing the river terraces of the Ticino River.

4.1.2 Soil

Regarding field analysis, the soil profiles examined in laboratory predominantly exhibit a sand/sandy loam texture (Figure 10), with an increasing sand-gravel fraction towards the proximity to the Ticino River. The sampling areas (Figure 5), as described in the 3.2.2 chapter, are located on various levels of the terraces of the Ticino River. The terrace level also determines the age of the soils, with the younger ones situated near the riverbed, while the more developed one is evolved on higher terraces.

- Coronate 1
- Coronate 2
- Lasso 1
- Lasso 2
- Cerina

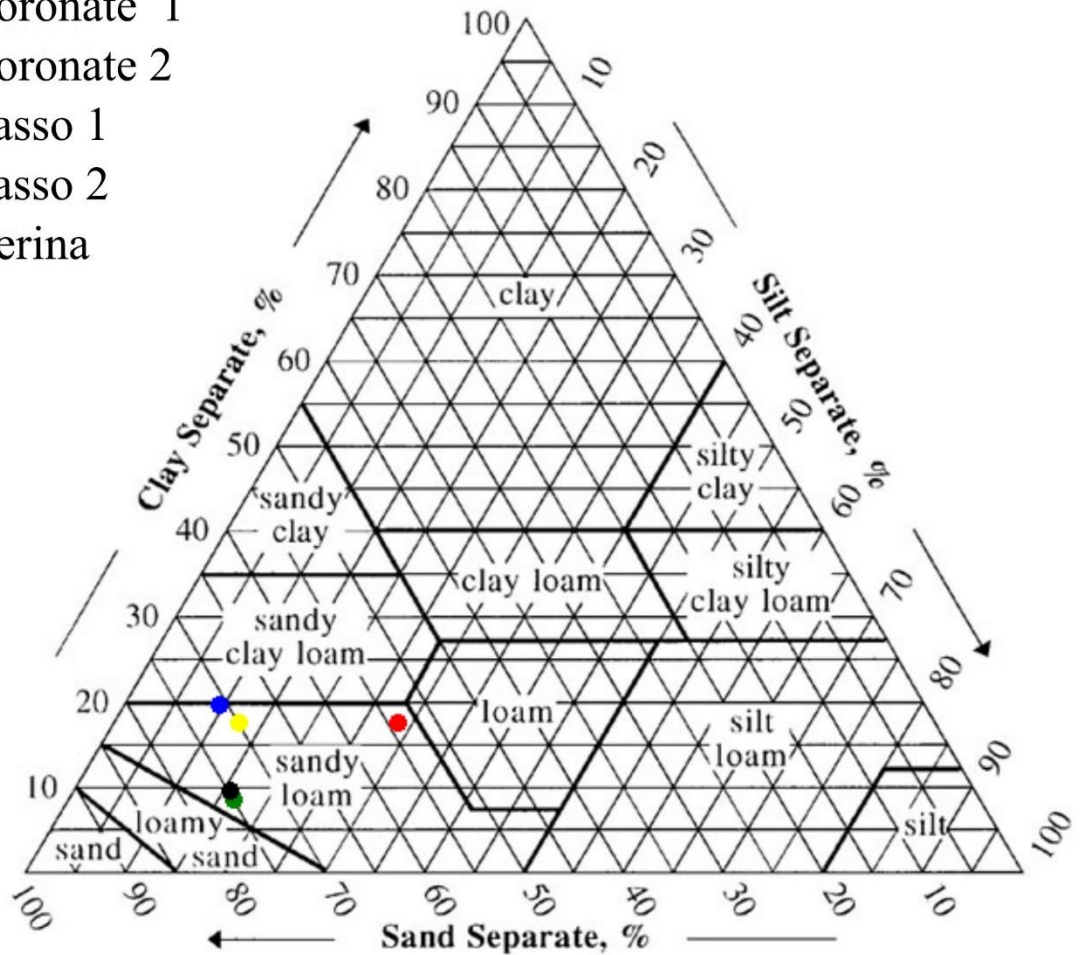


Figure 10: average texture of the soil samples analysed.

The fieldwork and general analysis showed that above the fluvial-fluvioglacial deposits in the study area, soil developed with different depths according to the age of the terrace level. The soil cover of the study area consists of Regosols on the lower terrace of the Ticino River and Luvisol and Umbrisols on the upper terraces, following the World Reference Base for soils (WRB) (IUSS Working Group WRB, 2015). Luvisol and Umbrisols are well-developed soils with a considerable thickness (more than 1 m), whereas Regosols represent younger and less evolved soils. The soil texture is sandy-loam (average values are 69% of sand, 15% of clay and a 6% of silt) following the ASTM Standards, with an increase in the gravel fraction in the areas closest to the Ticino River. This coarse texture is related to a good drainage, but even in hydraulic conductivity are observed differences varying between the soils near the Ticino River and those in the upper terrace level. Hydraulic conductivity is notably high

(approximately 87 mm/h) in the lower areas, consistent with the gravelly-sandy texture of the soils. In contrast, in the higher terraces, it is lower (ranging around 10 mm/h) due to the loamy-sandy texture and because of significant soil compaction caused from continuous agricultural activities.

In detail, the profiles dug near Cascina Coronate (Coronate 1 and Coronate 2) are situated on the level of the highest and oldest fluvial terraces and on the intermediate one, approximately 5 km away from the Ticino River at elevations of ~20 m and ~10 m, respect to the river, respectively. This area is characterized by Würmian fluvioglacial and fluvial deposits, predominantly consisting of sandy sediments. The higher fluvial terraces exhibit a flat topography and are primarily used for agricultural purposes. Coronate 1 and 2 are characterized by predominantly sandy loam textures, with percentages exceeding 50%. The pH values range between 6.3 and 7.4. The cation exchange capacity exhibits medium to low values, below 15 meq/100g. In terms of fertility, these values indicate low soil fertility. The C/N ratio is also in the medium to low range, ranging from 2.5 to 9.8. The organic matter content is <6%, indicating average values. The soil thickness is considerable, exceeding 1 m, and is characterized by A/Ap/Bw/B/Bt and A/Ap/C/A2/Gr, horizons, indicating well-developed soils.

Notably, Coronate 1 the top material exhibits altered pebbles and reveals a more compact soil, probably representing a fragipan layer, in the top 40 cm. A fragipan is characterized by a compacted layer with reduced pore volume and consequently lower hydraulic conductivity, in contrast with respective texture. The measured saturated hydraulic conductivity in these points (Table 7) is notably low, deviating from the sandy clay loam / sandy loam texture. This discrepancy provides a key factor to consider in the SWAT model, potentially influencing water dynamics within the soil.

The profile dug near Cascina Cerina is located approximately 2.5 km away from the Ticino River and the vertical distance is around 10 m. The site is characterized by sandy-silty deposits with on an intermediate fluvial terrace of the Ticino River. The terrain is mostly flat, and the profile was excavated in an area covered by woodland. The soils at the Cerina 1 site are well-developed with thicknesses exceeding 80 cm. The soils exhibit a sandy loam texture, and there is noticeable leaching of clay towards the lower part of the profile (>15cm). The profile is characterized by horizons A/B/Bw/Cw. The soil has formed on alluvial sandy-silty deposits. Due to the texture, the conductivity of the topsoil is relatively high (46.56 mm/h); however,

considering the leaching processes of clays, the hydraulic conductivity in the Bw horizon is lower (21.33 mm/h) compared to the topsoil. These soils have a gravel content of less than 15%. The pH is around 5.4. The organic matter content is relatively high, as the area is wooded.

The profiles near Cascina Lasso are located in close proximity (<1000 m) to the Ticino River, on the lowest terrace, with a flat topography of alluvial deposits. The sites exhibit an elevation above the Ticino of less than 3 m. The area is characterized by sandy-gravelly deposits from the Ticino River with spatial heterogeneity. Both excavations reveal A/C profiles, indicating rudimentary and young soils. These soils are characterized by high infiltration and hydraulic conductivity, leading to rapid drainage. Given the parent material, they exhibit a significant gravel content. The soil pH is around 7, indicating neutral soil conditions.

Overall, there is a trend of increasing saturated hydraulic conductivity closer the Ticino River (Table 7), aligning with the observed texture variations. Moreover, the values are generally higher in the topsoil compared to the subsoil.

Table 7: Ksat calculated with Amoozometer.

	Coronate 1	Coronate 2	Cerina 1	Lasso 1	Lasso 2
Ksat (mm/h) topsoil	1.26	10.13	46.56	360.23	91.05
Ksat (mm/h) subsoil	1.14	10.29	21.33	165.28	83.16

These measurements were cross-referenced with the "usersoil" table generated from ERSAP profiles and SPAW software. Preliminary analysis reveals some disparities, particularly in the often-smaller measured Ksat values compared to the calculated ones. Particularly at the Coronate 1 site, there appears to be a slightly more clayey texture, coupled with a lower Ksat, as previously noted, due to the presence of a fragipan. These variations are probably since spot analyses that have been conducted in distinct land use and management practices that can significantly alter soil properties, especially in heavily cultivated areas. Therefore, with

laboratory results, a more precise refinement of soil input data became feasible, enabling the subsequent execution and calibration of the SWAT model.

4.1.3 Landuse change.

Another finding of this study was the changes in land use patterns from 2007 to 2018 (Figure 11). Notably, a remarkable transformation is observed in the agricultural landscape, with a substantial increase in rice cultivation, expanding from 13% to 20% of the total area. Simultaneously, stable meadows experienced an expansion, increasing from 1% to 5%. In contrast, there is a decline in the areas designated for simple agricultural fields, diminishing from 46% to 38%, and permanent crops, decreasing from 3% to 1%. These fluctuations underscore the intricate interplay between human activities and the environment, highlighting the evolving dynamics of agricultural practices over the studied period. The urbanized area, instead, is constant in the years. Therefore, it is needed to comprehend these changes for a comprehensive understanding of the region's sustainability and resilience. Moreover, these understandings into land use changes are instrumental in considerate the evolving landscape and can be useful for future scenarios made with the SWAT model.

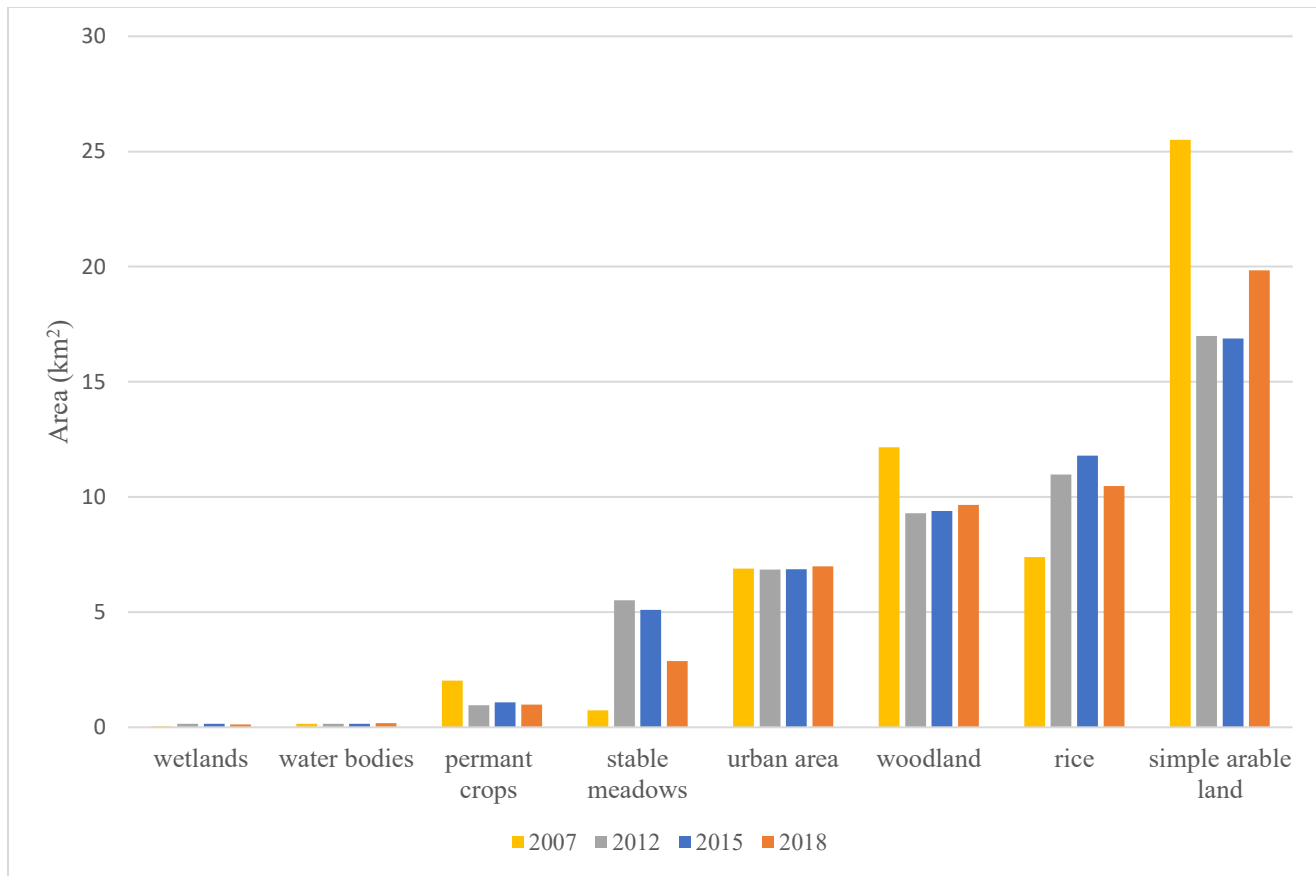


Figure 11: landuse changes from the DUSAF land use maps

4.1.4 Weather data and climate change

Concerning climate data, an in-depth analysis was conducted using GANTT diagrams (Figure 12) for each climate parameter to carefully comprehend the structure and quality of the data. The Gantt diagram is constructed with the time arc along the horizontal axis and the various ARPA stations depicted on the vertical axis. Horizontal blue bars, illustrate the sequences, duration, and period of each activity undertaken by the stations. The white areas denote periods without recorded data. From the GANTT diagram, it becomes evident that there are notable data gaps throughout the data. However, incorporating data from multiple meteorological stations, it is plausible to effectively fill these gaps.

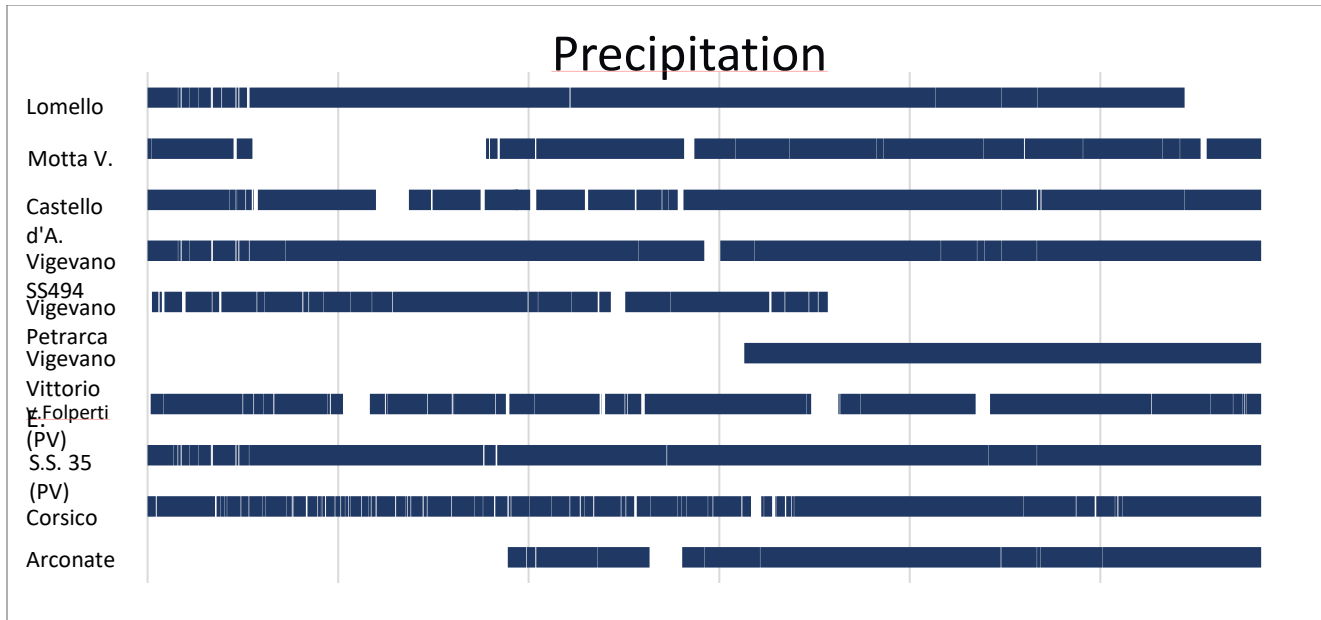


Figure 12: Gantt diagram of precipitation data.

Following the calibration and validation process (the results are presented in 4.5 paragraphs), an analysis of climate and hydrological data was performed. The temperature and precipitation trends were estimated throughout the entire period of SWAT simulation (2004-2022). Over this period of 19 years, a notable rise in the mean temperature was observed (Figure 13). Starting at around 13.8°C in 2004, it peaked at 14.7°C in 2022. Notably, 2005 marked the coldest year, while 2022 emerged as the warmest.

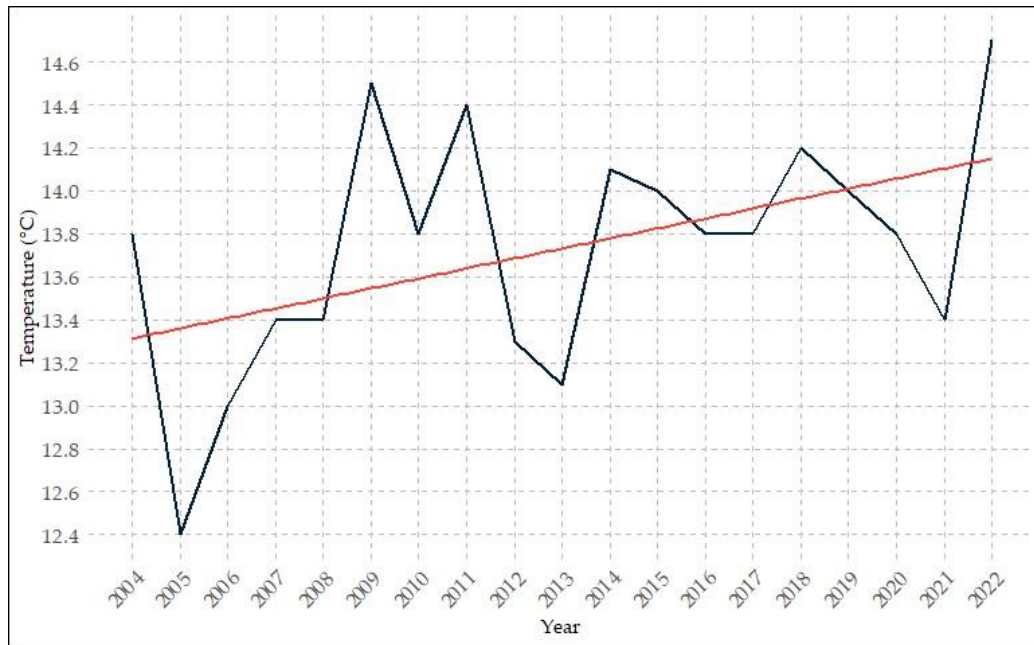


Figure 14: Mean temperature from 2004 to 2022, with the trend represented by the red line.

The analysis of precipitation patterns revealed a notable overall decrease, as illustrated in Figure 14, with the year 2022 prominently occurring as the driest in the observed period. Furthermore, a noteworthy increase was observed in the frequency of rain-free days, as represented in Figure 15, with both 2017 and 2022 documenting the highest occurrences of such meteorological events. This exploration of climatic trends contributes to our understanding of changing weather dynamics, particularly in terms of decreasing precipitation and the rising of rain-free days.

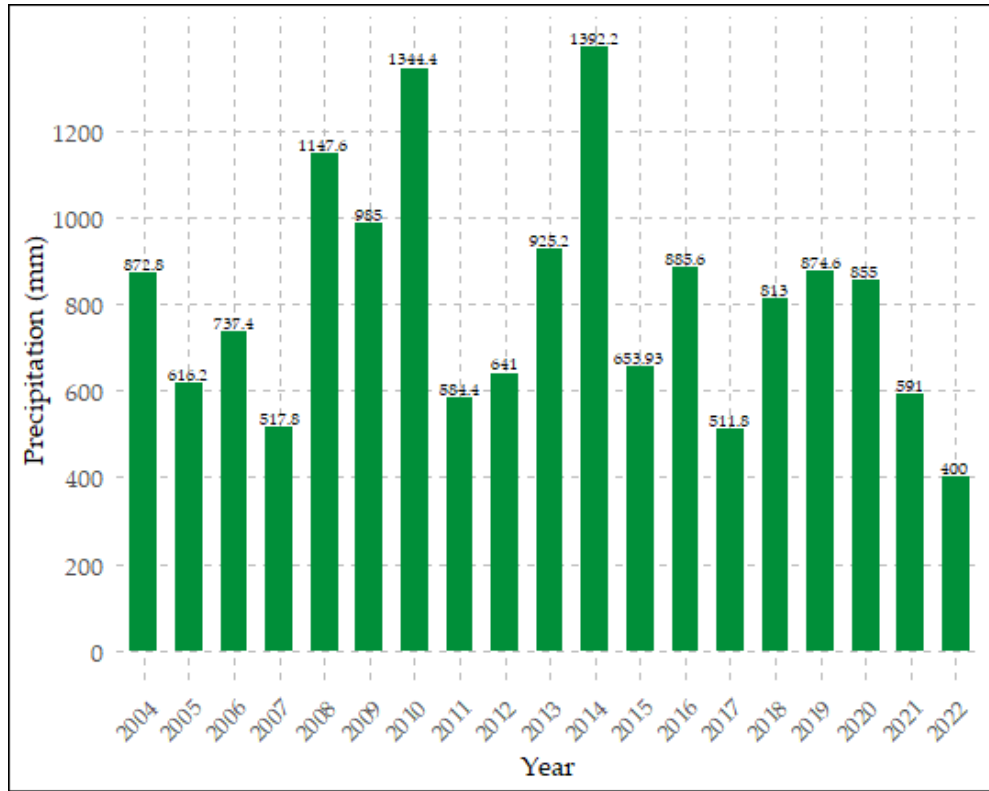


Figure 14: annual precipitation.

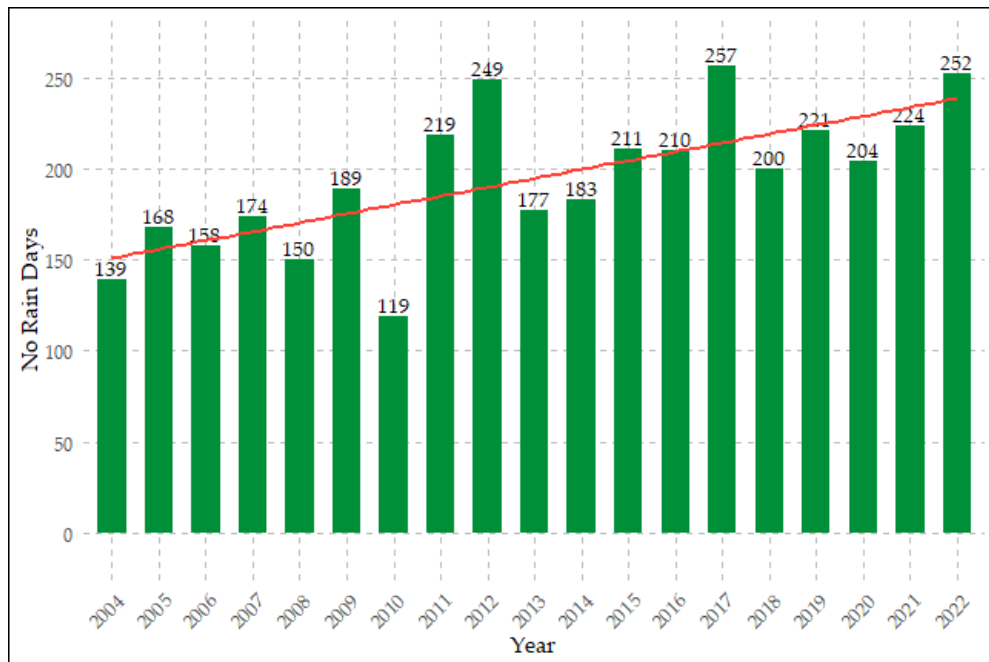


Figure 15: rain-free days over the past 19 years, with the trend reflected by the red line.

4.2 Soil water content sensors

The in-situ soil moisture measurements enabled, first, a correlation between soil water content and precipitation. This not only facilitated the identification of irrigation activities (as illustrated in Figure 16) but also enabled a comparative analysis of water content across different land uses.

As showed in Figure 16, the use of soil moisture sensors across various land-use conditions proved instrumental in recognizing distinct irrigation schedule. Within the forested area, the sensors reflected natural conditions where soil water content was predominantly influenced by precipitation. The peaks observed in soil water content in the forested region linked to rainfall events, also confirmed the peaks in both rice and corn fields. Conversely, in the corn and rice fields, the sensors revealed clear indications of irrigation practices. In the case of corn cultivation, additional peaks in soil water content were notable during irrigation periods, adding a layer of complexity to the moisture dynamics. Meanwhile, for rice fields, the timing of the initial irrigation flood was distinctly visible, indicating a significant increase in soil water content. This detailed analysis not only showed the influence of land-use practices on soil moisture but also emphasizes the importance of considering specific crop characteristics and irrigation schedules in understanding the dynamics of water availability in different agricultural settings.

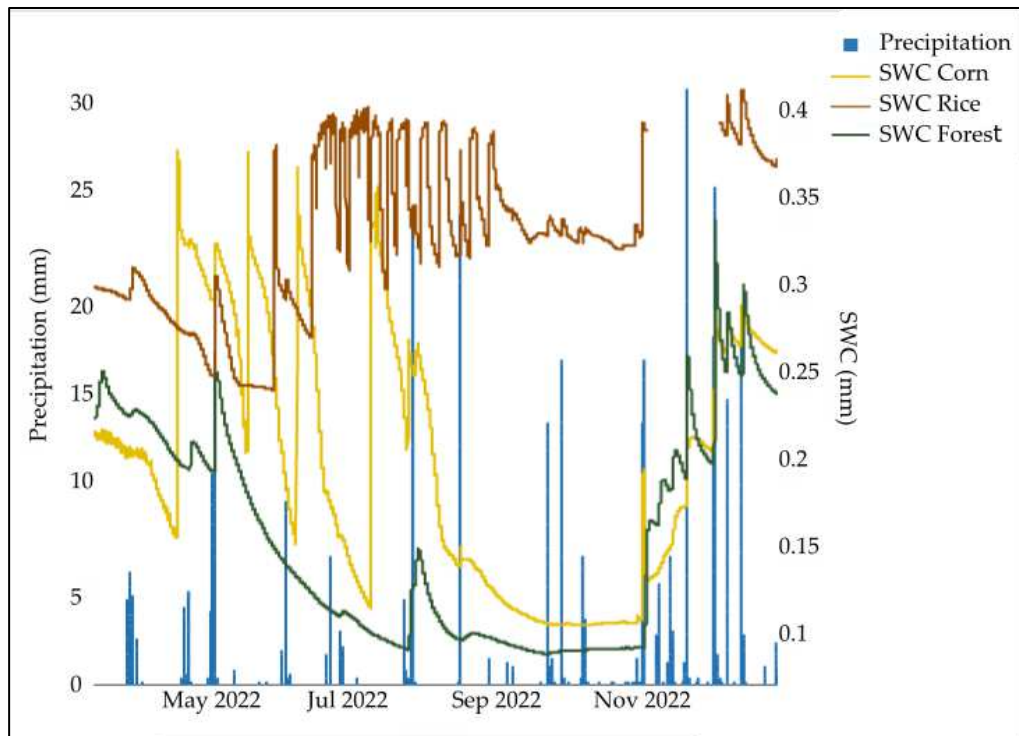


Figure 16: the correlation between soil water content and precipitation in the study area.

Analysing the modelled soil moisture content using SWAT in comparison with field measurements obtained through Soil moisture sensors (TEROS 12), a consistent underestimation in the model emerges. This discrepancy is probably due to the differences in measurement scales, with the sensors providing local water content data, while the SWAT simulations operate at the HRU scale. The incorporation of auto-irrigation in the SWAT further introduces a layer of complexity to the dynamics of soil moisture. The assumption was made that actual irrigation events might impact soil moisture levels differently than the model's HRUs, owing to their distinctive representative scales.

This evaluation underscores the crucial role of considering both spatial scale and local agricultural practices in comprehending and interpreting the intricate dynamics of soil moisture within the model system. These findings do not only contribute to the modelling techniques, but also emphasize the need to align simulations with in-situ realities to enhance the accuracy and applicability of such hydrological models.

4.3 SWAT model

As previously mentioned in the 3.4 paragraph, the initial SWAT run utilized the FAO-UNESCO soil map, which, however, represents only one type of texture in the area—specifically, a clayey composition that differs from the textures analysed. Despite this limitation, these preliminary test runs proved valuable in detecting and identifying both data and simulation issues.

The initial approach, employing "traditional topography driven drainages," revealed its inadequacy in accurately delineating streams and watersheds in an area with the described characteristics. Channels delineated by this method did not align with the actual artificial drainage system, resulting in dynamics that deviate from the real study area situation.

In the second approach, utilizing existing streams and watersheds, a challenge occurred with the use of channels sourced from Geoportale della Lombardia. Indeed, in the shapefile of watercourses (Streams) used in SWAT, LINKNO and DSLINKNO are important fields, which must be filled in necessarily. "LINKNO" is the field that must contain unique and non-negative values. Each value represents a stretch of watercourse. "DSLINKNO" is the field represents the downstream link. Each value must correspond to another value LINKNO or -1, where -1 indicates an exit point of the river basin. These two fields provide the connection between the sub-basins and the stretches of water streams, it is therefore impossible to conduct in the study area where the water streams are all irrigation channels managed by human.

Despite these challenges, the outputs of the initial SWAT model runs are considered acceptable, considering the use of only one type of soil, which is more clayey than the observed ones, and reliance on a single climate station. Consequently, the outputs exhibit excessive runoff compared to the expected values.

Subsequently, setting-up the model with more detailed input data, including a soil map delineating field-analysed characteristics, various climatic stations, manually delineated sub-basins following the fluvial terraces, and the incorporation of crop rotation and auto-irrigation, marked improvements in the results of the uncalibrated model were determined. The uncalibrated model, when subjected to this refined input dataset, exhibited markedly improved accuracy and reliability in capturing the intricate dynamics of the studied system. This improvement underscores the efficacy of the augmented model configuration and provides a solid foundation for advancing to the subsequent phase of model calibration.

4.5 Calibration and validation

First preliminary results of monthly SWAT calibration (during the period 2007-2013) using satellite actual evapotranspiration data showed that the model is able to simulate the general hydrological dynamics of the area. In the initial stages of approaching QSWAT and its calibration, the uncalibrated model achieved a KGE of 0.37 but overestimating it during the summer months and underestimating it during the winter months. While the calibrated model reached 0.56 and after calibration, the summer months appear to be quite consistent with the observed data, in the winter months this problem remains. Subsequent, including the crop rotation and auto-irrigation, coupled with model calibration from 2007 to 2010, led to an improvement in KGE values. Specifically, the uncalibrated model increased to 0.4, and the calibrated model demonstrated a higher performance at 0.59. These adjustments indicate a positive trajectory in the model's accuracy and effectiveness. The KGE efficiency, calculated as the mean of individual HRUs in SWAT-CUP, shows notable improvement when assessing the entire basin. Specifically, the KGE for the uncalibrated model rose from 0.41 to 0.83 for the calibrated AET (Figure 17).

From the graph, it is possible also analyse other method of evaluating the performance of the model. In particular, the Root Mean Square Error (RMSE), with a value of 14.52, and a Coefficient of Determination (R^2) with a value of 0.83. The RMSE quantifies the average difference between the observed and modelled values (Piñeiro et al., 2008) and, a lower RMSE indicates better model performance in capturing the variability. While the R^2 represents the proportion of variance in the observed data that can be explained by the model (Brown et al., 1999). An R^2 close to 1 indicates a strong relationship between the model and observed data. A closer examination of the calibration process reveals variations among the individual HRUs. The top performing HRU achieved an KGE value of 0.8 post-calibration, while some area exhibited values lower than -1, indicating a significant discrepancy between observed and simulated data. These underperforming HRUs, even though limited in area (less than 0.7 km²) contribute to the overall assessment. If we not considered these limited areas, after the calibration there is a satisfactory correlation between SWAT and MOD16 AET values, reflected in improved KGE values. In Figures 18 and 19, the calibrated SWAT model show the results of calibration in a field with rotation cycle of corn, and ryegrass, and a paddy rice. The observable improvement underscores the ability of the model to simulate the hydrological

dynamics of the study area. Here the results show a good KGE of 0.75 and 0.70 respectively, the R^2 is 0.79 and 0.77, while the RMSE 15.23 and 17.39, respectively for corn and rice. However, despite the similarity in seasonal trends for both AET SWAT-simulated and MOD16, the AET SWAT-simulation exhibits more fluctuations, especially during winter months. Notably, both uncalibrated and calibrated SWAT values remain lower than MOD16.

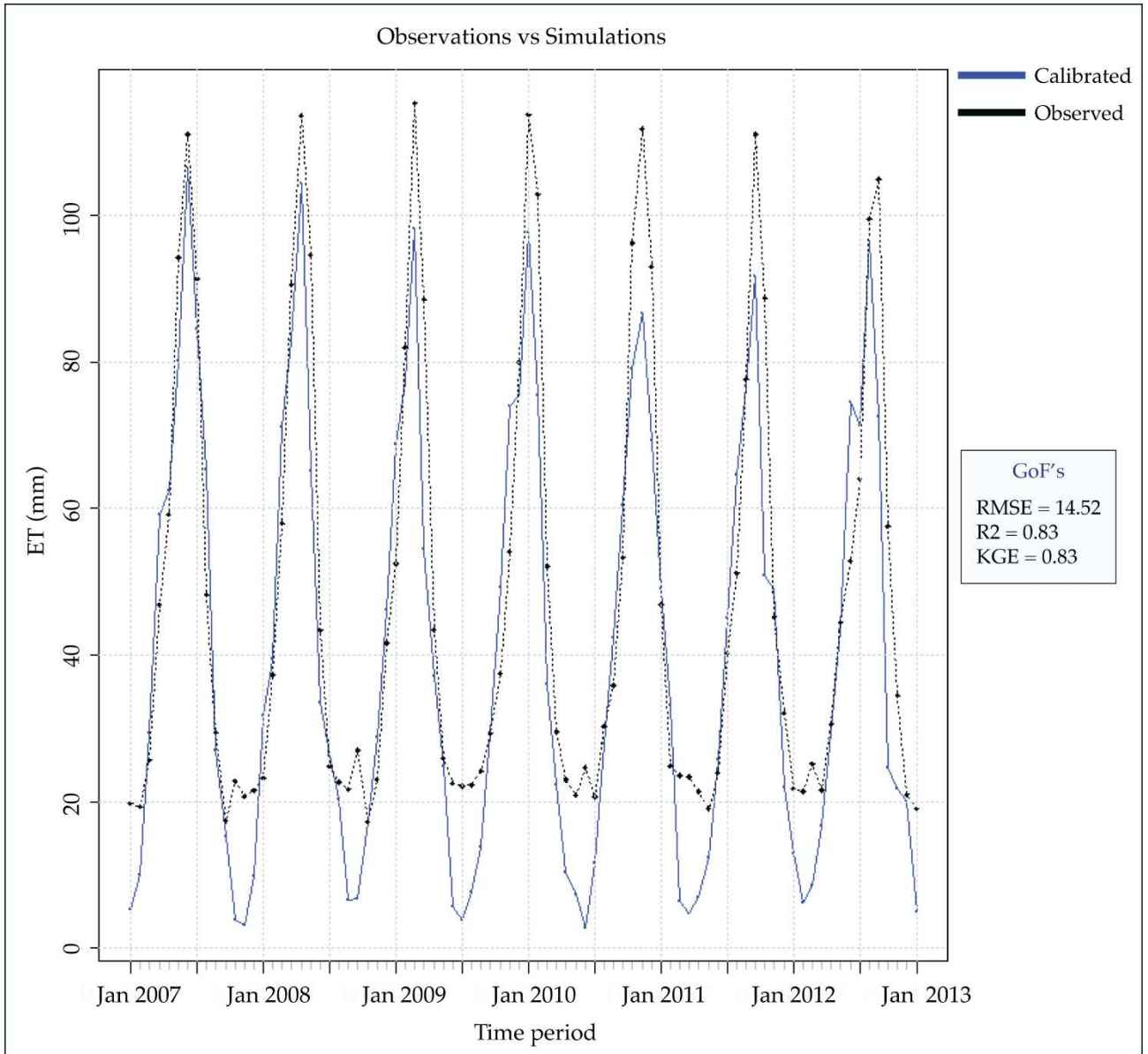


Figure 17: the time series of AET MOD16 (black) and SWAT (blue) after calibration for the study area.

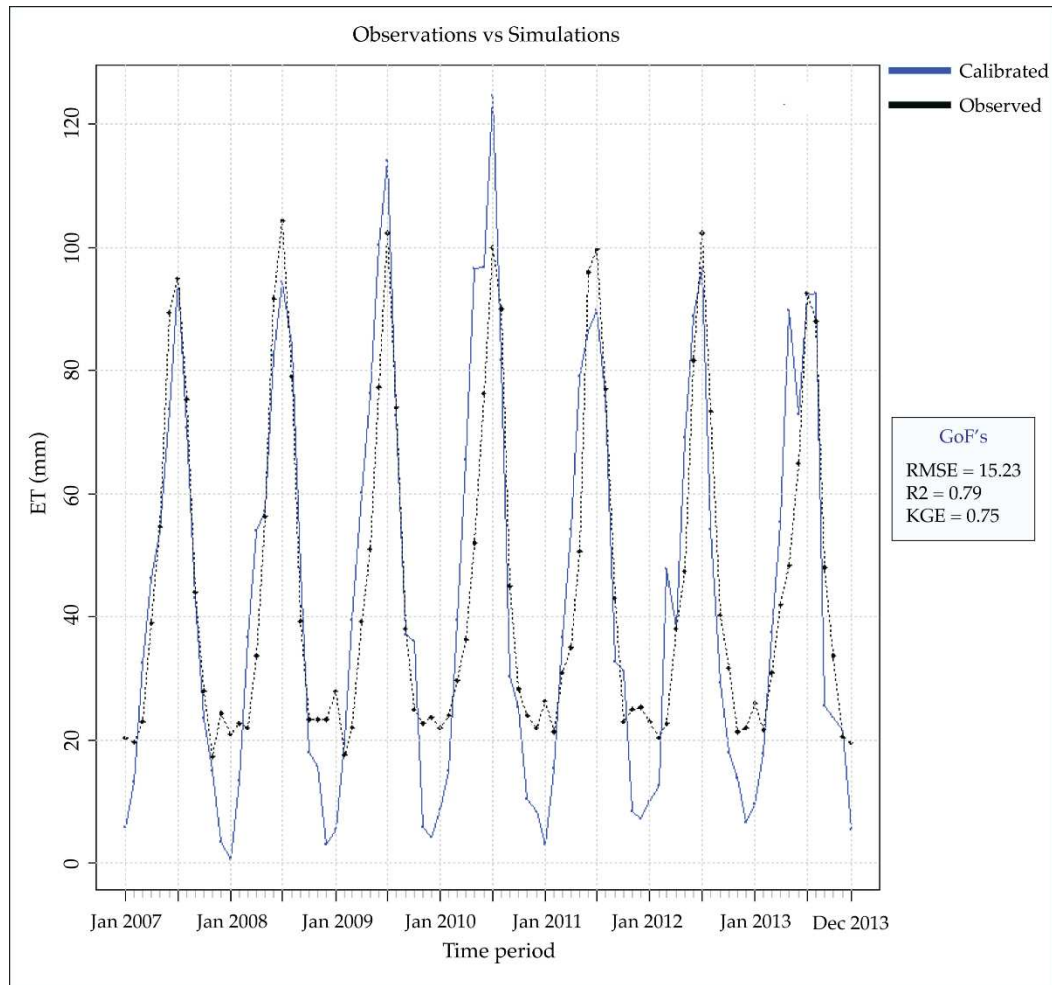


Figure 18: time series of AET MOD16 (black) and SWAT (blue) after calibration, in a corn-ryegrass field.

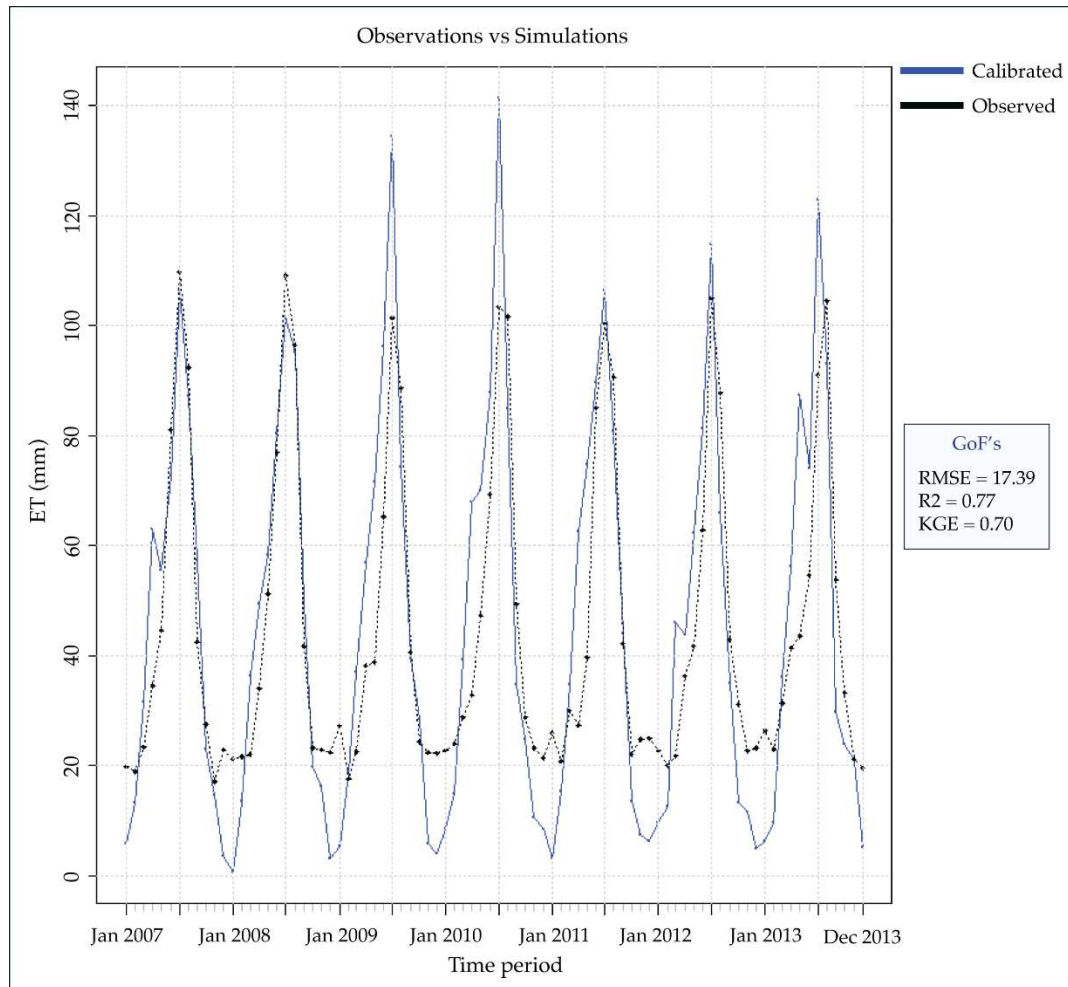


Figure 19: time series of AET MOD16 (black) and SWAT (blue) after calibration, in a rice field.

The validation results reveal an average KGE of 0.48, showing variability across HRUs, with some achieving high KGE values of up to 0.85 (Table 8). Notably, HRUs with limited areas tend to exhibit lower KGE. Conversely, regions of significance characterized by larger surfaces, often with an agricultural land-use, demonstrate good KGE values.

Despite the presence of lower KGE in select HRUs, this calibration and validation results are already estimated satisfactory, considering the intricate hydrological dynamics inherent to the study area, demonstrating the possibility of calibrating SWAT in an ungauged area using satellite-based actual evapotranspiration data.

Table 8: KGE calibration and validation results.

	Mean (all HRUs)	5th percentile	95th percentile
Calibration	0.59	0.22	0.85
Validation	0.49	-0.17	0.79

4.5.1 Sensitivity analysis

The 20 parameters were considered to be sensitive, six result to be more sensitive (Table 9).

The results of the global sensitivity analysis identified that the AWC (Available Water Capacity) and EPCO (Plant Uptake Compensation Factor) stand out as the most influential parameters in shaping the accuracy of SWAT-simulated actual evapotranspiration. AWC, which represents the soil's ability to retain water available to plants., this parameter determines how much water is taken from the lower layers of the soil when the water in the upper layers is insufficient. Higher values of EPCO indicate that more water is taken from the lower layers. Moreover, the other sensitive parameters are: ESCO (Soil Evaporation Compensation Factor), this parameter controls the ability of soil to "compensate" evaporation when water in the upper layers of soil is poor. Higher ESCO values indicate that more water is taken from the lower layers to compensate for evaporation. sol_z (Soil Depth): This parameter represents the maximum depth of the soil layer. SLSOIL (Slope Length for Lateral Subsurface Flow): This parameter represents the length of the slope for the lateral underground flow and CANMX (Maximum Canopy Storage): This parameter represents the maximum amount of water that can be retained by the foliage of the plants. During rain, water is trapped in the canopy, reducing the erosive energy of raindrops, and affecting infiltration, evapotranspiration, and erosion.

These parameters are sensitive in the model, which means that small variations in these parameters can have a significant impact on the model results.

Table 9: Calibrated sensitivity parameters

Parameter name	t-Stat	P-value
13:R__SOL_AWC.sol	52.385311864	0.000000000
9:V__EPCO.hru	25.728184428	0.000000000
6:V__ESCO.hru	14.966163373	0.000000000
18:R__SOL_Z(..).sol	12.986449854	0.000000000
17:R__SLSOIL.hru	9.934724489	0.000000000
11:V__CANMX.hru	5.944062659	0.000000005

4.6 Output analysis

The SWAT model results indicate that there is a marginal increase in actual evapotranspiration over the past 15 years in the study area. In contrast, the ratio of evapotranspiration to precipitation exhibits variability, providing valuable insight into the water balance dynamics within the study region.

The findings from the SWAT model output indicate, indeed, an evapotranspiration trend in the study area, revealing a relatively stable scenario with a marginal increase of only 4%, as illustrated in Figure 20. This apparent constancy in evapotranspiration, however, can be juxtaposed to the ration between actual evapotranspiration and precipitation. Figure 21 show the variability in the ratio of evapotranspiration to precipitation and notable spikes in the ratio are observed in 2015, 2017 and 2022, where actual evapotranspiration surpassed precipitation. The fluctuations in this ratio encourage a deeper exploration into the factors influencing the water balance dynamics within the study area.

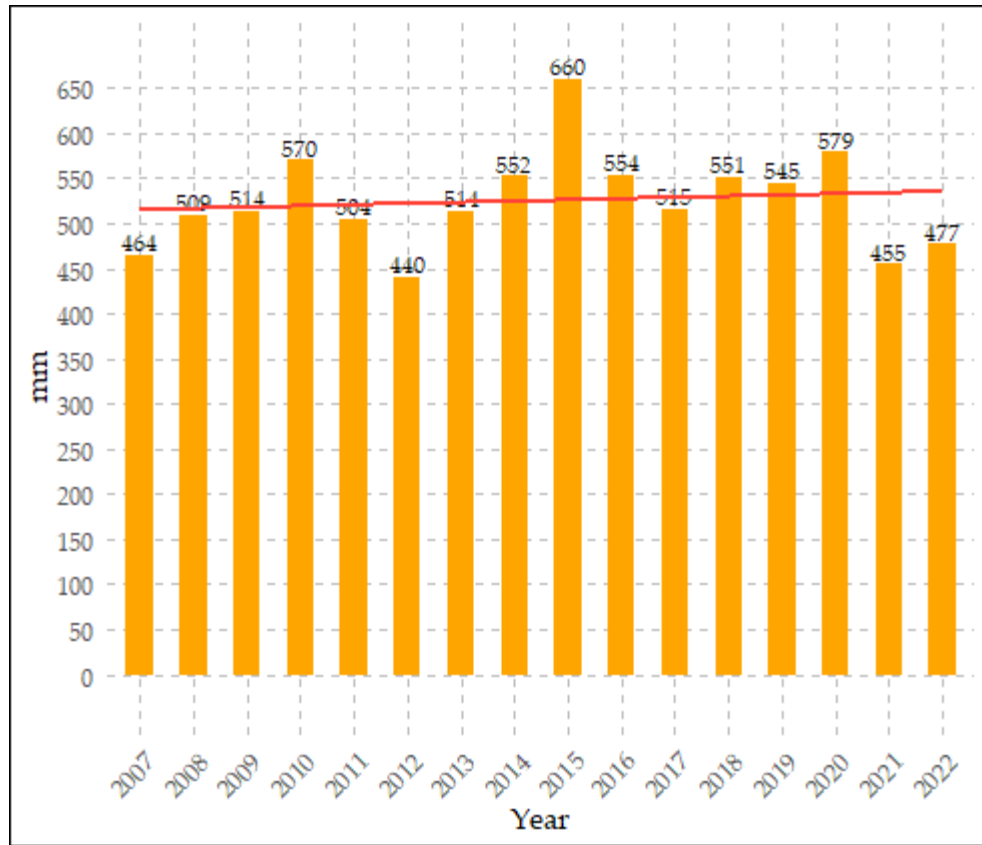


Figure 20: SWAT actual evapotranspiration trend in the study area.

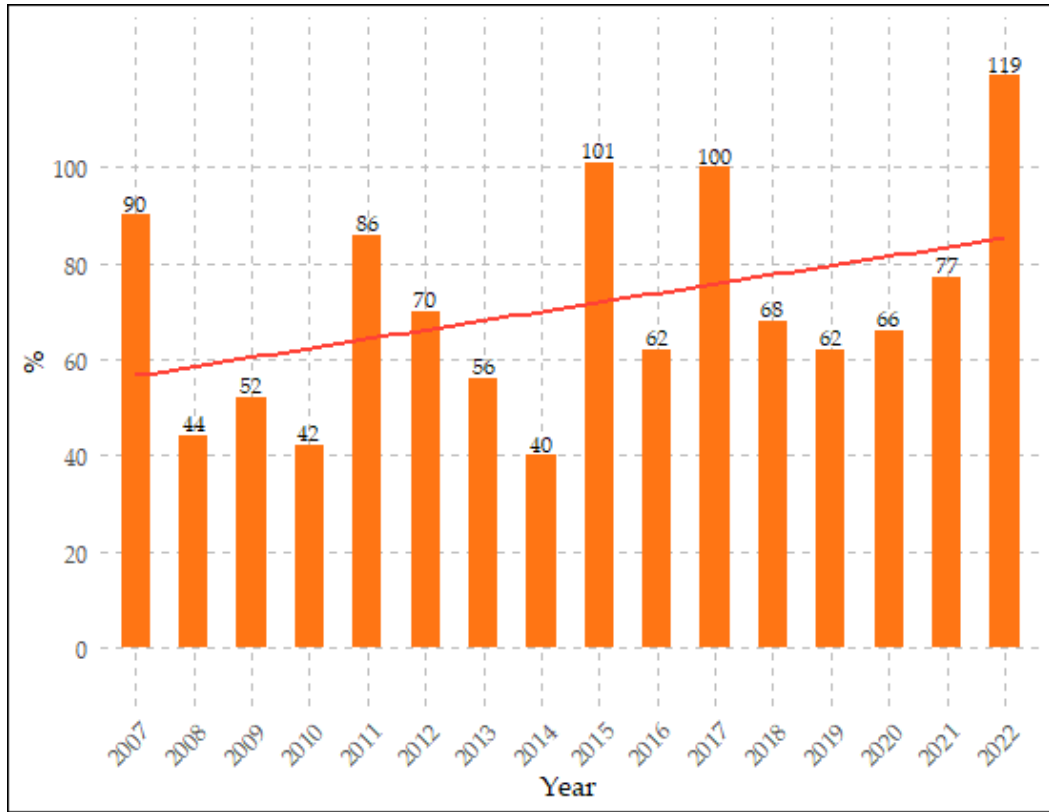


Figure 21: percentage ratio of evapotranspiration to precipitation in the study area.

This investigation also examined the Soil Water Content (SWC), particularly focusing on Hydrological Response Units (HRUs) characterized by agricultural land-use. The graphical representation in Figure 22 shows a declining trend in soil water content over the last 15 years. This substantial decrease, amounting to -7%, highlights a concerning shift in the moisture dynamics. This decline underscores the urgency of understanding the intricate factors contributing to this trend, prompting a deeper exploration into the potential implications for agricultural practices, ecosystem health, and overall water resource management.

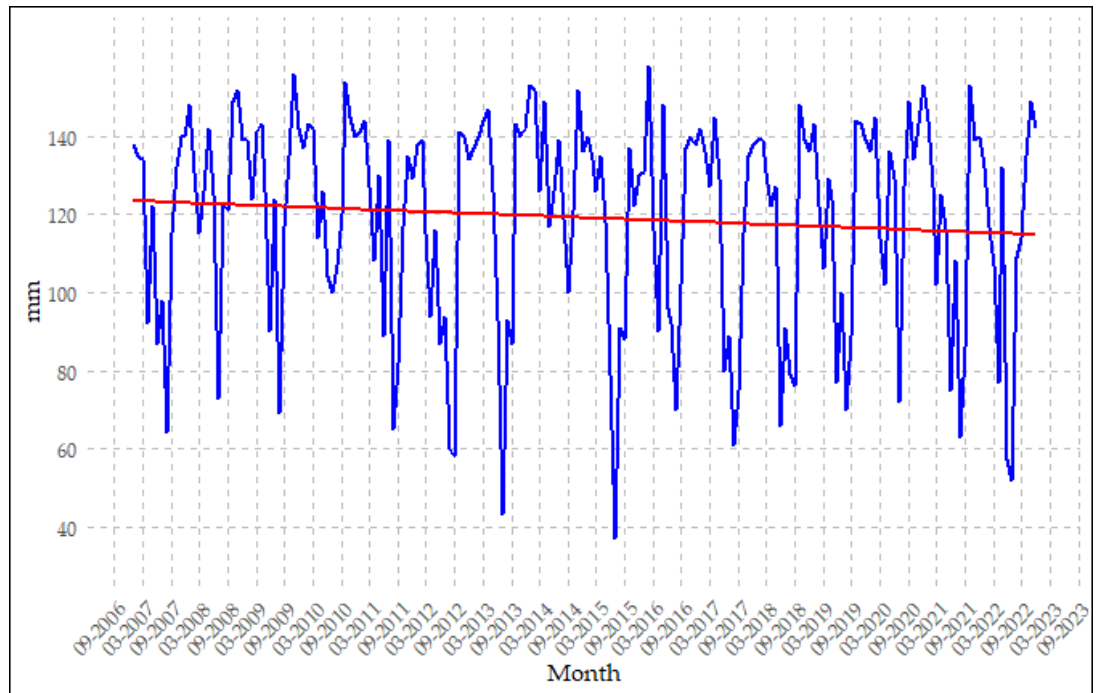


Figure 22: SWAT SWC trend in the last 15 years in the study area.

4.7 Trend analysis

Retaining the Mann-Kendall test, trends in temperature and rain-free days were examined. The Kendall coefficient for temperature indicates an upward trend, although the p-value lacks statistical significance. Conversely, the trend for rainless days is more pronounced, with a significant low p-value, pointing to a noteworthy increase in the number of rain-free days. The Mann-Kendall test was employed to assess the trends in actual evapotranspiration, the AET/precipitation ratio, and SWC too. AET values suggest that there is an upward trend, although p-value is not statistically significant. The AET/precipitation ratio exhibits a positive correlation with tau value, indicating a potential increase in evapotranspiration relative to precipitation over time; however, the p-value exceed the significance level. Regarding SWC, tau values suggest a weak negative correlation, implying a small decrease in soil water content over time.

5 DISCUSSION

Hydrological models, are valuable tools and fundamental for the understanding of the consequences of climate change in recent years (Liu et al., 2021). Hydrological models can be used to simulate rainfall-runoff regimes, groundwater-surface water interactions, water balance, and other hydrological phenomena in several types of basins. It is, however, difficult to apply these models in lowland areas (Waseem et al., 2020). Lowland areas, in fact, are often characterized by complex drainage systems, high infiltration rates and variable soil properties and are often subject to changes in land use and climate change. The application of a hydrological model in a lowland area requires careful analysis of the territory. Moreover, typically, hydrological models in the calibration and validation procedures use discharge data, but acquiring such data in lowland areas poses challenges. The flat topography prevalent in lowlands promotes vertical water dynamics, resulting in surface runoff often being negligible (Baker et al., 2022; Balestrini et al., 2021).

In particular, the study area presents a unique challenge, characterized by its intense cultivation, artificial irrigation channels, and the absence of a conventional "natural" channel network. Nevertheless, despite the crucial significance of the hydrological cycle for agriculture and water management in the region, the existing research is somewhat limited. From this study, in a particular and complex, but unique area, the importance of analysing input data is evident.

First of all, the 'hybrid' Digital Elevation Model (DEM) with a resolution of 10 meters, facilitated a comprehensive evaluation of the landscape, revealing distinctive features that define the area. Notably, the presence of fluvial terraces emerged as a defining characteristic of the region. These findings not only improve the understanding of the topography but also contribute significantly to highlight the unique landscape of the study area. It is precisely this feature of the terraces that generate the springs at the base of their escarpments and thus, creates a unique water reuse system, that in terms of sustainability is an exceptional example worldwide.

Additionally, while conducting fieldwork to assess hydraulic conductivity, the identification of densely compacted soils in elevated areas, influenced by ongoing agricultural practices, underscores the existence of local variations in soil characteristics. These compacted soils, often result from the use of heavy machinery, can induce alterations in soil structure, impeding

water and air penetration and limiting root development in the soil (Nawaz et al., 2013). Such soil compaction can significantly impact the physical condition of the soil, manifested in the diminishing hydraulic properties like infiltration rate and hydraulic conductivities. Therefore, it is evident that human activities, particularly those associated with agriculture, apply a substantial influence on the environment (Shaheb et al., 2021).

Furthermore, another aspect in continuous modification is the land use. Between 2007 and 2018, the study area experienced significant changes in land use and the impact of different land uses on soil properties can alter the components of the hydrological cycle, in particular, as regards agricultural areas, which are also those requiring a greater supply of water.

In the examined period, there was a decline in the simple arable land (such as maize, wheat, and sorghum), following in an increase. In contrast, for rice cultivation there was a substantial rise until 2015, succeeded by a decline from 2015 to 2018. This fluctuation is influenced by choices made by producers, often in response to drought conditions (Ente Risi, 2022). It is important to note that these changes in rice production can be influenced by numerous factors, such as climatic conditions, changes in agricultural practices and changes in market demand. For example, Coldiretti reported that national rice production in Italy has decreased by almost 30% due to increased costs and adverse weather conditions (Coldiretti, 2022). The Italian rice sector is facing a potential challenge due to climate change, which is causing a significant impact on rice cultivation, particularly in Northern Italy. Over 26,000 hectares of rice fields have been destroyed due to elevated temperatures and drought conditions. This has caused an extraordinary loss in production (Moraca, 2022). The decrease in rice production can explain the increase in simple arable crops, which require less irrigation water. However, the oscillation in rice cultivation carries significant hydrological and socioeconomic implications. A decrease in rice cultivation can alter water management, due to the substantial influence of traditional paddy rice fields on water flow and retention, particularly in the study area. Rice fields often function as natural reservoirs, contributing to flood control and groundwater recharge. A decline in rice cultivation has the potential to disturb this “delicate” water balance (Baker et al., 2022; Bove, 2021; Giuliana et al., 2022). Conversely, a growth in rice cultivation could accelerate water demand, resulting in elevated irrigation needs (Tsuchiya et al., 2018; Wu et al., 2019). This increased demand has the potential to strain local water resources. Therefore, preserving a sustainable equilibrium in rice cultivation practices is essential to save the hydrological balance in the study area.

The shifts in land use involve substantial implications for agricultural practices, biodiversity, and overall sustainability. Furthermore, alterations in land use can have a substantial impact on evapotranspiration (Crespi et al., 2021), thereby influencing water cycles and balances. Therefore, comprehending these dynamics is essential in formulating efficacious land management strategies and policies.

As evident, in this dynamic landscape, setting-up the Soil and Water Assessment Tool model poses a complex challenge. Several factors contribute to these complexities. First, the spatial variability of soil properties and land use. In addition, a flat topography and fertile soils promote intensive agriculture, particularly in areas such as the Ticino and Po Plains in northern Italy. This type of agriculture frequently involves irrigation. However, in numerous cases, comprehensive information regarding irrigation schemes and water supply is unavailable (Masseroni et al., 2017). Irrigation practices and precise information on irrigation, with the presence of artificial irrigation channels is a challenging task. Finally, the crop characteristics, as every crop exhibits distinct water requirements and varied responses to water stress, introducing an additional layer of complexity to the modelling process.

It is therefore essential to have high quality and detailed input data in order to calibrate and validate the model in an appropriate way.

After conducting an analysis of the study area and run SWAT simulations from 2004 to 2022, the model was calibrated by AET MODIS data. The calibrated SWAT model, applied to agricultural HRUs with a rotation of corn-ryegrass and paddy rice, demonstrated significant improvement, showing its capability to accurately simulate the hydrological dynamics of the study area. Therefore, results from SWAT calibration using MOD16 data are generally positive and indicate a good match between model simulations and observed data, for the KGE, used for evaluating the model performance, but also for other measure, such as RMSE and R^2 . Overall, the results suggest that the SWAT model, calibrated using MOD16 data, can adequately represent the hydrological dynamics of the study area. In particular, the R^2 results suggests that the model explains a large part of the variability in the data and the RMSE results are acceptable.

Validation results further confirmed the model's efficiency, with satisfactory results. Notably, regions of significance characterized by extensive surfaces and agricultural land-use exhibited good KGE values, indicating the model's excellence in areas of considerable size and specific land-use types, particularly in agricultural zones crucial for this study.

Despite encountering lower KGE values in selected HRUs, both calibration and validation results remained satisfactory, a crucial achievement considering the intricate hydrological dynamics of the study area. These findings highlight the possibility of calibrating the SWAT model in an ungauged area using satellite-based actual evapotranspiration data. The overall results underscore the SWAT model's potential as a valuable tool for simulating complex hydrological dynamics.

In particular if we consider all three methods to evaluate performance of the single HRUs, values of R^2 equal to 0.79 and 0.77 indicates that about 79% and 77% of the variability in the observed data can be explained by model simulations. While this is a positive result, it is important to note that there may be some variability components in the model. Moreover, the RMSE results can be considered acceptable. Finally, the KGE, R^2 and RMSE values may indicate that there may be a range for additional improvements in concordance and variability between model simulations and observed data.

However, the calibration results demonstrate that the seasonal patterns observed in both SWAT-simulated evapotranspiration and MODIS data exhibit similarities, yet the SWAT simulations exhibit more pronounced fluctuations. Initially, the uncalibrated SWAT-simulated evapotranspiration tends to overestimate ET in summer and underestimate it in winter. With the addition of crop rotation and auto-irrigation, KGE values have increased. In particular, through calibration, a notable correlation is achieved during the summer months between observed and simulated data, although challenges persist in accurately representing winter months. These differences could be due to utilizing satellite data for model calibration that yields slightly different output compared to calibrating with streamflow data, as highlighted by (Rajib et al., 2018). The hypothesis for these discrepancies is that SWAT's simulation of higher actual evapotranspiration in summer and lower AET in winter, relative to MODIS, arises from the utilization of satellite data and distinct input factor: SWAT's incorporate both weather data (precipitation, temperature, humidity, wind speed, and solar radiation) and surface conditions (soil, landuse, and slope) for evapotranspiration estimation. SWAT being a physical hydrological model designed to simulate the water cycle within a specific area at a heightened spatial resolution. This requires precise data on soil and land-use, unique for each HRU (Abiodun et al., 2018; Qiao et al., 2022). In contrast, MODIS includes only climate and vegetation data (Parajuli et al., 2022). Moreover, there are different resolutions compared to HRUs for AET calculation respect to MOD16 pixel size. Additionally, as highlighted by

Abiodun et al.(Abiodun et al., 2018), a potential factor contributing to this variation could be the differences in land cover. During winter months, vegetation typically undergoes dormancy or sheds foliage. If the land cover data utilized in SWAT significantly diverges from MOD16, it may lead to disparities in their respective simulations of evapotranspiration. In our study, the dissimilarities in land cover between SWAT and MOD16 were compounded by their data originating from different years. Additionally, as observed by (Parajuli et al., 2022), SWAT tends to project higher evapotranspiration during the crop growth season and lower during the inactive season, whereas MOD16-derived Actual Evapotranspiration (AET) remains relatively constant. Consequently, the discrepancies in simulated AET between SWAT and MOD16 were more pronounced during the less active winter months, attributed to SWAT's incorporation of climatic conditions, land-use, and soil characteristics. In conclusion, MOD16 data can have some limitations even if it provides valuable data for hydrological modelling and water resource management. Moreover, other studies have highlighted a significant uncertainty of evapotranspiration estimates using MOD16 data. These uncertainties are attributed, for example, to the lack of spatial heterogeneity due to the coarse MODIS imprint, the absence of local vegetation and microclimatic variability in the overall land cover classification and coarse spatial resolution of GMAO meteorological data used as input for evapotranspiration calculus (He et al., 2019; Velpuri et al., 2013).

However, despite these discrepancies, the calibration results are promising, particularly considering the complex hydrological dynamics of the study area. They emphasize the SWAT model's potential as a valuable tool for simulating hydrological processes. Nevertheless, vigilance is reasonable towards underperforming areas to ensure a comprehensive and precise representation of the entire basin.

An analysis of the recent drought was conducted (2004-2022). As outlined in the Annual Global Climate Report released by the National Center for Environmental Information (National Center for Environmental Information, 2022), the ten warmest years within the past 143 years occurred after 2010. The analysis of temperature trends indeed over the 19-year period reveals a significant increase in mean temperature, which rose from approximately 13.8°C in 2004 to a peak of 14.7°C in 2022, indicating a warming trend. The coldest year during this period was 2005, while the warmest was 2022. Italy faced challenges caused by heightened temperatures and drought in recent years, particularly in 2017 and 2022, resulting in substantial difficulties in water management (SNPA, 2023, 2018). The SNPA report

underscored that 2022 marked Italy's warmest and driest year on record, leading in various repercussions, particularly in the agricultural territory. The agricultural sector attested drought-induced damages and diminished crop yields, notably in corn cultivation, as reported by (Coldiretti, 2023). The warming trend observed aligns also with global temperature trends. According to NOAA, Earth's temperature has increased at an average rate of 0.08°C per decade since 1880 (Lindsey and Dahlman, 2023). The Intergovernmental Panel on Climate Change (IPCC) also notes that human-induced greenhouse gas emissions have contributed to an increased frequency and/or intensity of certain weather and climate extremes since pre-industrial times, particularly in temperature extremes (Seneviratne et al., 2021).

As for the examination of precipitation across the observed period, there is a significant decline in overall precipitation, reaching its lowest values in 2022. This discovery aligns with the trends in global climate change, forecasting a rise in the frequency and intensity of droughts (Seneviratne et al., 2021). Additionally, there is a conspicuous increase in the frequency of rain-free days, which may signify prolonged drought periods. Although the overall decline in precipitation over the past 19 years is marginal, the rise in rain-free days suggest heightened intensity in individual rainfall events and an increase in frequency of extreme precipitation events (SNPA, 2019). These findings contribute into evolving weather dynamics, particularly concerning the reduction in precipitation and the increase in rain-free days.

The effect of these trends, both temperature and precipitation, is significant. The rise in global average surface temperature caused the diminishing snow cover and sea ice and intensifying heavy rainfall (National Center for Environmental Information, 2022). Diminished precipitation and a rise in rain-free days can result in water scarcity, adversely affecting crop yields and the availability of water for irrigation, just as it occurred in the year 2022. The effects of these trends can impact various sectors, including agriculture and water resources management. In the agriculture sector, indeed, these shifts may result in alterations to growing seasons and diminished yields (Agriculture and Agrifood Canada, 2020). Therefore, it is essential to comprehend these trends and formulate adaptive strategies to ensure sustainable agriculture and innovative solutions to ensure in the evolving climate conditions.

In the specific context of my research, the observed warming trend holds profound implications for water resources management. Elevated temperatures can increase evapotranspiration rates, potentially impacting water availability for irrigation. This

underscores the critical need to incorporate climate change projections into water resources planning and management efforts.

The SWAT model output indicate a slight increase in actual evapotranspiration over the past 15 years in the study area. This trend is coupled with the variability in the ratio of evapotranspiration to precipitation. The relationship between calculated SWAT actual evapotranspiration and precipitation is a key indicator of water deficits in the area, leading to drought conditions and affecting water availability for plants and other purposes (Glenn et al., 2015; Milly, 1994). In particular, the ratio between actual evapotranspiration and precipitation shows fluctuations with distinct peaks occurred in 2015, 2017, and 2022, where actual evapotranspiration exceeded precipitation, indicating that the soil loses more water than it receives from the atmosphere, indicating periods of heightened water demand by plants due to drought conditions. The prolonged absence of precipitation over time, indeed, coupled with increasing temperatures, drove heightened water evaporation from both soils and plants (Faranda et al., 2023), concluding in a reduction in available water resources.

These oscillations induce a more in-depth exploration of the factors influencing the water balance dynamics within the study area. These findings underscore the potential of the SWAT model as a valuable tool for simulating hydrological dynamics, even in ungauged areas.

Finally, the investigation on SWC showed a trajectory in SWC over the last 15 years. One of the most significant factors affecting SWC is the amount of precipitation and its distribution over the years (Horel et al., 2022), that as previously reported, are undergoing changes and this could lead to this trend of decrease. Notably, a 7% reduction in soil water content over a 15-year was noted, a notable discovery considering the potential consequences for crop productivity and yield (Datta et al., 2017). The decrease in soil water content can be attributed to alterations in precipitation, increasing temperatures, and shifts in land management practices (Gao et al., 2014; Mimeau et al., 2021; Zhou et al., 2021). The diminishing SWC carries profound implications for agricultural practices, with impact on soil characteristics, like reduced water absorption capacity. This deterioration in soil quality, moreover, disrupts natural ecosystem cycles, affecting land, air, and sea, thereby influencing human health and lifestyles (Gomiero, 2016). Therefore, the decreasing trend in SWC poses a significant challenge for agricultural practices, ecosystem health, and water resource management. It emphasizes the need to comprehend the contributing factors to this trend and explore potential solutions urgently.

The results of trend analyses, using the Mann-Kendall test, a non-parametric method for identifying trends in time series data, underscore the presence of trends in the environmental parameters analysed. The results revealed a significant upward trend particularly in the increase of rain-free days. This observed trend holds significant implications for agriculture and water management. As already highlight, the rise in rain-free days indicate period of droughts that may contribute to a decrease in SWC (Chen et al., 2023), a critical factor for crop growth. Consequently, this could lead to lower crop yields, alterations in growing seasons, and exacerbation of water scarcity issues, especially in regions already vulnerable to drought.

Despite its utility, it is important to recognize the limitations of the Mann-Kendall test. It requires a substantial amount of data for increased accuracy. Hence, although the Mann-Kendall test provides valuable insights into rain-free day trends, additional research over an extended period is crucial for a more comprehensive analysis. Further examinations are judged necessary, particularly considering the potential impacts on local water resources. Anyway, the trends already observable with such a short historical series and the significant rain-free days definitely indicate a trend of climate change. These results, indeed, align with global concerns regarding climate change (Lindsey and Dahlman, 2023) and emphasize the necessary for additional explorations into the original factors.

In this context, on-site soil moisture measurements have provided valuable insights into the interaction among soil water content, precipitation, and the influence of different land uses on this relationship. Within forested areas, soil water content primarily reflected the influence of precipitation, with peaks in soil water content corresponding to rainfall events. These natural peaks were similarly observed in both rice and corn fields, underscoring the impact of precipitation on soil moisture across various land uses. However, in the corn and rice fields, additional peaks in soil water content are present, indicating the presence of irrigation practices. The timing of the initial irrigation flooding in the rice fields was evident, indicating a substantial increase in soil water content. These findings emphasize the significance of considering distinct crop characteristics and irrigation schemes when delving into the dynamics of water availability across diverse agricultural settings. Additionally, they underscore the potential of soil moisture sensors as a valuable tool for monitoring and managing water resources within agricultural landscapes. Regarding the comparison of SWC simulated by SWAT and the SWC of the soil moisture sensors, we observed that the measured

and modelled quantities of irrigation water and the timing of irrigation differ significantly, in line with other studies e.g., (Qi et al., 2018). However, due to the calibration we obtained a high reliability of the simulated SWAT output revealing, that farmers might use more irrigation water than needed compared to the SWAT's auto-irrigation procedure values. This suggests possibilities for optimizing irrigation practices and contributing to sustainable water resource management.

In conclusion, the application of the SWAT model in this study allowed for a more comprehensive and accurate analysis of the hydrological dynamics in intensively used agricultural and irrigated areas, considering crucial factors such as irrigation and crop rotation. This underscores the importance and versatility of the SWAT model in hydrological research and management.

6 CONCLUSION AND OUTLOOK

In conclusion, this PhD study has provided essential information giving valuable insights into the hydrological dynamics of an intensively used agricultural and irrigated region in northern Lombardy over the last 15 years, using a SWAT model application.

The findings highlight the intricate interplay of numerous factors, from unique landscape features to the impact of land use and climatic changes, on the water cycle.

Using the MOD16 data for the calibration was fundamental for precisely interpreting the impacts of climate change, especially in regions dominated by crops like rice and corn. These crops demand substantial irrigation, particularly crucial in times of drought.

The calibration and validation results were satisfactory, and the study revealed trends in temperature, precipitation, and rain-free days underscoring the influence of climate change on the region's hydrology. This warming and precipitation variation trends could have profound implications for various sectors, particularly agriculture and water security. The decrease in soil water content and shifts in land use patterns pose significant challenges for agricultural practices, soil erosion and sustainability. It is crucial to further investigate these trends and their potential impacts, as well as to develop adaptive strategies to mitigate the adverse effects of this warming trend.

However, it is important to note that the study area is a lowland area with complex hydrology and a lack of natural water courses. These characteristics introduced limitations in the conventional use of SWAT, depend on discharge for model calibration and validation. Nevertheless, the absence of irrigation data and only use of the auto-irrigation function within SWAT could affect the accuracy of the results. Therefore, the model offers optimal information that can assist farmers in refining their irrigation strategies, but the inclusion of actual irrigation data could improve the study's accuracy regarding water consumption in irrigation, groundwater recharge, and soil water dynamics.

Additionally, the study encourages the exploration of innovative solutions for sustainable agriculture and water resource management in the challenge of changing climate conditions.

In summary, this study is as a fundamental step towards a more comprehensive understanding of the Ticino irrigation cascade's hydrological dynamics, for decision-making and sustainable practices in agriculture and water resource management.

In recent years, the management of water resources has encountered formidable challenges, ranging from the limited availability of resources and pollution to the escalating demands of a growing population, and, notably, the impacts of climate change. Future studies could examine deeper into the causes of observed trends, considering the complex interactions between climate, land use, and human activities. Long-term monitoring and modelling could provide a more precise understanding of the evolving hydrological dynamics, thereby facilitating the development of adaptive strategies. The calibrated model would be able to explore potential solutions for the management of water resources. One could observe, for instance, how different types and periods of irrigation can affect groundwater. In fact, some studies have examined how, flooding the rice fields even in winter, when water is available, it can help the recharge of the aquifer for the summer irrigation periods, when water is frequently scarce. Moreover, with the calibrated and validated model there is the possibility of formulating future scenarios following the Shared Socioeconomic Pathways (SSPs). This approach could offer a valuable perspective for exploring the various directions that the context studied could take, based on different socio-economic development scenarios. In particular, it is contemplating to utilize an intermediate approach, the SSP2 where emissions continue to increase through the end of the century, with a resulting warming of 3.8-4.2C. Furthermore, past land use variations (from 2007 to 2018) have been analysed as an initial indication of the dynamics of anticipated future changes. Various land use and agricultural management scenarios, involving different irrigation techniques and field processing/preparation methods while maintaining a constant climate, have been explored. With climate change and water scarcity, land use is set to change. With the current situation, it is possible that maize cultivation will increase, compared to rice, as it requires less water, but also may change techniques. There may be the implementation of innovative technologies for water saving, such as precision irrigation and rainwater collection techniques. These technologies could help reduce water consumption and improve water use efficiency and could be analysed with SWAT model.

Finally, in the context of the research of the CE4WE project, a comparison between the SWAT model and HEC-HMS for the same area of study is currently being conducted. This study aims to understand the specific limitations of each model, thus allowing a more complete analysis of the hydrological dynamics of the area of interest. The ultimate goal is to synergistically

integrate the strengths of both models, thus optimizing the overall predictive capability and allowing a more accurate assessment of hydrological impacts.

REFERENCES

- Abbaspour, K.C., Johnson, C.A., Genuchten, M.T. van, 2004. Estimating Uncertain Flow and Transport Parameters Using a Sequential Uncertainty Fitting Procedure. *Vadose Zo. J.* 3, 1340–1352. <https://doi.org/https://doi.org/10.2113/3.4.1340>
- Abbaspour, K.C., Rouholahnejad, E., Vaghefi, S., Srinivasan, R., Yang, H., Kløve, B., 2015. A continental-scale hydrology and water quality model for Europe: Calibration and uncertainty of a high-resolution large-scale SWAT model. *J. Hydrol.* 524, 733–752. <https://doi.org/10.1016/j.jhydrol.2015.03.027>
- Abbaspour, K.C., Vaghefi, S.A., Srinivasan, R., 2017. A guideline for successful calibration and uncertainty analysis for soil and water assessment: A review of papers from the 2016 international SWAT conference. *Water (Switzerland)* 10. <https://doi.org/10.3390/w10010006>
- Abbaspour, K. C., Vejdani, M., Haghghat, S., 2007. SWAT-CUP calibration and uncertainty programs for SWAT. *MODSIM07 - Land, Water Environ. Manag. Integr. Syst. Sustain. Proc.* 1596–1602.
- Abbaspour, Karim C., Yang, J., Maximov, I., Siber, R., Bogner, K., Mieleitner, J., Zobrist, J., Srinivasan, R., 2007. Modelling hydrology and water quality in the pre-alpine/alpine Thur watershed using SWAT. *J. Hydrol.* 333, 413–430. <https://doi.org/10.1016/j.jhydrol.2006.09.014>
- Abbaszadeh, M., Bazrafshan, O., Mahdavi, R., Sardooi, E.R., Jamshidi, S., 2023. Modeling Future Hydrological Characteristics Based on Land Use/Land Cover and Climate Changes Using the SWAT Model. *Water Resour. Manag.* 37, 4177–4194. <https://doi.org/10.1007/s11269-023-03545-6>
- Abiodun, O.O., Guan, H., Post, V.E.A., Batelaan, O., 2018. Comparison of MODIS and SWAT evapotranspiration over a complex terrain at different spatial scales. *Hydrol. Earth Syst. Sci.* 22, 2775–2794. <https://doi.org/10.5194/hess-22-2775-2018>
- Aboelnour, M., Gitau, M.W., Engel, B.A., 2020. A comparison of streamflow and baseflow responses to land-use change and the variation in climate parameters using SWAT. *Water (Switzerland)* 12. <https://doi.org/10.3390/w12010191>
- Agriculture and Agrifood Canada, 2020. Climate change impacts on agriculture [WWW Document]. URL <https://agriculture.canada.ca/en/environment/climate-change/climate-scenarios-agriculture> (accessed 1.7.24).
- Amoozegar, A., 1989. A Compact Constant-Head Permeameter for Measuring Saturated Hydraulic Conductivity of the Vadose Zone. *Soil Sci. Soc. Am. J.* 53, 1356–1361. <https://doi.org/https://doi.org/10.2136/sssaj1989.03615995005300050009x>
- Arnold, J.C., Moriasi, D.N., Gassman, P.W., Abbaspour, K.C., White, M.J., Srinivasan, R., Santhi, C., Harmel, R.D., Griensven, A. Van, Van Liew, M.W., Kannan, N., Jha, M.K., 2012. SWAT: MODEL USE, CALIBRATION, AND VALIDATION. *Trans. ASABE* 55, 1491–1508.
- Arnold, J.G., Kiniry, J.R., Srinivasan, R., Williams, J.R., Haney, E.B., Neitsch, S.L., 2012. Input/Output Documentation Soil & Water Assessment Tool 1–650.
- Arnold, Jeffrey G., Srinivasan, R., Muttiah, R.S., Williams, J., 1998. LARGE AREA

HYDROLOGIC MODELING AND ASSESSMENT PART I : MODEL DEVELOPMENT '.
J. Am. Water Resour. Assoc. 34, 73–89.

- Arnold, J.G., Srinivasan, R., Muttiah, R.S., Williams, J.R., 1998. Large area hydrologic modeling and assessment Part I : Model Development' basin scale model called SWAT (Soil and Water speed and storage , advanced software debugging policy to meet the needs , and the management to the tank model 34, 73–89.
- Azar, R., Villa, P., Stroppiana, D., Crema, A., Boschetti, M., Brivio, P.A., 2016. Assessing in-season crop classification performance using satellite data: A test case in Northern Italy. *Eur. J. Remote Sens.* 49, 361–380. <https://doi.org/10.5721/EuJRS20164920>
- Baker, E.A., Cappato, A., Todeschini, S., Tamellini, L., Sangalli, G., Reali, A., Manenti, S., 2022. Combining the Morris method and multiple error metrics to assess aquifer characteristics and recharge in the lower Ticino Basin, in Italy. *J. Hydrol.* 614, 128536. <https://doi.org/10.1016/j.jhydrol.2022.128536>
- Balestrini, R., Delconte, C.A., Sacchi, E., Buffagni, A., 2021. Groundwater-dependent ecosystems as transfer vectors of nitrogen from the aquifer to surface waters in agricultural basins: The fontanili of the Po Plain (Italy). *Sci. Total Environ.* 753, 141995. <https://doi.org/10.1016/j.scitotenv.2020.141995>
- Becker, R., Koppa, A., Schulz, S., Usman, M., aus der Beek, T., Schüth, C., 2019. Spatially distributed model calibration of a highly managed hydrological system using remote sensing-derived ET data. *J. Hydrol.* 577, 123944. <https://doi.org/10.1016/j.jhydrol.2019.123944>
- Bernini, A., Becker, R., Adeniyi, O.D., Pilla, G., Sadeghi, S.H., Maerker, M., 2023. Hydrological Implications of Recent Droughts (2004 – 2022): A SWAT-Based Study in an Ancient Lowland Irrigation Area in Lombardy , Northern Italy.
- Beven, K.J., Binley, A., 1992. The Future of Distributed Models: Model Calibration and Uncertainty Prediction. *Hydrol. Process.* 6, 279–298.
- Bian, G., Zhang, J., Chen, J., Song, M., He, R., Liu, C., Liu, Y., Bao, Z., Lin, Q., Wang, G., 2021. Projecting Hydrological Responses to Climate Change Using CMIP6 Climate Scenarios for the Upper Huai River Basin, China. *Front. Environ. Sci.* 9, 1–14. <https://doi.org/10.3389/fenvs.2021.759547>
- Bove, M., 2021. Allarme acqua, quali sono le cause? Il risicoltore 2–3.
- Brauer, C.C., Teuling, A.J., Torfs, P.J.J.F., Uijlenhoet, R., 2013. Investigating storage-discharge relations in a lowland catchment using hydrograph fitting, recession analysis, and soil moisture data. *Water Resour. Res.* 49, 4257–4264. <https://doi.org/10.1002/wrcr.20320>
- Brown, S., Lo, K., Lys, T., 1999. Use of R2 in accounting research: Measuring changes in value relevance over the last four decades. *J. Account. Econ.* 28, 83–115. [https://doi.org/10.1016/S0165-4101\(99\)00023-3](https://doi.org/10.1016/S0165-4101(99)00023-3)
- Bux, C., Lombardi, M., Varese, E., Amicarelli, V., 2022. Economic and Environmental Assessment of Conventional versus Organic Durum Wheat Production in Southern Italy. *Sustain.* 14, 1–14. <https://doi.org/10.3390/su14159143>
- Certini, G., Ugolini, F.C., 2021. Basi di Pedologia. Cos'è il suolo, come si forma, come va descritto

e classificato., 2nd ed.

- Chen, Y., Leng, Y.-N., Zhu, F.-Y., Li, S.-E., Song, T., Zhang, J., 2023. Water-saving techniques: physiological responses and regulatory mechanisms of crops. *Adv. Biotechnol.* 1, 1–24. <https://doi.org/10.1007/s44307-023-00003-7>
- Cheng, C., Zhang, F., Shi, J., Kung, H. Te, 2022. What is the relationship between land use and surface water quality? A review and prospects from remote sensing perspective. *Environ. Sci. Pollut. Res.* 29, 56887–56907. <https://doi.org/10.1007/s11356-022-21348-x>
- Coldiretti, 2023. Siccità, 250mila aziende a rischio crack. [WWW Document]. URL [https://www.coldiretti.it/economia/siccita-250mila-aziende-a-rischio-crack#:~:text=Con le piogge praticamente dimezzate,Sud del Paese%2C secondo Coldiretti. \(accessed 10.14.23\)](https://www.coldiretti.it/economia/siccita-250mila-aziende-a-rischio-crack#:~:text=Con le piogge praticamente dimezzate,Sud del Paese%2C secondo Coldiretti. (accessed 10.14.23)).
- Coldiretti, 2022. Siccità: devasta il raccolto di riso italiano (-30%) [WWW Document]. URL [https://www.coldiretti.it/economia/siccita-devasta-il-raccolto-di-riso-italiano-30 \(accessed 1.4.24\)](https://www.coldiretti.it/economia/siccita-devasta-il-raccolto-di-riso-italiano-30 (accessed 1.4.24)).
- Crevaschi, M., Rodolfi, G., 1991. Il suolo.
- Crespi, A., Brunetti, M., Ranzi, R., Tomirotti, M., Maugeri, M., 2021. A multi-century meteorological hydrological analysis for the Adda river basin (Central Alps). Part I: Gridded monthly precipitation (1800–2016) records. *Int. J. Climatol.* 41, 162–180. <https://doi.org/10.1002/joc.6614>
- Cuceloglu, G., Abbaspour, K.C., Ozturk, I., 2017. Assessing the water-resources potential of Istanbul by using a soil and water assessment tool (SWAT) hydrological model. *Water (Switzerland)* 9. <https://doi.org/10.3390/w9100814>
- Datta, S., Taghvaeian, S., Stivers, J., 2017. Understanding Soil Water Content and Thresholds for Irrigation Management Managing Irrigations Based on Soil Water Content Managing irrigations based on VWC data Managing Irrigations based on SMP data. *Oklahoma Coop. Ext. Serv. BAE-1537-1-BAE-1537-7*.
- De Luca, D.A., Destefanis, E., Forno, M.G., Lasagna, M., Masciocco, L., 2013. The genesis and the hydrogeological features of the Turin Po Plain fontanili, typical lowland springs in Northern Italy. *Bull Eng Geol Env.* <https://doi.org/10.1007/s10064-013-0527-y>
- Devi, G.K., Ganasri, B.P., Dwarakish, G.S., 2015. A Review on Hydrological Models. *Aquat. Procedia* 4, 1001–1007. <https://doi.org/10.1016/j.aqpro.2015.02.126>
- Donmez, C., Sari, O., Berberoglu, S., Cilek, A., Satir, O., Volk, M., 2020. Improving the applicability of the swat model to simulate flow and nitrate dynamics in a flat data-scarce agricultural region in the mediterranean. *Water (Switzerland)* 12, 1–24. <https://doi.org/10.3390/w12123479>
- Douglas-Mankin, K.R., Srinivasan, R., Arnold, J.G., 2010. Soil and water assessment tool (SWAT) model: Current developments and applications. *Trans. ASABE* 53, 1423–1431. <https://doi.org/10.13031/2013.34915>
- Ente Risi, 2022. Riso Italiano [WWW Document]. URL [https://www.risoitaliano.eu/ci-siamo-giocati-la-lombardia/ \(accessed 10.9.23\)](https://www.risoitaliano.eu/ci-siamo-giocati-la-lombardia/ (accessed 10.9.23)).

- ERSAF “Ente Regionale per i Servizi alla Agricoltura e alle Foreste - Regione Lombardia, 2019. Uso del suolo in Regione Lombardia. Atlante descrittivo.
- Faranda, D., Pascale, S., Bulut, B., 2023. Persistent anticyclonic conditions and climate change exacerbated the exceptional 2022 European-Mediterranean drought. *Environ. Res. Lett.* 18. <https://doi.org/10.1088/1748-9326/acbc37>
- Ferreira, A. do N., de Almeida, A., Koide, S., Minoti, R.T., de Siqueira, M.B.B., 2021. Evaluation of evapotranspiration in Brazilian cerrado biome simulated with the SWAT model. *Water (Switzerland)* 13, 1–14. <https://doi.org/10.3390/w13152037>
- Flugel, W.A., 1995. Delineating hydrological response units by geographical information system analyses for regional hydrological modelling using PRMS/MMS in the drainage basin of the River Bröl, Germany. *Hydrol. Process.* 9, 423–436.
- FORM RICHIESTA DATI [WWW Document], n.d. URL <https://www.arpalombardia.it/temi-ambientali/meteo-e-clima/form-richiesta-dati/>
- Gao, X., Wu, P., Zhao, X., Wang, J., Shi, Y., 2014. Effects of land use on soil moisture variations in a semi-arid catchment: Implications for land and agricultural water management. *L. Degrad. Dev.* 25, 163–172. <https://doi.org/10.1002/ldr.1156>
- Gassman, P.W., Sadeghi, A.M., Srinivasan, R., 2014. Applications of the SWAT Model Special Section: Overview and Insights. *J. Environmental Qual.* 43, 1–8.
- Giuliana, V., Lucia, M., Marco, R., Simone, V., 2022. Environmental life cycle assessment of rice production in northern Italy: a case study from Vercelli. *Int. J. Life Cycle Assess.* <https://doi.org/10.1007/s11367-022-02109-x>
- Glenn, E.P., Scott, R.L., Nguyen, U., Nagler, P.L., 2015. Wide-area ratios of evapotranspiration to precipitation in monsoon-dependent semiarid vegetation communities. *J. Arid Environ.* 117, 84–95. <https://doi.org/10.1016/j.jaridenv.2015.02.010>
- Gomiero, T., 2016. Soil degradation, land scarcity and food security: Reviewing a complex challenge. *Sustain.* 8, 1–41. <https://doi.org/10.3390/su8030281>
- He, M., Kimball, J.S., Yi, Y., Running, S.W., Guan, K., Moreno, A., Wu, X., Maneta, M., 2019. Satellite data-driven modeling of field scale evapotranspiration in croplands using the MOD16 algorithm framework. *Remote Sens. Environ.* 230, 111201. <https://doi.org/10.1016/j.rse.2019.05.020>
- Henry, M., 1945. *Nonparametric Tests Against Trend* Author (s): Henry B . Mann Published by : The Econometric Society Stable URL : <https://www.jstor.org/stable/1907187> REFERENCES Linked references are available on JSTOR for this article : You may need to log in to JSTOR. *Econometrica* 13, 245–259.
- Horel, Á., Zsigmond, T., Farkas, C., Gelybó, G., Tóth, E., Kern, A., Bakacsi, Z., 2022. Climate Change Alters Soil Water Dynamics under Different Land Use Types. *Sustain.* 14. <https://doi.org/10.3390/su14073908>
- IUSS Working Group WRB, 2015. World reference base for soil resources 2014, update 2015. International soil classification system for naming soils and creating legends for soil maps, World Soil. ed. Rome.

- Janjić, J., Tadić, L., 2023. Fields of Application of SWAT Hydrological Model—A Review. *Earth (Switzerland)* 4, 331–344. <https://doi.org/10.3390/earth4020018>
- Jayakrishnan, R., Srinivasan, R., Santhi, C., Arnold, J.G., 2005. Advances in the application of the SWAT model for water resources management. *Hydrol. Process.* 19, 749–762. <https://doi.org/10.1002/hyp.5624>
- Kendall, A.M.G., 1955. Further Contributions to the Theory of Paired Comparisons Published by : International Biometric Society Stable URL : <https://www.jstor.org/stable/3001479>
REFERENCES Linked references are available on JSTOR for this article : [reference # references _ tab 11](#), 43–62.
- Kottek, M., Grieser, J., Beck, C., Rudolf, B., Rubel, F., 2006. World map of the Köppen-Geiger climate classification updated. *Meteorol. Zeitschrift* 15, 259–263. <https://doi.org/10.1127/0941-2948/2006/0130>
- Kour, R., Patel, N., Krishna, A.P., 2016. Climate and hydrological models to assess the impact of climate change on hydrological regime: a review. *Arab. J. Geosci.* 9. <https://doi.org/10.1007/s12517-016-2561-0>
- Krysanova, V., Srinivasan, R., 2015. Assessment of climate and land use change impacts with SWAT. *Reg. Environ. Chang.* 15, 431–434. <https://doi.org/10.1007/s10113-014-0742-5>
- Lam, Q.D., Schmalz, B., Fohrer, N., 2010. Modelling point and diffuse source pollution of nitrate in a rural lowland catchment using the SWAT model. *Agric. Water Manag.* 97, 317–325. <https://doi.org/10.1016/j.agwat.2009.10.004>
- Lasagna, M., Mancini, S., De Luca, D.A., 2020. Groundwater hydrodynamic behaviours based on water table levels to identify natural and anthropic controlling factors in the Piedmont Plain (Italy). *Sci. Total Environ.* 716, 137051. <https://doi.org/10.1016/j.scitotenv.2020.137051>
- Lin, Y.P., Hong, N.M., Wu, P.J., Lin, C.J., 2007. Modeling and assessing land-use and hydrological processes to future land-use and climate change scenarios in watershed land-use planning. *Environ. Geol.* 53, 623–634. <https://doi.org/10.1007/s00254-007-0677-y>
- Lindsey, R., Dahlman, L., 2023. Climate Change: Global Temperature [WWW Document]. Climate.gov. URL <https://www.climate.gov/news-features/understanding-climate/climate-change-global-temperature#:~:text=Highlights,2° F in total> (accessed 9.30.23).
- Liu, X., Li, Z., Pedram, A., 2021. Editorial: Understanding Hydrological Extremes and Their Impact in a Changing Climate: Observations, Modeling and Attribution. *Front. Environ. Sci.* 8. <https://doi.org/https://doi.org/10.3389/feart.2020.632186>
- Maier, N., Dietrich, J., 2016. Using SWAT for Strategic Planning of Basin Scale Irrigation Control Policies: a Case Study from a Humid Region in Northern Germany. *Water Resour. Manag.* 30, 3285–3298. <https://doi.org/10.1007/s11269-016-1348-0>
- Maja, M.M., Ayano, S.F., 2021. The Impact of Population Growth on Natural Resources and Farmers' Capacity to Adapt to Climate Change in Low-Income Countries. *Earth Syst. Environ.* 5, 271–283. <https://doi.org/10.1007/s41748-021-00209-6>
- Masseroni, D., Ricart, S., de Cartagena, F.R., Monserrat, J., Gonçalves, J.M., de Lima, I., Facchi, A., Sali, G., Gandolfi, C., 2017. Prospects for improving gravity-fed surface irrigation systems

- in mediterranean european contexts. *Water (Switzerland)* 9. <https://doi.org/10.3390/w9010020>
- McLeod, A.I., 2005. Kendall Rank Correlation and Mann-Kendall Trend Test. R Package “Kendall”. [WWW Document]. URL <https://cran.r-project.org/web/packages/Kendall/> (accessed 11.27.23).
- Milly, P.C.D., 1994. Climate, soil water storage, and the average annual water balance. *Water Resour. Res.* 30, 2143–2156. <https://doi.org/10.1029/94WR00586>
- Mimeau, L., Tramblay, Y., Brocca, L., Massari, C., Camici, S., Finaud-Guyot, P., 2021. Modeling the response of soil moisture to climate variability in the Mediterranean region. *Hydrol. Earth Syst. Sci.* 25, 653–669. <https://doi.org/10.5194/hess-25-653-2021>
- Moraca, S., 2022. Protecting Italian rice from a warming climate [WWW Document]. *Nat. Italy*. [https://doi.org/doi: https://doi.org/10.1038/d43978-022-00159-1](https://doi.org/doi:https://doi.org/10.1038/d43978-022-00159-1)
- Mu, Q., Faith Ann, H., Zhao, M., Steven, W.R., 2007. Development of a global evapotranspiration algorithm based on MODIS and global meteorology data. *Remote Sens. Environ.* 106, 285–304. <https://doi.org/10.1016/j.rse.2006.07.007>
- Mu, Q., Zhao, M., Running, S.W., 2011. Improvements to a MODIS global terrestrial evapotranspiration algorithm. *Remote Sens. Environ.* 115, 1781–1800. <https://doi.org/10.1016/j.rse.2011.02.019>
- Narsimlu, B., Gosain, A.K., Chahar, B.R., 2013. Assessment of Future Climate Change Impacts on Water Resources of Upper Sind River Basin, India Using SWAT Model. *Water Resour. Manag.* 27, 3647–3662. <https://doi.org/10.1007/s11269-013-0371-7>
- Nasa, n.d. MODIS [WWW Document]. URL <https://modis.gsfc.nasa.gov/data/dataproduct/mod16.php> (accessed 12.27.23).
- National Center for Environmental Information, 2022. Annual 2022 Global Climate Report [WWW Document]. URL <https://www.ncei.noaa.gov/access/monitoring/monthly-report/global/202213> (accessed 10.10.23).
- Nawaz, M.F., Bourrié, G., Trolard, F., 2013. Soil compaction impact and modelling. A review. *Agron. Sustain. Dev.* 33, 291–309. <https://doi.org/10.1007/s13593-011-0071-8>
- Neitsch, S., Arnold, J., Kiniry, J., Williams, J., 2011. Soil & Water Assessment Tool Theoretical Documentation Version 2009, Texas Water Resources Institute. <https://doi.org/10.1016/j.scitotenv.2015.11.063>
- Nkwasa, A., Chawanda, C.J., Jägermeyr, J., Van Griensven, A., 2022. Improved representation of agricultural land use and crop management for large-scale hydrological impact simulation in Africa using SWAT+. *Hydrol. Earth Syst. Sci.* 26, 71–89. <https://doi.org/10.5194/hess-26-71-2022>
- Odusanya, A.E., Mehdi, B., Schürz, C., Oke, A.O., Awokola, O.S., Awomeso, J.A., Adejuwon, J.O., Schulz, K., 2019. Multi-site calibration and validation of SWAT with satellite-based evapotranspiration in a data-sparse catchment in southwestern Nigeria. *Hydrol. Earth Syst. Sci.* 23, 1113–1144. <https://doi.org/10.5194/hess-23-1113-2019>
- Parajuli, P.B., Jayakody, P., Ouyang, Y., 2018. Evaluation of Using Remote Sensing

- Evapotranspiration Data in SWAT. *Water Resour. Manag.* 32, 985–996.
<https://doi.org/10.1007/s11269-017-1850-z>
- Parajuli, P.B., Risal, A., Ouyang, Y., Thompson, A., 2022. Comparison of SWAT and MODIS Evapotranspiration Data for Multiple Timescales. *Hydrology* 9, 103.
<https://doi.org/10.3390/hydrology9060103>
- Perego, A., Sanna, M., Giussani, A., Chiadini, M.E., Fumagalli, M., Pilu, S.R., Bindi, M., Moriando, M., Acutis, M., 2014. Designing a high-yielding maize ideotype for a changing climate in Lombardy plain (northern Italy). *Sci. Total Environ.* 499, 497–509.
<https://doi.org/10.1016/j.scitotenv.2014.05.092>
- Pereira, L.S., 2017. Water, Agriculture and Food: Challenges and Issues. *Water Resour. Manag.* 31, 2985–2999. <https://doi.org/10.1007/s11269-017-1664-z>
- Piñeiro, G., Perelman, S., Guerschman, J.P., Paruelo, J.M., 2008. How to evaluate models: Observed vs. predicted or predicted vs. observed? *Ecol. Modell.* 216, 316–322.
<https://doi.org/10.1016/j.ecolmodel.2008.05.006>
- Qi, J., Zhang, X., McCarty, G.W., Sadeghi, A.M., Cosh, M.H., Zeng, X., Gao, F., Daughtry, C.S.T., Huang, C., Lang, M.W., Arnold, J.G., 2018. Assessing the performance of a physically-based soil moisture module integrated within the Soil and Water Assessment Tool. *Environ. Model. Softw.* 109, 329–341. <https://doi.org/10.1016/j.envsoft.2018.08.024>
- Qiao, L., Will, R., Wagner, K., Zhang, T., Zou, C., 2022. Improvement of evapotranspiration estimates for grasslands in the southern Great Plains: Comparing a biophysical model (SWAT) and remote sensing (MODIS). *J. Hydrol. Reg. Stud.* 44.
<https://doi.org/10.1016/j.ejrh.2022.101275>
- Rajib, A., Evenson, G.R., Golden, H.E., Lane, C.R., 2018. Hydrologic model predictability improves with spatially explicit calibration using remotely sensed evapotranspiration and biophysical parameters. *J. Hydrol.* 567, 668–683. <https://doi.org/10.1016/j.jhydrol.2018.10.024>
- Regione Lombardia, 2013. Basi informative dei suoli. Geoportale della Lombardia. [WWW Document], n.d. URL https://www.geoportale.regione.lombardia.it/metadati?p_p_id=detailSheetMetadata_WAR_gptmetadataportlet&p_p_lifecycle=0&p_p_state=normal&p_p_mode=view&_detailSheetMetadata_WAR_gptmetadataportlet_uuid=%257BA7138B8A-9025-4802-82BC-52267B60A3D7%257D# (accessed 12.18.23).
- Ritchie, J.T., 1972. Model for predicting evaporation from a row crop with incomplete cover. *Water Resour* 8, 1204-1213.
- Running, S.W., Mu, Q., Zhao, M., Moreno, A., 2019. MODIS Global Terrestrial Evapotranspiration (ET) Product (NASA MOD16A2/A3) Algorithm Theoretical Basis Document Collection 6 1–40.
- Saxton, K.E., n.d. SPAW - Soil - Plant -Air - Water Field & Pond Hydrology.
- Schuol, J., Abbaspour, K.C., Srinivasan, R., Yang, H., 2008. Estimation of freshwater availability in the West African sub-continent using the SWAT hydrologic model. *J. Hydrol.* 352, 30–49.
<https://doi.org/10.1016/j.jhydrol.2007.12.025>





- Sconfiatti, R., Pesci, I., Paganelli, D., 2018. Terrace springs: Habitat haven for macrobenthic fauna in the lower plain of the River Ticino (Lombardy, Northern Italy). *Nat. Hist. Sci.* 5, 19–26. <https://doi.org/10.4081/nhs.2018.376>
- Seneviratne, S.I., X. Zhang, M., Adnan, W., Badi, C., Dereczynski, A., Di Luca, S., Ghosh, I., Iskandar, J., Kossin, S., Lewis, F. Otto, I., Pinto, M., Satoh, S.M., Vicente-Serrano, Wehner, M., Zhou, B., 2021. Weather and Climate Extreme Events in a Changing Climate. In *Climate Change 2021: The Physical Science Basis. Contribution of Working Group I to the Sixth Assessment Report of the Intergovernmental Panel on Climate Change 1513–1766*. <https://doi.org/https://doi.org/10.1017/9781009157896.013>
- Shaheb, M.R., Venkatesh, R., Shearer, S.A., 2021. A Review on the Effect of Soil Compaction and its Management for Sustainable Crop Production. *J. Biosyst. Eng.* 46, 417–439. <https://doi.org/10.1007/s42853-021-00117-7>
- SNPA, 2023. IL CLIMA IN ITALIA NEL 2022.
- SNPA, 2019. Cambiamento climatico: in Lombardia, oltre un secolo di dati dall’osservatorio Milano Brera [WWW Document]. URL <https://www.snpambiente.it/2019/03/13/cambiamento-climatico-in-lombardia-oltre-un-secolo-di-dati-a-milano-brera/> (accessed 10.10.23).
- SNPA, 2018. SNPA presenta il Rapporto “GLI INDICATORI DEL CLIMA IN ITALIA NEL 2017”.
- Sun, Y., Bao, W., Valk, K., Brauer, C.C., Sumihar, J., Weerts, A.H., 2020. Improving Forecast Skill of Lowland Hydrological Models Using Ensemble Kalman Filter and Unscented Kalman Filter. *Water Resour. Res.* 56. <https://doi.org/10.1029/2020WR027468>
- Tsuchiya, R., Kato, T., Jeong, J., Arnold, J.G., 2018. Development of SWAT-paddy for simulating lowland paddy fields. *Sustain.* 10. <https://doi.org/10.3390/su10093246>
- Velpuri, N.M., Senay, G.B., Singh, R.K., Bohms, S., Verdin, J.P., 2013. A comprehensive evaluation of two MODIS evapotranspiration products over the conterminous United States: Using point and gridded FLUXNET and water balance ET. *Remote Sens. Environ.* 139, 35–49. <https://doi.org/10.1016/j.rse.2013.07.013>
- Waseem, M., Kachholz, F., Klehr, W., Tränckner, J., 2020. Suitability of a coupled hydrologic and hydraulic model to simulate surfacewater and groundwater hydrology in a typical north-eastern germany lowland catchment. *Appl. Sci.* 10. <https://doi.org/10.3390/app10041281>
- Wu, D., Cui, Y., Luo, Y., 2019. Irrigation efficiency and water-saving potential considering reuse of return flow. *Agric. Water Manag.* 221, 519–527. <https://doi.org/10.1016/j.agwat.2019.05.021>
- Zhou, T., Han, C., Qiao, L., Ren, C., Wen, T., Zhao, C., 2021. Seasonal dynamics of soil water content in the typical vegetation and its response to precipitation in a semi-arid area of Chinese Loess Plateau. *J. Arid Land* 13, 1015–1025. <https://doi.org/10.1007/s40333-021-0021-5>

APPENDIX

-Bernini et al., 2023

Article

Hydrological Implications of Recent Droughts (2004–2022): A SWAT-Based Study in an Ancient Lowland Irrigation Area in Lombardy, Northern Italy

Alice Bernini ¹, Rike Becker ², Odunayo David Adeniyi ¹, Giorgio Pilla ¹, Seyed Hamidreza Sadeghi ^{1,3} and Michael Maerker ^{1,4,*}

¹ Department of Earth and Environmental Sciences, Università degli Studi di Pavia, Via Ferrata 1, 27100 Pavia, Italy; alice.bernini01@universitadipavia.it (A.B.); odunayodavid.adeniyi01@universitadipavia.it (O.D.A.); giorgio.pilla@unipv.it (G.P.); sadeghi@modares.ac.ir (S.H.S.)

² Department of Agroecosystem Analysis and Modelling, Faculty of Organic Agricultural Sciences, University of Kassel, 37213 Witzenhausen, Germany; rike.becker@uni-kassel.de

³ Department of Watershed Management Engineering, Faculty of Natural Resources, Tarbiat Modares University, Noor 46417-76489, Iran

⁴ Department of Landscape Functioning, Leibniz Centre for Agricultural Landscape Research, 15374 Müncheberg, Germany

* Correspondence: michael.maerker@zalf.de or michael.maerker@unipv.it; Tel.: +49-176-6266-3563

Abstract: This study examines the hydrological dynamics of the Ticino irrigation cascade in northern Italy from 2004 to 2022. The region, which is shaped by human activity, is characterized by its flat topography and complex management of water resources, featuring a unique historic irrigation cascade. Utilizing the Soil and Water Assessment Tool (SWAT), we investigated the water availability during recent severe droughts in this complex agricultural environment, which lacks natural drainage. This area faces risks due to increasing temperatures and increased rainless days. Therefore, understanding the soil water dynamics is essential for maintaining the system's sustainability. Calibrating and validating the SWAT model with runoff data was challenging due to the absence of natural drainage. Thus, we utilized MOD16 evapotranspiration (AET) data for calibration. Generally, the calibration and validation of the SWAT model yielded satisfactory results in terms of the Kling–Gupta efficiency (KGE). Despite some discrepancies, which were mainly related to the data sources and resolution, the calibrated model's outputs showed increased actual evapotranspiration that was influenced by climate and irrigation, leading to water deficits and droughts. The soil water content (SWC) decreased by 7% over 15 years, impacting crop productivity and environmental sustainability. This also resulted in rising water stress for crops and the ecosystem in general, highlighting the direct impact of adverse climate conditions on soil hydrology and agriculture. Our research contributes to the understanding of soil–water dynamics, as it specifically addresses recent droughts in the Lombardy lowlands.

Keywords: agricultural water; drought management; hydrological modeling; water shortage; evapotranspiration; climate change adaption



Citation: Bernini, A.; Becker, R.; Adeniyi, O.D.; Pilla, G.; Sadeghi, S.H.; Maerker, M. Hydrological Implications of Recent Droughts (2004–2022): A SWAT-Based Study in an Ancient Lowland Irrigation Area in Lombardy, Northern Italy. *Sustainability* **2023**, *15*, 16771. <https://doi.org/10.3390/su152416771>

Academic Editors: Mir Jafar Sadegh Safari and Gokmen Tayfar

Received: 31 October 2023
Revised: 29 November 2023
Accepted: 11 December 2023
Published: 12 December 2023



Copyright: © 2023 by the authors. Licensee MDPI, Basel, Switzerland. This article is an open access article distributed under the terms and conditions of the Creative Commons Attribution (CC BY) license (<https://creativecommons.org/licenses/by/4.0/>).

1. Introduction

It is widely accepted that global climate change can cause significant changes in hydrological processes due to the higher temperatures, more frequent and intense heatwaves, and changes in precipitation regimes [1–3]. In particular, droughts have been recognized as natural phenomena that can significantly impact ecosystems, agriculture, and water resources, posing substantial challenges to societies worldwide [4–6].

Italy has experienced several droughts in recent years, with drought episodes that have become stronger in frequency and length since 2001. In Northern Italy, 2022 was the warmest year since 1800 according to the Institute of Atmospheric and Climate Sciences

(ISAC) of the National Research Council (CNR) [7]. Anomalies were found in February and March with 88% and 55% less precipitation, respectively, and in the summer of 2022—especially in July—with 65% less precipitation. Indeed, a significant lack of rain was observed across most of the European continent during 2022 [8]. This led to significant water shortages, affecting agricultural production and, thus, impacting the local and regional economies [9]. In this context, irrigation plays a crucial role in supporting local agricultural production, as it ensures that crops have adequate water supply in periods of droughts. Without irrigation, crops may experience water stress, resulting in reduced growth, adverse impacts on plant health [10], and lower yields in terms of both quantity and quality. Furthermore, in our study area, irrigation is fundamental for groundwater recharge. Particularly, the flooding of rice fields during winter alleviates water scarcity in spring and early summer by recharging aquifers. Essentially, irrigation serves as a fundamental tool for managing agricultural production during periods of drought. It helps to mitigate the effects of water scarcity, promotes crop productivity, and keeps the whole system balanced. The region of Lombardy in Northern Italy, which is renowned for its ancient lowland irrigation areas characterized by the presence of springs [11,12], has historically been a vital agricultural region due to its rich soils and favorable water supply. The area covers the main terraces and escarpments of the Ticino River. In the past, irrigation water was diverted from the Ticino River through irrigation channels and infiltrated as irrigation water on the uppermost terrace level, re-emerging in the form of springs at the base of the fluvial terrace escarpments [13]. Over centuries, this represented a sustainable water-use cycle that was quite unique in the world and allowed for intensive rice cultivation. However, this traditional irrigation system is now facing new challenges due to changing climate patterns. The region experienced significant droughts in the last few years that affected the water cycle and groundwater levels, e.g., through variations in recharge rates [14]. Therefore, traditional irrigation schemes based on water reuse, which have operated in the region since the eleventh century [15], might be seriously affected. Specific measures and strategies for water scarcity situations should be developed to prevent and mitigate the effects of any severe reductions in water resource availability and to protect agricultural production as much as possible.

In this context, our study aims to examine the complex hydrological dynamics of the area using the Soil and Water Assessment Tool (SWAT), a physically based and complex hydrological model designed to operate at the basin scale [16,17]. The SWAT is widely used to model runoff, non-point source pollution, and other intricate hydrological, ecological, and environmental processes under changing land uses and climate conditions [18–24]. We used the SWAT to investigate the occurrence and severity of last year's droughts in Lombardy's ancient lowland irrigation area. Despite the existence of several hydrological models that were used to study droughts in recent years, such as the DTVM, GWAVA, SWAT, and HEC-HMS [25], their application in lowland areas is still challenging [26]. Lowlands are characterized by a flat topography and low hydraulic gradients [27]. Furthermore, these areas are often heavily modified in terms of drainage systems due to human activity, such as intensive agriculture. These characteristics make it challenging to delineate first-order watersheds [28] and to assess their hydrological dynamics. Moreover, it is difficult to obtain adequate information about the quantity and quality of irrigation water. Irrigation schemes are highly variable, as they depend on the actual crop water availability and the agricultural management strategies. The dense network of irrigation channels is managed at different administrative levels, ranging from the local field scale to large consortia (consorzio di bonifica Est Ticino Villoresi) that manage general water resources. Thus, a detailed assessment of the irrigation schemes is challenging due to the various levels of administrative competences, as well as missing monitoring and/or documentation activity.

However, in this intensely used agricultural lowland area, calibrating and validating a hydrological model in a traditional way using discharge data is difficult or impossible due to the lack of natural drainage and information on the water resources used for

irrigation [29]. Therefore, we propose alternative procedures for calibrating and validating the model. As shown by Becker et al., Odusanya et al., and Shah et al. [29–31], model calibration can also be conducted using evapotranspiration data. Various products that provide evapotranspiration information based on remotely sensed data are freely available. Satellite-based products, such as the Global Evaporation data (MOD16), which are based on measurements from the Moderate-Resolution Imaging Spectroradiometer (MODIS), were successfully used to calibrate spatially distributed hydrological models [30,32–34]. However, as stated by Becker et al. [29], the calibration of a hydrological model in a flat, complex agricultural environment is quite challenging, particularly when human activities such as irrigation interfere with the natural system or there is a general lack of observed information in terms of their spatiotemporal scales [30].

In this study, we aim to contribute to the understanding of the conditions and dynamics of local water resources in this intensively used agricultural region, with a particular emphasis on the impacts of droughts, especially in the last few years. By addressing the challenges of hydrological modeling in an anthropic landscape, our research represents an innovative approach to understanding the complexities of hydrological dynamics in response to changing climatic conditions.

2. Materials and Methods

2.1. Study Area

The study area (Figure 1) covers approximately 50 km² and was located about 20 km southwest of the city of Milan in the intensively used agricultural lowlands of Lombardy, close to the border with the region of Piedmont.

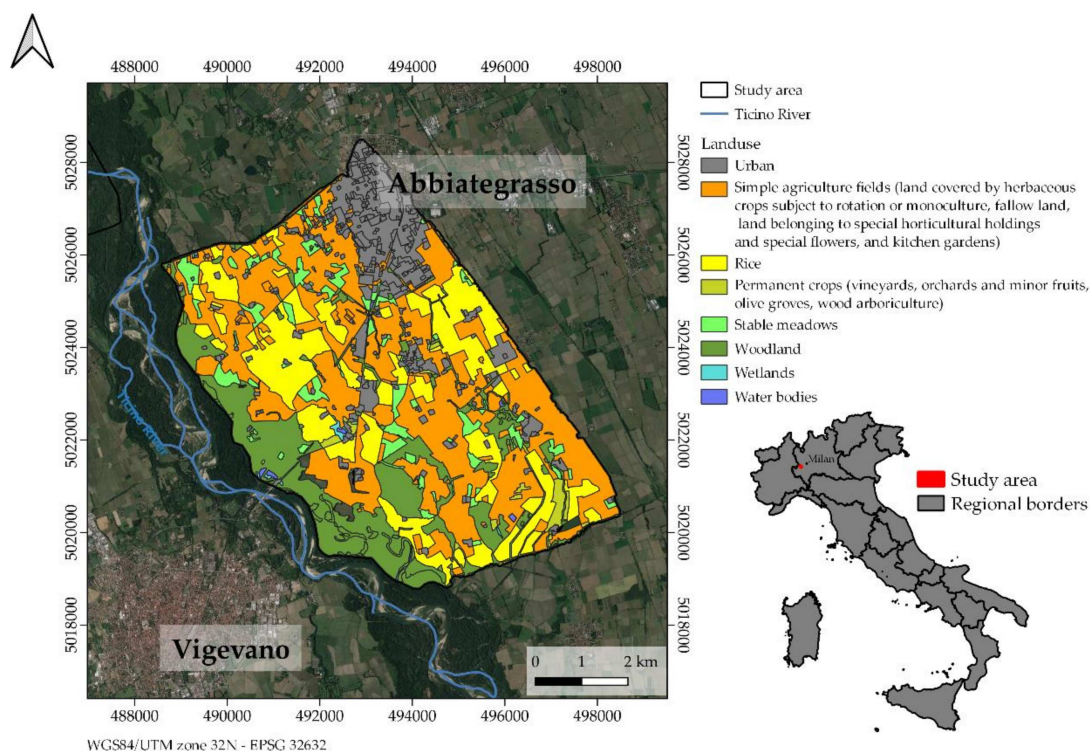


Figure 1. Right: Location of the study area in Italy. Left: Overview of the study area with its dominant land-use classes based on the “Atlante descrittivo—Uso del Suolo Regione Lombardia” [35]. Simple agricultural fields include herbaceous crops that are subjected to rotation or monoculture (excluding permanent grasslands and pastures), fallow land, and land belonging to special horticultural crops, special flowers, and gardens (excluding those in private residences), while the permanent crops included vineyards, orchards and minor fruits, olive groves, and wood arboriculture.

The area covered parts of the Ticino River Valley, with elevations ranging between 76 m.a.s.l. in the southwestern part of the Ticino River to 127 m.a.s.l. around the town of Abbiategrasso (Figure 2). The region is characterized by a humid subtropical climate (Cfa) according to the Köppen climate classification [36], with warm summers, cold winters, and a mean annual temperature of 14 °C. The mean annual rainfall amounts to 782 mm/year—measured at Vigevano SS494 Arpa Lombardia station (Figure 2), which is located close to the Ticino River in the central part of the study area at an elevation of 94 m.a.s.l.

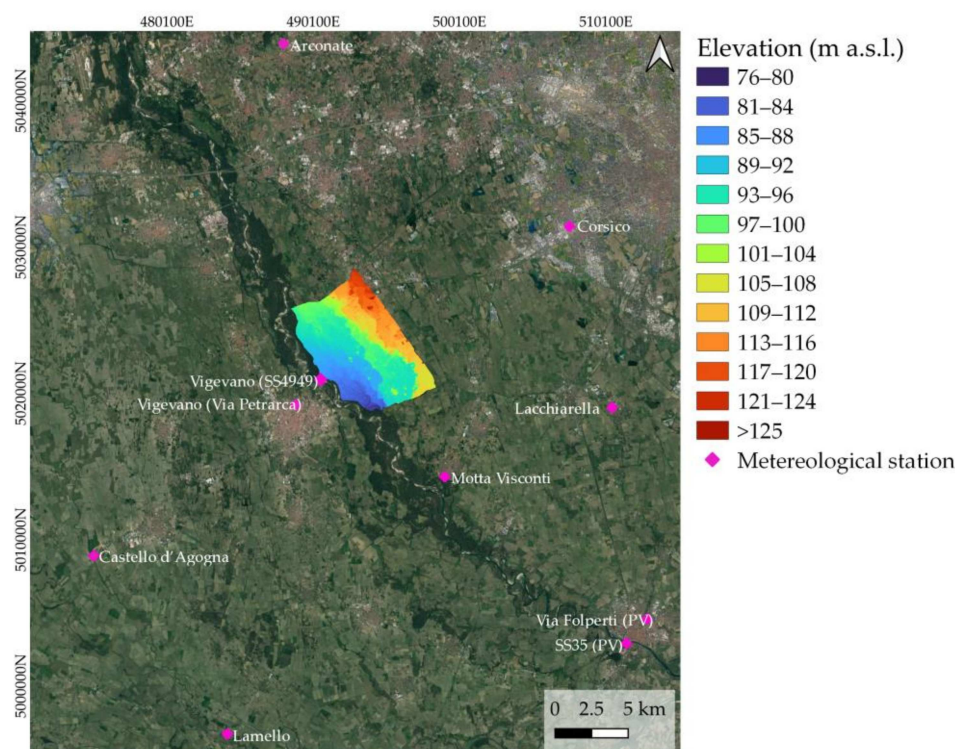


Figure 2. Elevation of the study area and geographical locations of the meteorological stations.

The Ticino River is the only natural drainage system in the area flowing towards the southeast. This area is characterized by artificial drainage and irrigation channels that completely modify the natural drainage system. The study area is flat, except for the river terraces that were formed as a result of the erosive activity of the Ticino River. The area can be divided into three main terrace levels that stretch parallel to the Ticino River. On the left side, these terraces are more developed, while on the right side, there is only one order of terraces. The terrace escarpments have a slope of approximately 20° and are characterized by springs at their base. The oldest terrace, with higher topographic altitudes, is known as the “Ripiano Generale della Pianura,” and it dates back to the upper Pleistocene. It consists of gravelly–sandy fluvio-glacial deposits [12] of the last Würmian glaciation [37]. These coarse deposits allow water to infiltrate and serve as a significant source of aquifer recharge. The intermediate level, which was formed during a subsequent phase of erosive action of the Ticino River, is characterized by terraced fluvial deposits of the Middle Holocene, and it consists of sandy–gravelly and silty textures. The most recent fluvial deposits represent the youngest level of the Ticino valley, attributed to the Upper Holocene, and they are composed of sandy–gravelly and slightly silty textures. Soil has developed above these fluvial and fluvio-glacial deposits, with varying depths based on the age of the terrace level. According to the World Reference Base for Soil Resources [38], the soil types range from regosols in the lower part to luvisols and umbrisols on the upper terrace level, which is characterized by a sandy–loamy texture.

From the hydrogeological point of view, groundwater primarily flows towards the Ticino River (Figure 3).

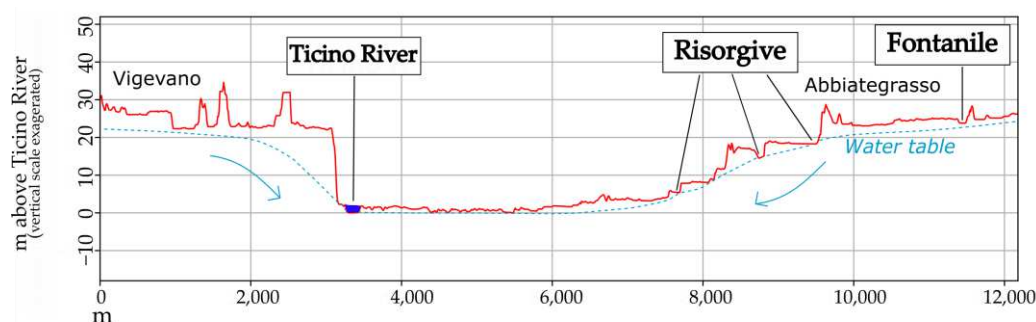


Figure 3. Schematic representation of the geohydrological settings of the study area. The topographical profile was obtained from a “hybrid” DEM (10 m resolution) joining a 12 m TanDemX and 1 m Lidar. The figure represents the different orders of terraces with the respective springs at their bases and the drainage action of the Ticino River. The water table shows where it has contact with the surface (Fontanile, Risorgive) (after the CE4WE report, Pilla 2020).

As mentioned previously, this part of the Ticino Valley is characterized by the presence of springs, which are classified as “risorgive” and “fontanili.” “Risorgive” are formed by groundwater that naturally emerges due to changes in topography and the permeability of sediments at the base of the terrace escarpments. On the other hand, “fontanili” refers to springs in lowland areas that have been modified by human intervention [15,39].

The *fontanili* and *risorgive* are primarily fed by groundwater. The phreatic aquifer is supplied by local infiltration, streams, and irrigation channels [32]. However, due to the flat nature of the study area (except for the terrace’s slope), the contribution of the surface runoff is negligible [15]. The variation in spring discharge is mainly attributable to water infiltration after periods of rain or irrigation [11].

During the spring–summer period, substantial quantities of water are distributed through a complex channel network for field irrigation. Thus, the water allocated for irrigation serves a dual purpose: It supports agriculture and significantly contributes to recharging the water table, subsequently sustaining the springs at different terrace base levels (see Figure 3). The region has a long history of distinctive land-use and land management practices dating back to the eleventh century, and these involve the construction of irrigation channels [39] and the reuse of water along the fluvial terrace cascade of the Ticino River (risorgive). This has represented a sustainable and effective method of reusing irrigation water for centuries.

Presently, based on the DUSAF 6.0 land-use map (Regione Lombardia, 2019) [40], the main crops in the area are corn and rice. Corn—including maize, along with other simple arable crops, such as wheat, sorghum, and barley—for both grain or silage covers approximately 32% of the area. However, rice covers up to 21%. Furthermore, about 18% of the study area is covered by woodlands, which are predominantly concentrated on the lowermost terrace level. Both corn and rice require substantial amounts of irrigation water [11,41]. As indicated in Figure 4, the irrigation seasons for corn typically run from June to September [14], and furrow irrigation is usually performed. In contrast, the rice fields are generally flooded from mid-April to early May and remain submerged until the end of August or September [11,14,15]. In 2022, one of the hottest years of the century in the study area, the rice fields were flooded from late May to late August, with intermittent flooding. The substantial water usage in rice paddies significantly affects the recharging of the water table [42]. In these rice paddy areas, the primary factor influencing water levels is the agricultural technique for rice cultivation, as described by Lasagna et al. [14].

Crop rotation patterns, sowing and harvesting times, and irrigation practices were obtained through a comprehensive study that included a detailed literature analysis (e.g., [43,44]), on-site inspections, and interviews with local farmers (Figure 4).

Our findings revealed that the most cultivated summer crops were corn and rice, with corn being sown between mid-April and early May, reaching maturity by mid-June, and being harvested in late September. Rice, on the other hand, was typically sown later than

corn—between mid-April and late May. It grew from early June to mid-October and was harvested in the middle and end of October. Double cultivation with crops such as corn and sorghum after the harvesting of fodder crops such as ryegrass or winter cereals (such as barley or wheat) is common. Additionally, herbaceous legumes such as alfalfa and clover were prevalent and were usually mowed and harvested multiple times from May to August.

For our study area, the most common crop rotation (ryegrass–corn rotation) was considered by defining the sowing, irrigation, and harvesting times, as shown in Figure 4.

	Jan	Feb	Mar	Apr	May	Jun	Jul	Aug	Sep	Oct	Nov	Dec
Ryegrass	Yellow	Yellow	Yellow	Yellow	Orange	Orange				Green	Green	Yellow
Corn				Green	Green	Yellow	Yellow	Yellow	Orange	Orange		
Barley	Yellow	Yellow	Yellow	Yellow	Yellow	Orange				Green	Green	Yellow
Wheat	Yellow	Yellow	Yellow	Yellow	Yellow	Orange				Green	Green	Yellow
Rice	Blue	Blue	Blue	Green	Yellow	Yellow	Yellow	Yellow	Yellow	Orange	Blue	Blue
Sorghum				Green	Green	Yellow	Yellow	Yellow	Yellow	Orange		

Figure 4. Crop calendar of the main crops in the study area. Green represents the sowing of crops, yellow represents their development/growth, orange represents harvesting, and blue represents residues.

2.2. Application of the SWAT

The approach used to study the hydrological dynamics of the study area over the last decade is depicted in Figure 5.

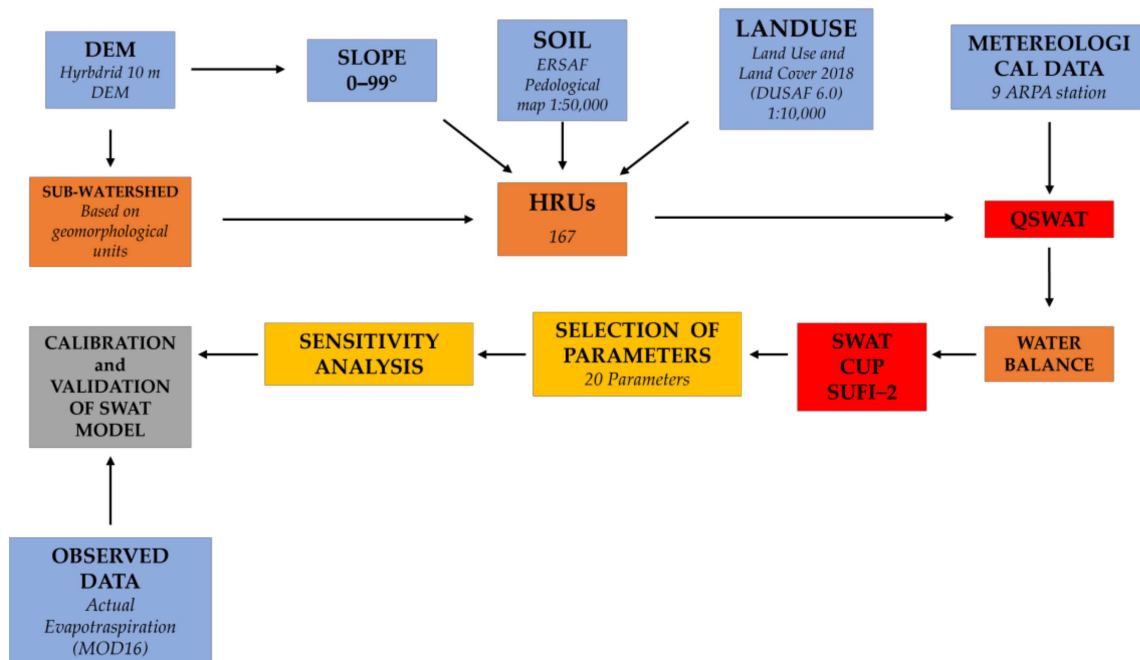


Figure 5. Flowchart of the methodology and results: The red color indicates the software used, blue indicates the input data, orange indicates the outputs, gray indicates the actions conducted, and yellow indicates the steps performed for the calibration and validation.

To assess the effects of droughts on the hydrological dynamics of a Lombardy lowland system, the Soil and Water Assessment Tool (SWAT) model [17] was applied. The SWAT is a physically based model that operates at the basin scale, and it was developed to predict

the impacts of climate and land management practices on water, sediment, and chemical yields [16]. It requires specific input data, such as an elevation model, soil and land-use maps, and climate data (precipitation, temperature, solar radiation, relative humidity, and wind speed) [45]. The sources and the temporal and spatial resolutions of the datasets used are documented in Table 1.

Table 1. Sources and descriptions of the input data utilized to set up the SWAT model.

Data Type	Sources	Resolution and Description
Topography	Deutsches Zentrum für Luft und Raumfahrt (DLR) and Ministero dell’Ambiente: Geoportale Nazionale, 2019 [46]	10 m “Hybrid” Digital Elevation Model
Soil	Geoportale della Lombardia [47]	1:50,000, Soil information bases
Land-Use	Geoportale della Lombardia [40]	1:10,000, Land Use and Land Cover 2018 (DUSAF 6.0)
Climate	Arpa Lombardia [48]	Daily, ARPA Lombardia hydro-nivo-meteorological data archive.

The SWAT divides a watershed into sub-basins, which are further split into hydrological response units (HRUs) that represent areas with homogenous topographies, soils, and land uses. The SWAT also considers spatially distributed changes in land use and management (e.g., irrigation schemes) and their effects on individual components of the water balance, such as the actual evapotranspiration (AET) [29], which was used as a variable in the calibration procedure.

In this study, the Penman–Monteith method was applied to calculate the evapotranspiration for the SWAT. Sub-basins were delineated in a GIS environment based on geomorphological units (river terrace levels), since traditional watershed subdivision methods were not feasible in this flat, intensively irrigated area. The 5 sub-basins obtained were further divided into 167 HRUs, with varying surface areas ranging from approximately 100 m² to 4.7 km² and an average extension of approximately 0.308 km². We ran the SWAT model on a monthly basis to match the temporal resolution of the observed AET data. A monthly AET time series was generated for each HRU, and these AET values were used in the calibration phase from 2007 to 2010 and in the validation phase from 2011 to 2013.

Due to a lack of information on irrigation schemes and practices (see above), the SWAT auto-irrigation module was applied. Auto-irrigation can be triggered within HRUs by soil water deficiency or plant water stress [49,50]. If sufficient water is available from the irrigation source, the model adds water to the soil until it reaches field capacity [51].

2.3. Calibration and Validation of the Model

The SWAT model was calibrated and validated using the SWAT-CUP software (Calibration and Uncertainty Procedures) version 5.1.6.2. [52,53] and applying the “Sequential Uncertainty Fitting” (SUFI-2) algorithm [54]. This algorithm performs a “stochastic” calibration, considers uncertainties related to parameters, the conceptual model, or input data, and reflects these uncertainties in the model’s output [55]. The Kling–Gupta efficiency (KGE) was used as the objective function [56] to assess the model’s performance. The KGE index ranges from negative infinity to 1, and a value closer to 1 indicates a better match between the model and the observed data.

In this study, monthly evapotranspiration data provided by Moderate-Resolution Imaging Spectroradiometer (MODIS) were used as the observed data for the calibration period from 2007 to 2010 and the validation period from 2011 to 2013. Runoff data were not considered because the study area lacks natural streams. The latter was the main reason for why AET data derived from satellite products were selected. Consequently, MOD16 data with a resolution of 1 km were used for the calibration.

In order to compare the monthly SWAT-AET values of each HRU with the respective MOD16 AET pixel, the mean monthly evapotranspiration of each HRU was extracted. The

model was calibrated for 149 HRUs out of a total of 167—excluding urbanized areas—from 2007 to 2010.

A set of 20 calibration parameters (Table 2) were selected based on previous SWAT calibration studies [27,29,52], and the parameters' sensitivity to changes in AET was determined. These parameters were adjusted to optimize the KGE criteria between the SWAT and MODI16 AET values.

Table 2. Parameters selected for the calibration and the range of the corrections.

Parameter Name	Min_Value	Max_Value	Description
1:R_HRU_SLP.hru	0	0.2	Average slope steepness for overland flow
2:V_ESCO.hru	0.6	1	Soil evaporation compensation factor
3:R_CN2.mgt	−0.2	0.2	SCS runoff curve number for moisture conditions
4:V_ALPHA_BF.gw	−0.07076	0.109	Baseflow recession coefficient
5:V_GW_DELAY.gw	0	20.281	Groundwater delay
6:V_GWQMN.gw	0	500	Threshold depth of water in the shallow aquifer required for return flow to occur
7:V_GW_REVAP.gw	0.1	0.2	Groundwater 'revap' coefficient
8:V_REVAPMN.gw	143.0484	342.720	Threshold depth for water in the shallow aquifer for revap or percolation to occur
9:V_EPCO.hru	0	1	Plant evaporation compensation factor
10:V_RCHRG_DP.gw	0.009108	0.336	Deep aquifer percolation fraction
11:V_CANMX.hru	9.93414	29.805	Maximum canopy storage
12:R_SOL_BD(..).sol	0.190512	1.571	Moist bulk density
13:R_SOL_AWC(..).sol	−0.5	0.95	Available water capacity of the soil layer
14:R_SOL_K(..).sol	−0.8	0.8	Saturated hydraulic conductivity
15:R_SOL_ALB(..).sol	−0.03	0.2	Moist soil albedo
16:R_SOL_ZMX.sol	24.9602	141.659	Maximum rooting depth of soil profile
17:V_SLSOIL.hru	0	150	Slope length for lateral subsurface flow
18:R_SOL_Z(..).sol	−0.03	0.2	Depth from the soil surface to the bottom of the layer
19:R_SOL_CBN(..).sol	0.041925	0.1855	Organic carbon content
20:V_FFCD.bsn	0	1	Initial soil water storage

2.4. Trend Analysis

In our study, we also conducted a trend analysis using the Mann–Kendall test [57,58] to discern patterns and directional trends in the climate and hydrological data. The Mann–Kendall test is a non-parametric statistical method that is commonly used in environmental studies to detect monotonic trends in time-series data [59–61]. Specifically, the test assesses the presence of an increasing or decreasing trend over time by evaluating the rank correlation of data points. In this study, climate data graphs, including those of temperature and rainless days, were subjected to the Mann–Kendall test. For each dataset, the Kendall coefficient (τ) was calculated to quantify the strength and direction of the observed trend. Simultaneously, p -values were determined to ascertain the statistical significance of the identified trends. A p -value below a predetermined significance level (e.g., 0.05) indicated a statistically significant trend. The test was performed using the “MannKendall” function in the “Kendall” package [61] in R [62].

2.5. Soil Moisture Sensors

In 2022, three TEROS 12 soil moisture sensors were installed at various depths, facilitating a preliminary correlation between the soil moisture and precipitation patterns allowing

the identification of irrigation activities. The sensors were deployed in three distinct areas characterized by different land uses as follows: (i) simple arable land with a rotation of ryegrass and corn—sensors were installed at depths of 10 cm and 35 cm; (ii) rice cultivation, with sensor depths of 10 cm and 30 cm; (iii) a forested area in which sensors were placed at depths of 10 cm, 30 cm, and 65 cm. This configuration enabled a comparative analysis of the soil moisture across the three distinct land uses.

3. Results

3.1. Input Data Analysis

Figure 6 presents the trend of temperature in the study area from 2004 to 2022 according to measurements at the Vigevano SS494 station. There was a noticeable increase in the mean temperature over the 19-year period. Starting at around 13.8 °C in 2004, the temperature peaked at 14.7 °C in 2022. The coldest year was registered in 2005, while 2022 was the hottest. Though there were notable fluctuations, the overall trend showed an increase in temperature.

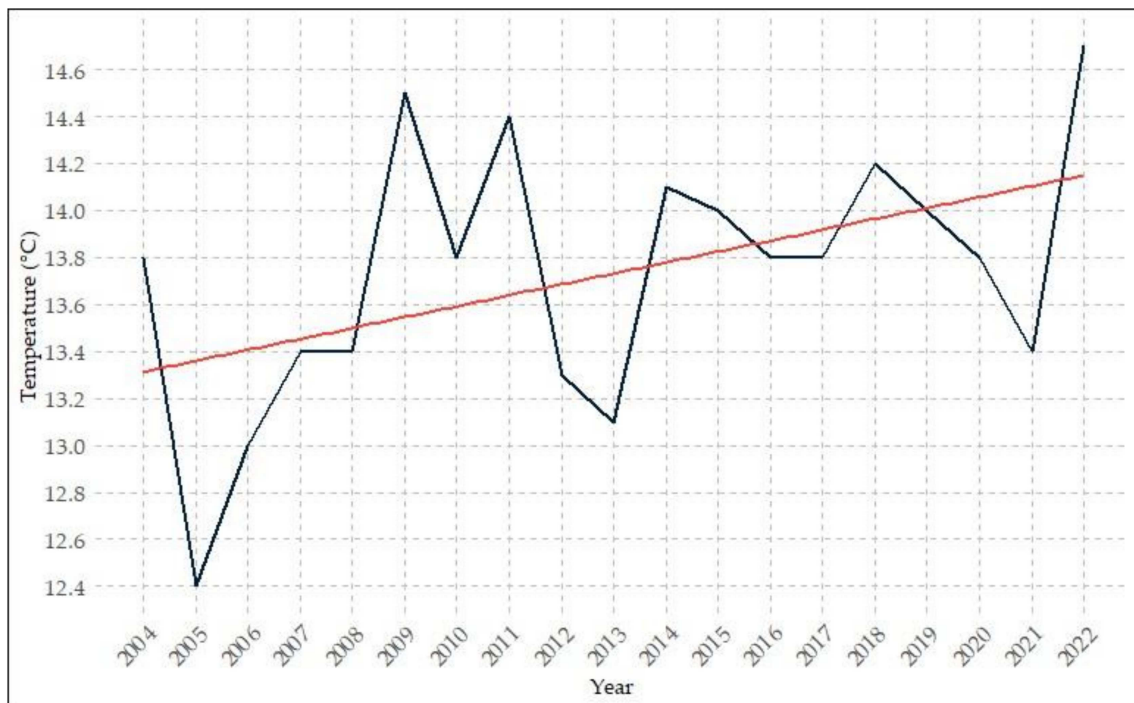


Figure 6. Mean temperature from 2004 to 2022, with the trend represented by the red line.

Figure 7 illustrates the amount of precipitation over the same 19-year period. There was an overall decrease of 0.86%. The rainiest year was observed in 2014, while the driest year was 2022. Moreover, a notable increase in rain-free days was observed (Figure 8). The two years with the most precipitation-free days were 2017 and 2022. Generally, precipitation only marginally decreased over the last 19 years, but the number of rain-free days increased. This suggested that, on average, single precipitation events were more intensive, and the number of extreme precipitation events increased [63]. Examining the data from the Vigevano station revealed that in 2022, the year with the least rainfall and the fewest rainless days, 11 extreme weather events occurred. While this aligned with the mean for the other years, the prolonged drought periods have significant consequences.

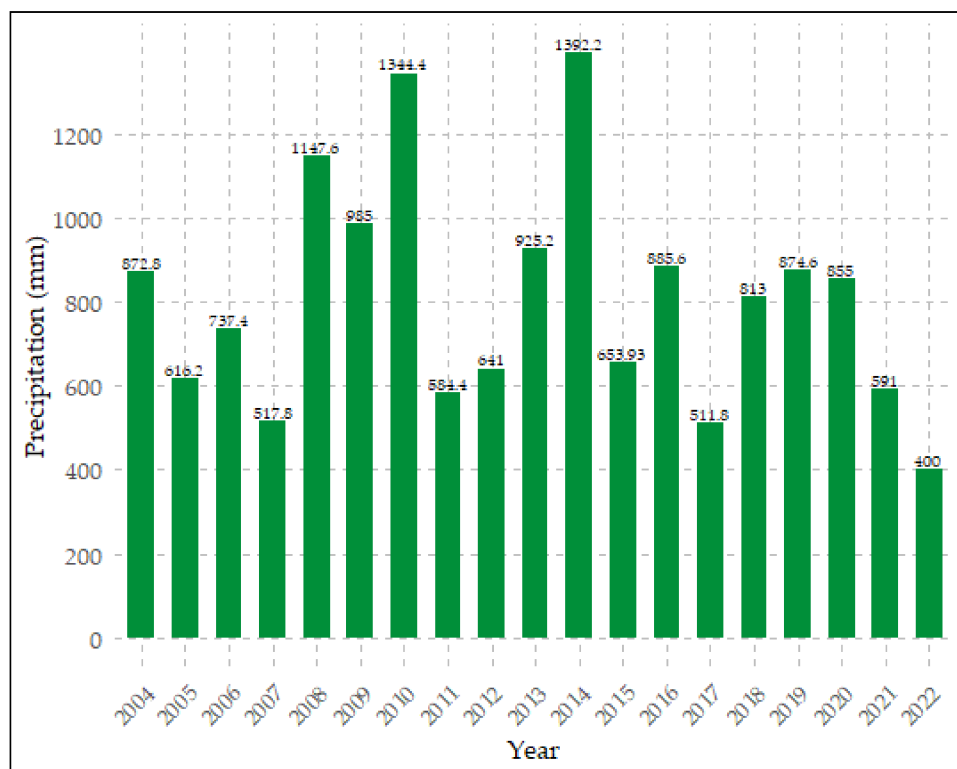


Figure 7. Mean annual precipitation.

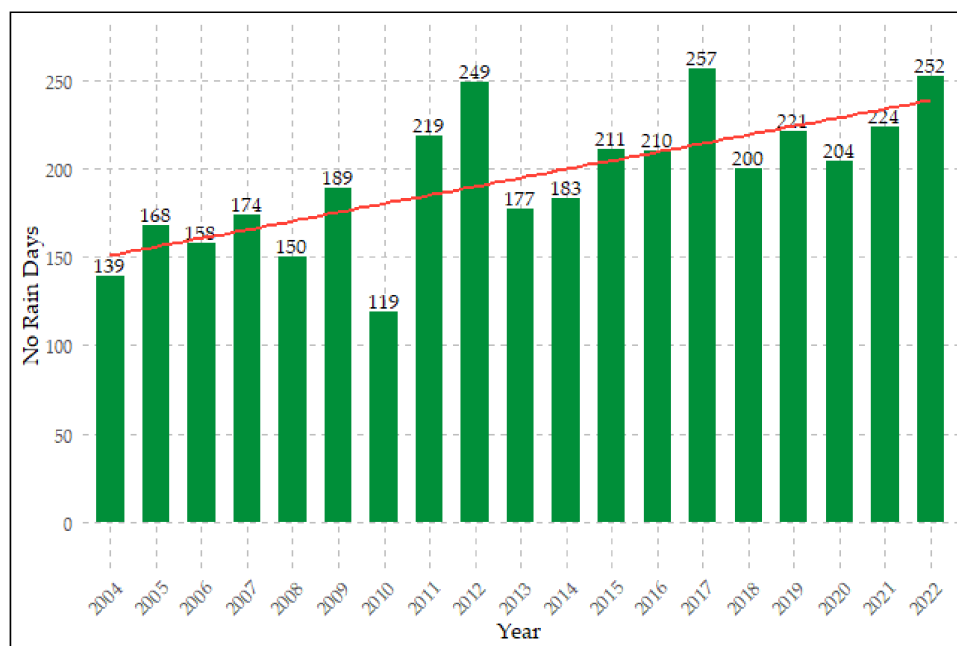


Figure 8. Rain-free days over the last 19 years, with the trend represented by the red line.

The Mann–Kendall test [57,58] was conducted to analyze the climate data trends, with a focus on temperature (Figure 6) and rainless days (Figure 8). For temperature, a positive Kendall coefficient (τ) of 0.287 implied that there was an increasing trend, but the non-statistically significant p -value of 0.10294 at the 5% confidence level suggested caution in interpreting this trend. The proximity of the p -value to 5% signaled the potential for further investigation or analysis. On the other hand, the rainless days exhibit a more pronounced trend, with a τ value of 0.567 and a significantly low p -value of 0.00078332 (<0.05). This

indicated a noteworthy and statistically significant increase in rain-free days. The results highlight the complexity of the climate dynamics, urging a nuanced interpretation that considers statistical significance and the need for additional scrutiny, especially in the context of potential impacts on the local environment and water resources.

3.2. Calibration and Validation of the Model

The uncalibrated SWAT model's output demonstrated a tendency to underestimate the AET when compared to the AET data derived from the MOD16 satellite observations. This underestimation was particularly pronounced during the winter months. However, from the uncalibrated model to the calibrated model, there was a remarkable improvement in the Kling–Gupta efficiency values, which were calculated by averaging the individual KGEs of all 149 HRUs in the SWAT-CUP. Initially, the uncalibrated SWAT model exhibited a KGE value of 0.4. Through the calibration of the SWAT model using the SUFI-2 algorithm, an increase in the KGE from 0.4 to 0.59 was achieved. The KGE of 0.59 was derived from the mean of the individual HRUs. Notably, a KGE value that changed from 0.41 to 0.83 for the entire basin (Figure 9) was observed. Furthermore, a more in-depth analysis of the results of this calibration process revealed that the calibration results clearly differed between the individual HRUs. The best HRU reached KGE values of up to 0.8 after the calibration, while some areas showed values lower than -1 , indicating a poor fit between the observed and simulated data. These HRUs with low values had very limited areal dimensions (less than 0.7 km^2) (Table 3).

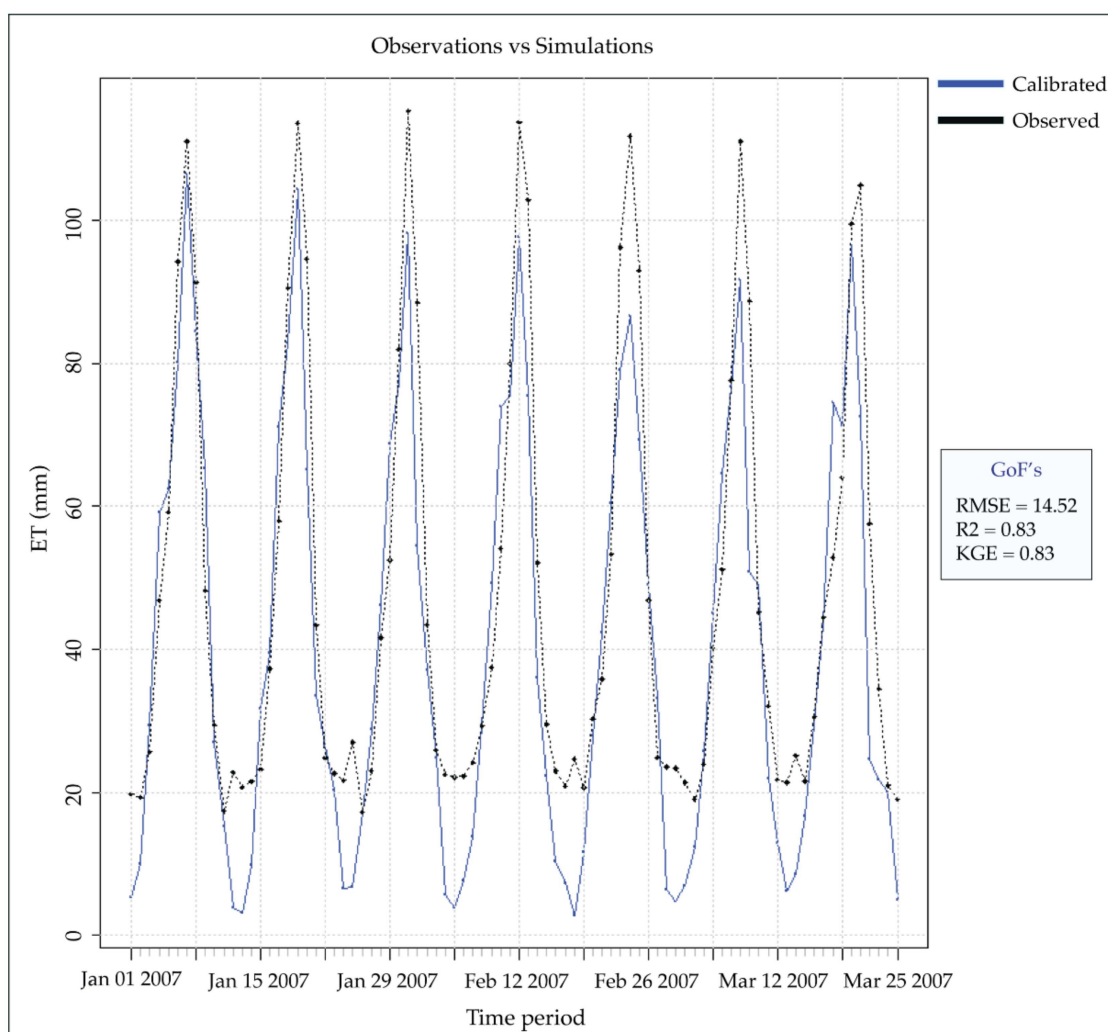


Figure 9. Time series of AET for the study area from MOD16 (black) and the SWAT (blue) after calibration.

Figures 10 and 11 present the calibrated SWAT model in a field with a rotation of corn-ryegrass and rice paddies. Here, a clear improvement in the model’s performance was observed during the calibration process.

Calibration increased the AET found with the SWAT model, particularly during the summer months. While during most of the year, there was a good match between the values from the SWAT and MOD16, during the winter months, the SWAT values (both calibrated and uncalibrated) were much lower than those of MOD16.

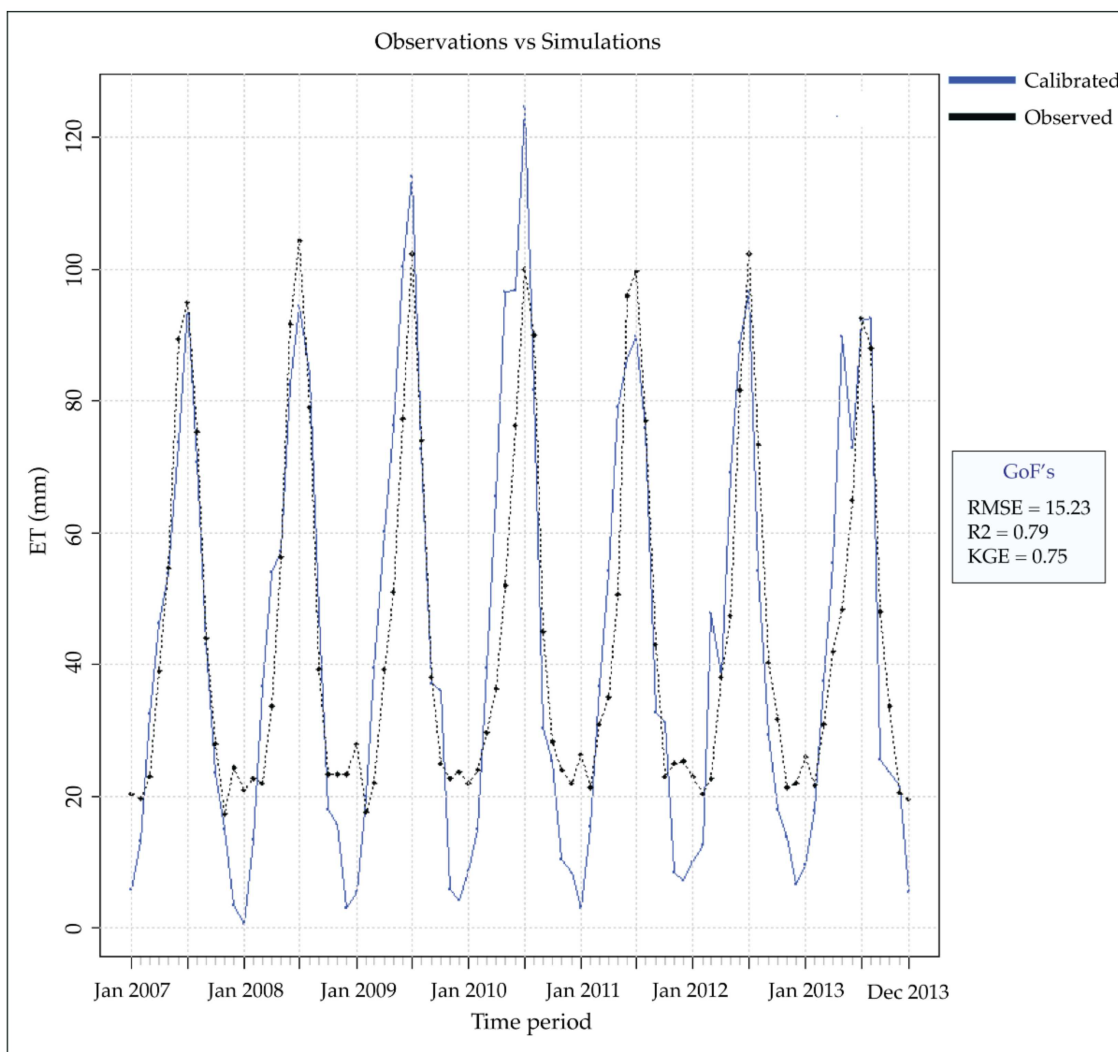


Figure 10. Time series of AET in a corn–ryegrass field from MOD16 (black) and the SWAT (blue) after calibration.

The validation results showed a mean KGE of 0.48, with the highest KGE values reaching up to 0.85 for some HRUs (Table 3). Even in this case, the HRUs in extremely limited areas had low KGE values, while areas of our interest with larger surface areas and agricultural land use had satisfactory KGE values.

Table 3. KGE results for the calibration and validation.

	Mean (All HRUs)	5th Percentile	95th Percentile
Calibration	0.59	0.22	0.85
Validation	0.49	−0.17	0.79

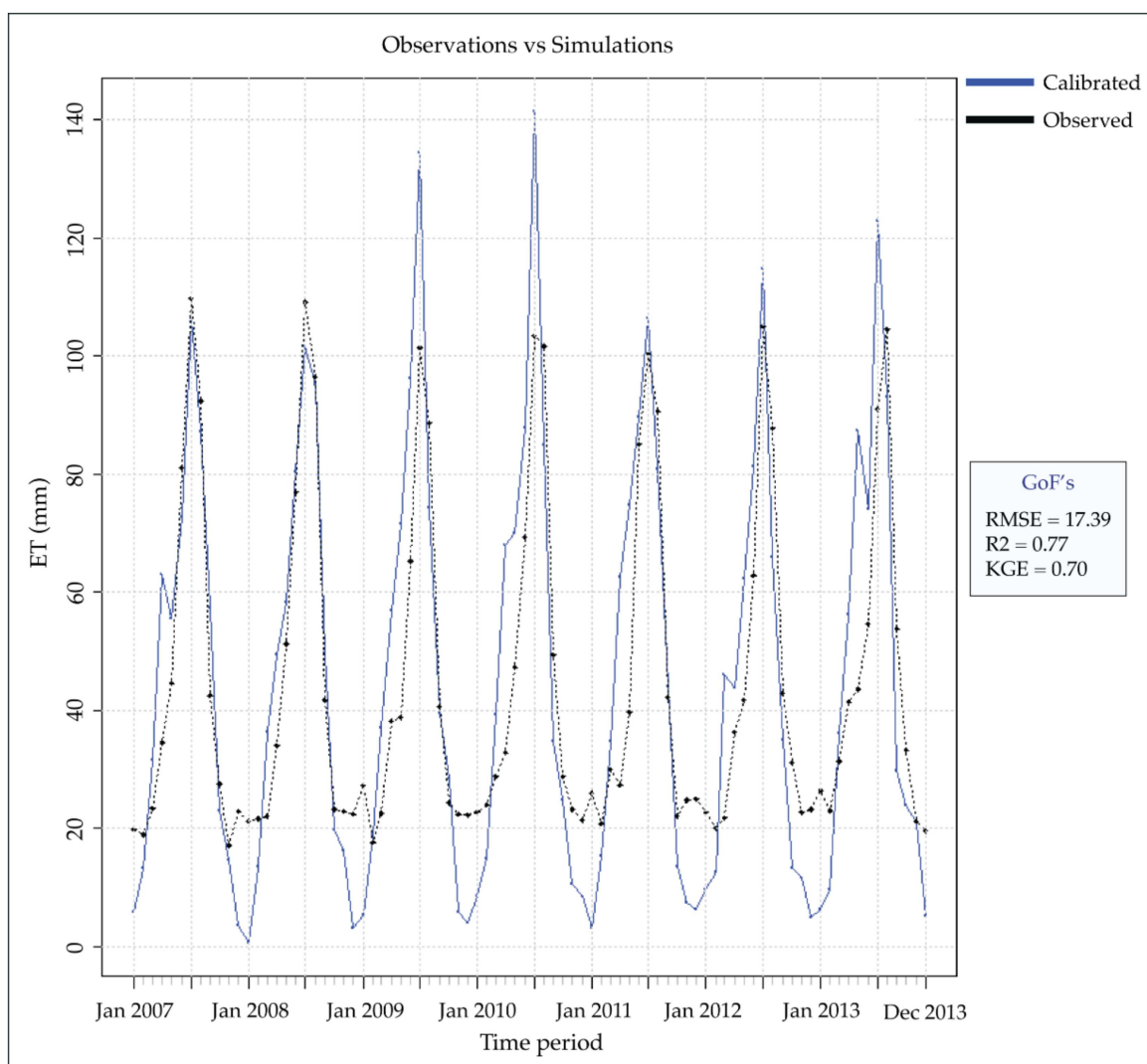


Figure 11. Time series of AET in a rice field from MOD16 (black) and the SWAT (blue) after calibration.

3.3. Model Results

The SWAT output results showed that there was no significant increase in evapotranspiration over the last 15 years (+4%) in the study area (Figure 12). However, it turned out that the ratio of evapotranspiration and precipitation varied (Figure 13). The graphical representation of the evapotranspiration-to-precipitation ratio provides valuable insights into the water balance dynamics in the study area. Peaks in the ratio, such as in 2015, 2017, and 2022, where the precipitation was less than the actual evapotranspiration, are indicative of periods with increased water demand by plants due to drought conditions.

Additionally, we analyzed the soil water content (SWC), which showed a declining trend for HRUs with agricultural land use. The graph in Figure 14 illustrates that there was a significant decrease (−7%) in soil water content over the last 15 years.

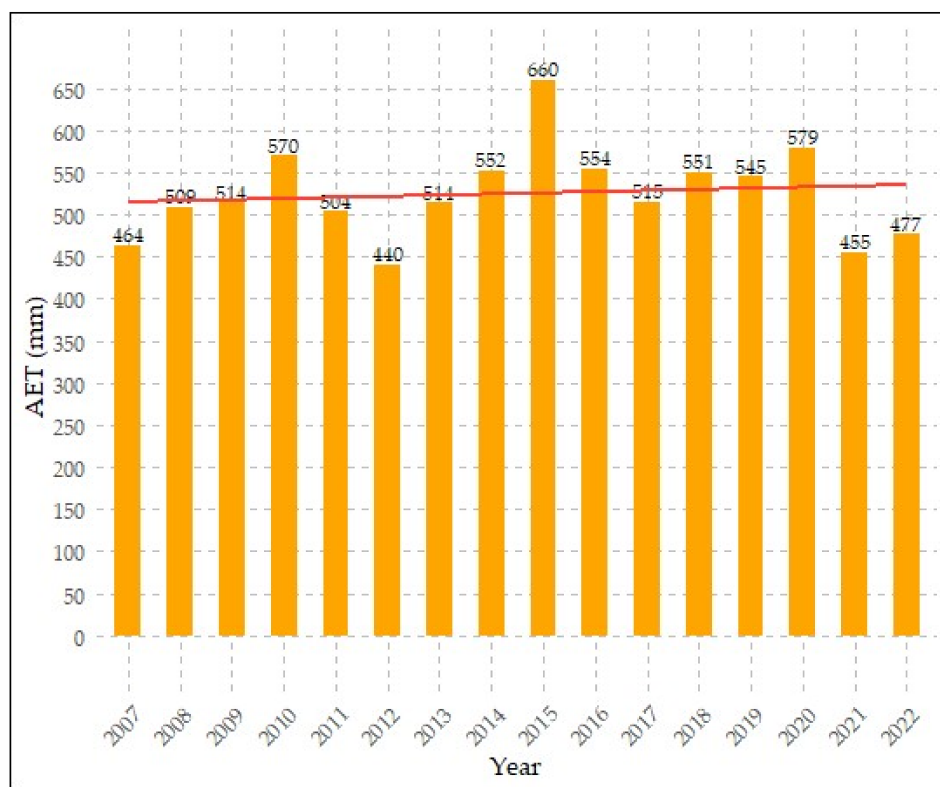


Figure 12. Actual evapotranspiration trend in the study area according to the SWAT, with the trend represented by the red line.

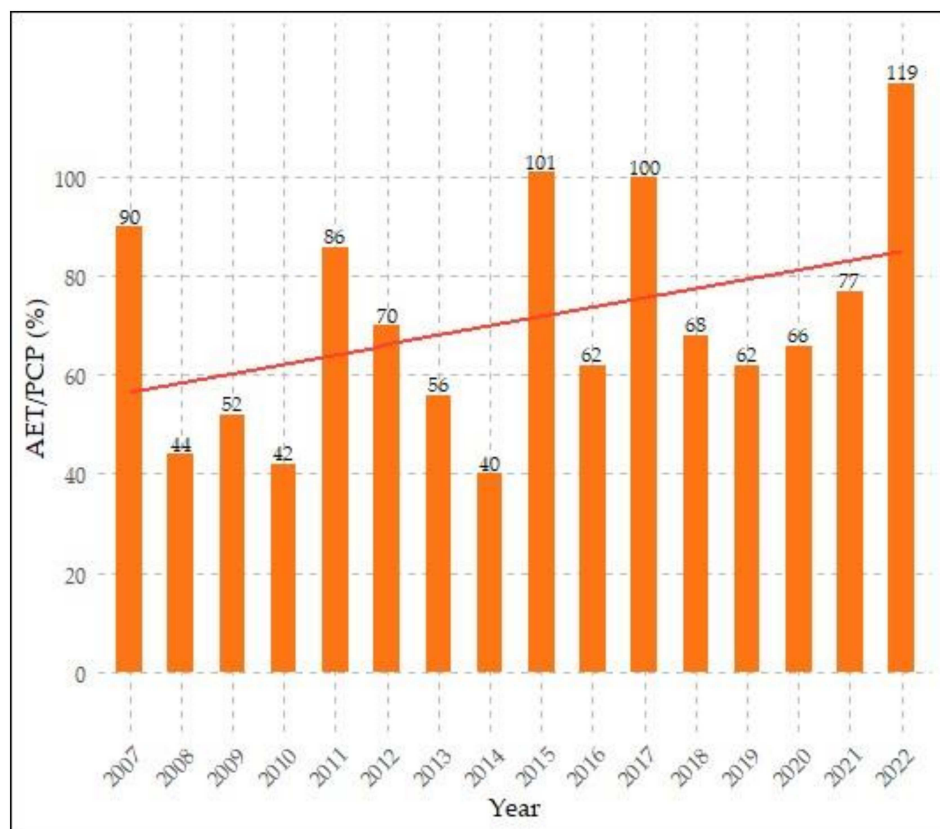


Figure 13. The ratio of evapotranspiration to precipitation (as a percentage) in the study area, with the trend represented by the red line.

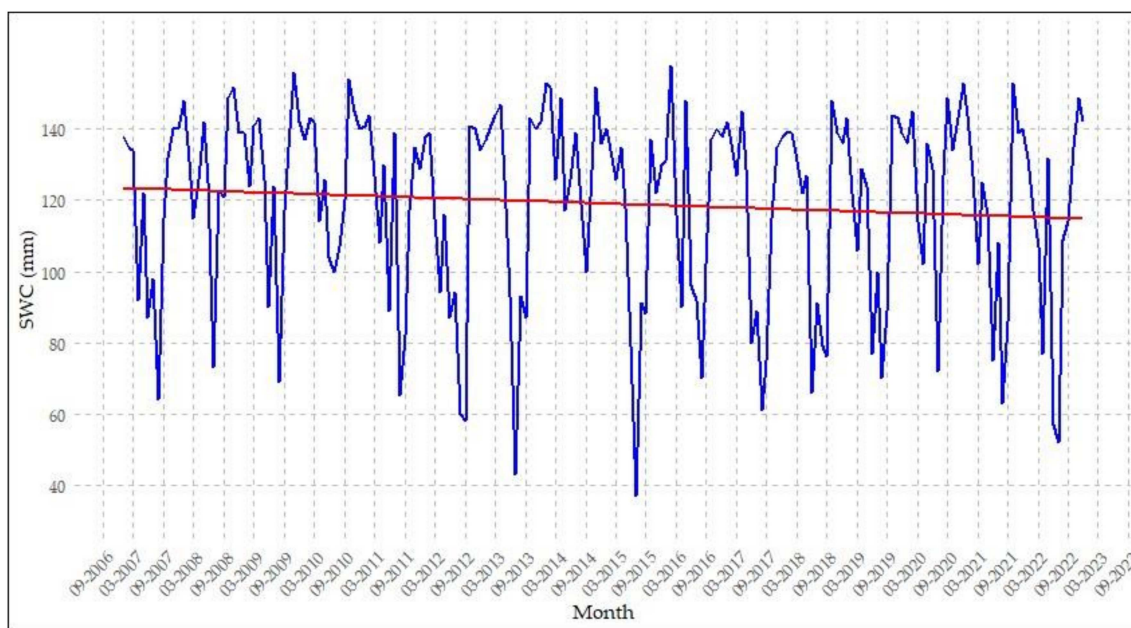


Figure 14. SWC trend over the last 15 years in the study area according to the SWAT, with the trend represented by the red line.

The Mann–Kendall test was also applied to assess trends in the AET (Figure 12), AET/PCP ratio (Figure 13), and SWC (Figure 14). For the AET, a tau value of 0.142 indicated an increasing trend, but the non-significant p -value of 0.47085 warrants caution in interpreting the trend's statistical significance. The AET/PCP ratio demonstrated a positive correlation with a tau value of 0.259, suggesting a tendency to increase evapotranspiration relative to precipitation over time. Despite the p -value of 0.1763 being higher than the significance level, this underscores the need for careful consideration. Regarding the SWC, the tau value of -0.0522 implied a weak negative correlation, indicating a slight tendency toward a decrease in soil water content over time. However, the p -value of 0.2867 is not statistically significant, emphasizing the absence of evidence for a significant decreasing trend for the SWC.

3.4. Soil Moisture Sensor Results

Comparing the soil moisture content modeled with the SWAT with field measurements taken with soil moisture sensors (TEROS 12), we observed a consistent underestimation in the model. This discrepancy can be attributed to the differences in measurement scales, as the sensors measured the water content locally [64], while the SWAT simulated it at the HRU scale. Furthermore, the inclusion of auto-irrigation in the SWAT added a certain degree of complexity to the soil moisture dynamics. It was assumed that actual irrigation events may have impacted the soil moisture levels differently from the model's HRUs due to their representative scale. These findings highlight the importance of considering both the spatial scale and local practices in understanding and interpreting soil moisture dynamics within the model system.

As shown in Figure 15, the soil moisture sensors in different land-use conditions helped to identify irrigation patterns. The sensors in the forest area reflected natural conditions in which the soil water content depended solely on precipitation. In contrast, the sensors in the corn and rice fields indicated irrigation. Notably, the peaks in the soil water content in the forest area were related to rainfall, and this trend was also observed in rice and corn. In the case of corn, additional peaks occurred during irrigation periods, while for rice, the timing of the first irrigation flood was clearly visible.

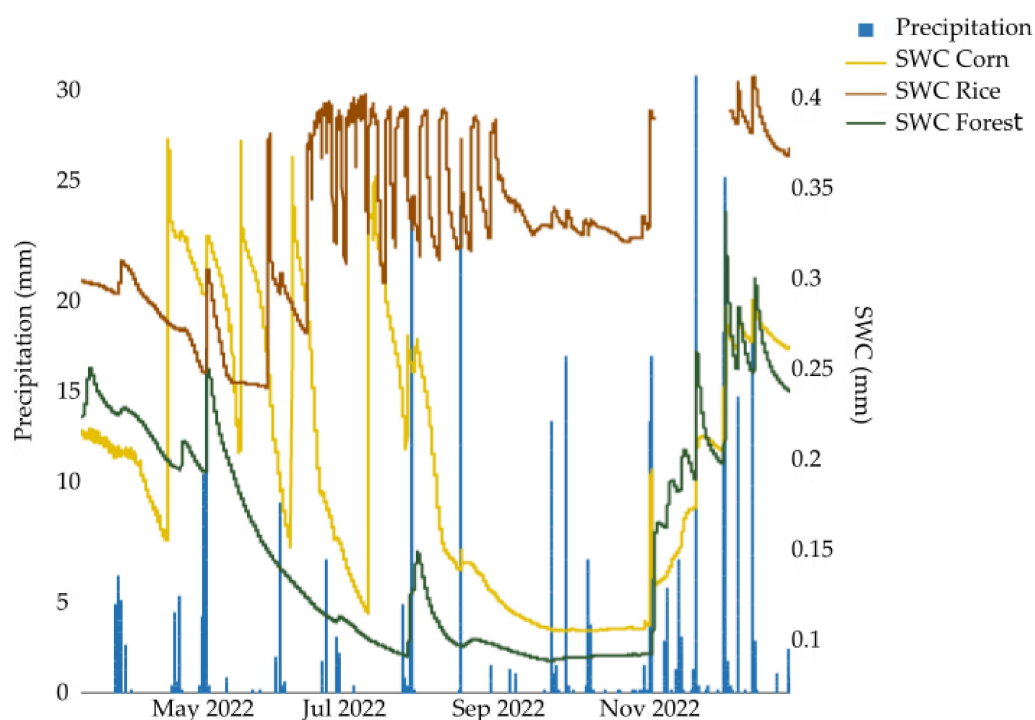


Figure 15. Correlation between soil water content and precipitation in the study area.

4. Discussion

The process-based modeling of hydrological dynamics is a valuable tool for gaining insights into the general water cycle and for assessing future conditions through scenario analysis. However, it has been noted by various authors that applying physically based hydrological models such as the SWAT in lowland areas presents unique challenges. In general, hydrological models are calibrated and validated with discharge data, but in lowland areas, obtaining discharge data can be difficult. Additionally, the flat topography of lowlands promotes vertical water dynamics; thus, the surface runoff is often negligible [11,15]. Furthermore, flat topographies and fertile soils favor intensive agriculture, particularly in areas such as the Ticino and Po Plains in northern Italy. This type of agriculture often involves irrigation, but in many cases, information about irrigation schemes and water supplies is lacking [65]. Irrigation can also lead to significant alterations in drainage patterns due to the construction of irrigation and drainage channels, as seen in the ancient Ticino irrigation cascade system dating back to the 11th century.

To assess the hydrological dynamics of the Ticino Plain between Abbiategrosso and Pavia, the SWAT was applied for the period of 2004–2022. Since there were no reliable discharge data available and there were no clear drainage patterns, the SWAT model was calibrated using AET observations derived from MOD16 data. Generally, the calibration and validation of the model yielded satisfactory KGE values of 0.59 HRUs; these were derived from the mean of the individual HRUs. This result served as a valuable indicator of the model's ability to capture and simulate the hydrological processes within HRUs, but there was a substantial improvement in the model's performance when considering the basin as a whole (0.83). This result is particularly encouraging due to the accuracy in representing the hydrological dynamics of the entire study area. However, notably lower KGE values were found in HRUs classified as having a "WATER" land use. These areas primarily consisted of irrigation channels and small artificial lakes, and their representation within the HRU framework was problematic. Excluding these "WATER" areas led to an increase in the overall average KGE value to 0.64 (not considering WATER HRUs), as seen in Table 3. Referring individual HRUs, instead, as seen in Figures 10 and 11, the model was able to simulate the AET in an area with different crops and land-use practices, highlighting the success of the calibration process. However, differences between the model's output

and the observed data were noted. These differences could be attributed to the fact that the MOD16 data relied on remote satellite measurements with a 1 km resolution, which covered areas with heterogeneous land uses. MOD16 also used parameters such as Earth's surface temperature, the NDVI, and other indicators to calculate evapotranspiration. In contrast, the SWAT is a physical hydrological model that simulates the water cycle in a specific area with a higher spatial resolution, necessitating detailed data on soil and land uses that are unique for each HRU (e.g., [66,67]). Consequently, examining the differences between the SWAT and MOD16, we noticed that HRUs with a low KGE were characterized by a smaller area than the resolution provided by MOD16. This meant that the MOD16 data always yielded a mean of the land use in the 1 km pixel covering the area, whereas the HRUs were specifically related to a single land use and, thus, represented the hydrological processes within the HRUs in a much more detailed way. The differences between the SWAT and MOD16 were mainly observed during winter months. As mentioned by Abiodun et al. [66], one potential reason could be the variance in land cover. Winter months are typically characterized by vegetation entering a dormant phase or losing foliage. If the land cover information used in the SWAT differs significantly from that in MOD16, this could result in discrepancies in the respective simulations of evapotranspiration. In our study, the land cover differences between the SWAT and MOD16 were compounded by their data coming from different years. Additionally, as noted in [68], the simulated evapotranspiration from the SWAT tends to be higher during the crop growth season and lower during the inactive season, while the MOD16-derived AET remains relatively constant. Consequently, the differences in the simulated AET between the SWAT and MOD16 were more significant during the less active winter months due to the SWAT's consideration of climatic conditions, land uses, and soil characteristics.

Analysis of meteorological input data revealed significant climate changes over recent decades. Notably, there has been an alarming upward trend in the mean temperature with a pronounced increase in the number of rain-free days, despite the modest 0.86% decrease in overall precipitation. The results of the Mann–Kendall test confirmed that the temperature showed an increasing trend, but this trend was not statistically significant. However, the number of days without rain significantly increased, and these trends could have important implications for agriculture, water supply, and other climate-related aspects, and further research may be needed to better understand these trends and their potential consequences. These findings align with global concerns about climate change [69] and highlight the need for further investigations of the underlying factors. The impacts of changes in temperature and precipitation patterns on water availability, especially in intensely cultivated environments, are of major concern. The data indicate a trajectory toward increasing temperatures and related drought conditions, consistently with global and national patterns. As delineated in the Annual Global Climate Report issued by the National Centre for Environmental Information [70], the ten warmest years within the past 143 years occurred after 2010. Notably, Italy faced challenges due to elevated temperatures and droughts in recent years, particularly in 2017 and 2022, causing significant issues in water management [71,72]. The report from the SNPA emphasized that 2022 was Italy's warmest and driest year on record, leading to multifaceted consequences, especially in the agricultural sector, where drought-induced damages and reduced crop yields, particularly in corn cultivation, were reported [73]. These repercussions have had strong implications for the national economy. The growing complexity and unpredictability of climate change and its repercussions underscore the need to understand its impacts on various components of the hydrological cycle.

Analysis of the calibrated model's output data confirmed these general changes. The actual evapotranspiration, under the influence of various climatic factors, such as temperature, wind, relative humidity, and irrigation practices, increased. The relationship between the SWAT's calculated actual evapotranspiration and precipitation is a key indicator of water deficits in an area, leading to drought conditions and affecting water availability for plants and other purposes [74,75]. The persistent lack of precipitation over time and

the rising temperatures led to increased evaporation of water from soils and plants [76], resulting in a decrease in the available water resources.

These changes were also reflected in the dynamics of the soil water content. The reduction in soil water content (Figure 14) could be attributed to changes in precipitation patterns, rising temperatures, and modifications in land management practices [77–79]. Notably, we observed a 7% decrease in soil water content over a 15-year period, which is a notable finding due to the potential impact of soil water content on crop productivity and yield [80].

The results of the Mann–Kendall test suggested that there were trends in the data too, such as an increase in the AET and a decrease in SWC, but none of these trends were statistically significant at the 0.05 level. This means that while there were trends in the data, we cannot conclusively say that these were not due to random variations. However, given the limited number of years, these trends can be considered significant in this context. In future research, it will be necessary to extend the analyzed data.

Understanding this long-term trend may have significant implications for water resource management and environmental sustainability in the study area. In this context, considering the differences between the SWAT and soil moisture sensors, the measured and modeled quantities of irrigation water and the timing of irrigation differed significantly, in line with other studies (e.g., [81]). Given the model's accurate calibration and the reliability of the simulated results, it can be assumed that farmers may be applying more irrigation water than predicted by the SWAT's auto-irrigation, opening avenues for optimizing irrigation practices and contributing to sustainable water resource management.

Land-use changes—especially variations in rice cultivation—significantly impact water use and the hydrological balance. While the SWAT model used a static land use, it is important to note that land use changes over time. For example, from 2007 to 2018, the land area used for rice cultivation significantly increased (41%), but from 2015 to 2018, it decreased (−11%). This fluctuation was influenced by choices made by producers, often in response to drought conditions [82]. This fluctuation in rice cultivation has substantial consequences both hydrologically and socioeconomically. A reduction in rice cultivation can modify water-use patterns, as traditional paddy rice fields significantly influence water flow and retention, particularly in the study area. Rice fields often serve as a natural reservoir that aids in flood control and groundwater recharge. A decline in rice cultivation can disrupt this balance [15,42,83]. Conversely, an increase in rice cultivation could intensify water demand, leading to higher irrigation requirements [84,85]. This can strain local water resources. Therefore, maintaining a sustainable equilibrium in rice cultivation practices is, thus, crucial for maintaining the hydrological balance in the study area. Moreover, land-use changes can significantly impact evapotranspiration [38], affecting the water cycle and balances. An analysis of the land-use history shows an expansion of the agricultural areas and a decrease in woodlands, thus influencing the amount of water absorbed and released through plant transpiration.

5. Conclusions

This study provides a comprehensive overview of the hydrological dynamics within the Ticino irrigation cascade in northern Lombardy over the last 15 years. The integration of the SWAT calibrated with MOD16 data is a crucial step in accurately interpreting the effects of climate change, especially in areas characterized by crops such as rice and corn, which require a large quantity of irrigation water, particularly during periods of drought. However, it is important to note that the study area represents a lowland area with complex hydrology and a lack of natural water courses. These features led to limitations in terms of the traditional application of the SWAT using discharge for the calibration and validation of the model. In particular, the lack of irrigation data and the use of the auto-irrigation function in the SWAT may affect the results obtained. On the one hand, the model yields optimal irrigation patterns that might help farmers optimize their own irrigation schemes. However, real irrigation data might further improve the work in

terms of the actual water consumption in irrigation, groundwater recharge, and soil water dynamics. Nevertheless, the calibration and validation results were satisfactory, and the study revealed a significant increase in temperatures in recent years, even though the decrease in rainfall was relatively small. However, there was a substantial increase in the number of rain-free days. These factors collectively led to reduced water availability. The increased actual evapotranspiration and the decreased soil water content are indicative of the growing water stress for crops and the surrounding ecosystem. These findings highlight the need for resilient and sustainable water management strategies that consider the increasing frequency of climate challenges.

Our research explored the peculiarities of a unique area, shedding light on its morphological and hydrological characteristics that, up till now, have been little studied. This region, although complex, poses a challenge because of the limited data available, particularly for hydrological modeling. Therefore, we applied a hydrological model that was adapted to the complex study area and was calibrated and validated with MOD16 evapotranspiration data, and this yielded valuable insights into the impacts of climate change on the water resources of the unique landscape setting of the Ticino irrigation cascade. Emphasizing the importance of adapting water management strategies and suggesting possible future developments will help refine further research, such as through a better understanding of the hydrological dynamics in the study area and the development of innovative solutions for mitigating the impacts of droughts. In particular, the application of advanced water management technologies and the development of more climate-resilient agricultural strategies should be tackled. Furthermore, given the increasing frequency of climate challenges, integrated approaches involving both hydrological management and agricultural practices should be further explored.

Author Contributions: Conceptualization, A.B., M.M. and R.B.; methodology, A.B. and R.B.; software, A.B.; validation, R.B., M.M. and A.B.; formal analysis, A.B.; investigation, A.B. and M.M.; resources, A.B.; data curation, A.B. and R.B.; writing—original draft preparation, A.B. and M.M.; writing—review and editing, R.B., O.D.A., S.H.S. and G.P.; visualization, A.B. and O.D.A.; supervision, M.M. and R.B.; project administration, M.M.; funding acquisition, M.M. All authors have read and agreed to the published version of the manuscript.

Funding: This research was supported by Regione Lombardia, POR FESR 2014–2020—Call HUB Ricerca e Innovazione, Project 1139857 CE4WE: Approvvigionamento energetico e gestione della risorsa idrica nell’ottica dell’Economia Circolare (Circular Economy for Water and Energy).

Institutional Review Board Statement: Not applicable.

Informed Consent Statement: Not applicable.

Data Availability Statement: Data is available on request.

Acknowledgments: We acknowledge the DLR and the TDX Science Team for providing the Tandem-X dataset of the study area.

Conflicts of Interest: The authors declare no conflict of interest.

References

1. Giorgi, F.; Im, E.S.; Coppola, E.; Diffenbaugh, N.S.; Gao, X.J.; Mariotti, L.; Shi, Y. Higher hydroclimatic intensity with global warming. *J. Clim.* **2011**, *24*, 5309–5324. [[CrossRef](#)]
2. Egidio, E.; Mancini, S.; De Luca, D.A.; Lasagna, M. The Impact of Climate Change on Groundwater Temperature of the Piedmont Po Plain (NW Italy). *Water* **2022**, *14*, 2797. [[CrossRef](#)]
3. Forootan, E.; Sadeghi, S.H.R. Relative importance of climatic and anthropogenic factors on runoff change at watershed scale. *Int. J. Environ. Sci. Technol.* **2023**, *20*, 3059–3070. [[CrossRef](#)]
4. Kuwayama, Y.; Thompson, A.; Bernknopf, R.; Zaitchik, B.; Vail, P. Estimating the impact of drought on agriculture using the U.S. Drought Monitor. *Am. J. Agric. Econ.* **2019**, *101*, 193–210. [[CrossRef](#)]
5. Wilhite, D.A.; Svoboda, M.D.; Hayes, M.J. Understanding the complex impacts of drought: A key to enhancing drought mitigation and preparedness. *Water Resour. Manag.* **2007**, *21*, 763–774. [[CrossRef](#)]
6. Ding, Y.; Hayes, M.J.; Widhalm, M. Measuring economic impacts of drought: A review and discussion. *Disaster Prev. Manag.* **2011**, *20*, 434–446. [[CrossRef](#)]

7. ISAC. CNR MEAN TEMPERATURE—Latest Month Analysis. Available online: https://www.isac.cnr.it/climstor/climate/latest_month_TMM.html (accessed on 10 July 2023).
8. Straffelini, E.; Tarolli, P. Climate change-induced aridity is affecting agriculture in Northeast Italy. *Agric. Syst.* **2023**, *208*, 103647. [[CrossRef](#)]
9. Freire-González, J.; Decker, C.; Hall, J.W. The Economic Impacts of Droughts: A Framework for Analysis. *Ecol. Econ.* **2017**, *132*, 196–204. [[CrossRef](#)]
10. Walker, W.R. *Guidelines for Designing and Evaluating Surface Irrigation Systems*; FAO, Ed.; FAO: Rome, Italy, 1989; ISBN 92-5-102879-6.
11. Balestrini, R.; Delconte, C.A.; Sacchi, E.; Buffagni, A. Groundwater-dependent ecosystems as transfer vectors of nitrogen from the aquifer to surface waters in agricultural basins: The fontanili of the Po Plain (Italy). *Sci. Total Environ.* **2021**, *753*, 141995. [[CrossRef](#)]
12. De Caro, M.; Perico, R.; Crosta, G.B.; Frattini, P.; Volpi, G. A regional-scale conceptual and numerical groundwater flow model in fluvio-glacial sediments for the Milan Metropolitan area (Northern Italy). *J. Hydrol. Reg. Stud.* **2020**, *29*, 100683. [[CrossRef](#)]
13. Fumagalli, N.; Senes, G.; Ferrario, P.S.; Toccolini, A. A minimum indicator set for assessing fontanili (lowland springs) of the Lombardy Region in Italy. *Eur. Countrys.* **2017**, *9*, 1–16. [[CrossRef](#)]
14. Lasagna, M.; Mancini, S.; De Luca, D.A. Groundwater hydrodynamic behaviours based on water table levels to identify natural and anthropic controlling factors in the Piedmont Plain (Italy). *Sci. Total Environ.* **2020**, *716*, 137051. [[CrossRef](#)]
15. Baker, E.A.; Cappato, A.; Todeschini, S.; Tamellini, L.; Sangalli, G.; Reali, A.; Manenti, S. Combining the Morris method and multiple error metrics to assess aquifer characteristics and recharge in the lower Ticino Basin, in Italy. *J. Hydrol.* **2022**, *614*, 128536. [[CrossRef](#)]
16. Neitsch, S.; Arnold, J.; Kiniry, J.; Williams, J. *Soil and Water Assessment Tool Theoretical Documentation Version 2009*; Report No. 406; Texas A&M University System: College Station, TX, USA, 2011.
17. Arnold, J.G.; Srinivasan, R.; Muttiah, R.S.; Williams, J. Large area hydrologic modeling and assessment part I: Model development. *J. Am. Water Resour. Assoc.* **1998**, *34*, 73–89. [[CrossRef](#)]
18. Janjić, J.; Tadić, L. Fields of Application of SWAT Hydrological Model—A Review. *Earth* **2023**, *4*, 331–344. [[CrossRef](#)]
19. Norouzi Nazar, M.; Asgari, E.; Baaghdeh, M.; Lotfi, S. Quantifying the long-term flood regulation ecosystem service under climate change using SWAT Model. *Ecopersia* **2020**, *8*, 169–180.
20. Mahzari, S.; Kiani, F.; Azimi, M.; Khormali, F. Using SWAT Model to Determine Runoff, Sediment Yield and Nitrate Loss in Gorganrood Watershed, Iran. *Ecopersia* **2016**, *4*, 1359–1377. [[CrossRef](#)]
21. Sareshtehdari, A.; Ghafouri, M.; Ardakani, A.J.; Bayat, R. Reliability of Land Capability Map in Watershed Hydrological Simulation using SWAT Model. *Ecopersia* **2015**, *2*, 715–725.
22. Arnold, J.C.; Moriasi, D.N.; Gassman, P.W.; Abbaspour, K.C.; White, M.J.; Srinivasan, R.; Santhi, C.; Harmel, R.D.; Van Griensven, A.; Van Liew, M.W.; et al. SWAT: Model use, calibration, and validation. *Trans. ASABE* **2012**, *55*, 1491–1508. [[CrossRef](#)]
23. Francesconi, W.; Srinivasan, R.; Pérez-Miñana, E.; Willcock, S.P.; Quintero, M. Using the Soil and Water Assessment Tool (SWAT) to model ecosystem services: A systematic review. *J. Hydrol.* **2016**, *535*, 625–636. [[CrossRef](#)]
24. Baker, T.J.; Miller, S.N. Using the Soil and Water Assessment Tool (SWAT) to assess land use impact on water resources in an East African watershed. *J. Hydrol.* **2013**, *486*, 100–111. [[CrossRef](#)]
25. Xing, Z.; Ma, M.; Su, Z.; Lv, J.; Yi, P.; Song, W. A review of the adaptability of hydrological models for drought forecasting. *Proc. Int. Assoc. Hydrol. Sci.* **2020**, *383*, 261–266. [[CrossRef](#)]
26. Sun, Y.; Bao, W.; Valk, K.; Brauer, C.C.; Sumihar, J.; Weerts, A.H. Improving Forecast Skill of Lowland Hydrological Models Using Ensemble Kalman Filter and Unscented Kalman Filter. *Water Resour. Res.* **2020**, *56*, e2020WR027468. [[CrossRef](#)]
27. Lam, Q.D.; Schmalz, B.; Fohrer, N. Modelling point and diffuse source pollution of nitrate in a rural lowland catchment using the SWAT model. *Agric. Water Manag.* **2010**, *97*, 317–325. [[CrossRef](#)]
28. Donmez, C.; Sari, O.; Berberoglu, S.; Cilek, A.; Satir, O.; Volk, M. Improving the applicability of the swat model to simulate flow and nitrate dynamics in a flat data-scarce agricultural region in the mediterranean. *Water* **2020**, *12*, 3479. [[CrossRef](#)]
29. Becker, R.; Koppa, A.; Schulz, S.; Usman, M.; aus der Beek, T.; Schüth, C. Spatially distributed model calibration of a highly managed hydrological system using remote sensing-derived ET data. *J. Hydrol.* **2019**, *577*, 123944. [[CrossRef](#)]
30. Odusanya, A.E.; Mehdi, B.; Schürz, C.; Oke, A.O.; Awokola, O.S.; Awomeso, J.A.; Adejuwon, J.O.; Schulz, K. Multi-site calibration and validation of SWAT with satellite-based evapotranspiration in a data-sparse catchment in southwestern Nigeria. *Hydrol. Earth Syst. Sci.* **2019**, *23*, 1113–1144. [[CrossRef](#)]
31. Shah, S.; Duan, Z.; Song, X.; Li, R.; Mao, H.; Liu, J.; Ma, T.; Wang, M. Evaluating the added value of multi-variable calibration of SWAT with remotely sensed evapotranspiration data for improving hydrological modeling. *J. Hydrol.* **2021**, *603*, 127046. [[CrossRef](#)]
32. Parajuli, P.B.; Jayakody, P.; Ouyang, Y. Evaluation of Using Remote Sensing Evapotranspiration Data in SWAT. *Water Resour. Manag.* **2018**, *32*, 985–996. [[CrossRef](#)]
33. López, P.L.; Sutanudjaja, E.H.; Schellekens, J.; Sterk, G.; Bierkens, M.F.P. Calibration of a large-scale hydrological model using satellite-based soil moisture and evapotranspiration products. *Hydrol. Earth Syst. Sci.* **2017**, *21*, 3125–3144. [[CrossRef](#)]
34. Immerzeel, W.W.; Droogers, P. Calibration of a distributed hydrological model based on satellite evapotranspiration. *J. Hydrol.* **2008**, *349*, 411–424. [[CrossRef](#)]

35. ERSAF. Ente Regionale per i Servizi alla Agricoltura e alle Foreste—Regione; Lombardia. Losan Database. Available online: https://losan.ersaf Lombardia.it/oss/oss_index.html (accessed on 12 February 2022).
36. Kottek, M.; Grieser, J.; Beck, C.; Rudolf, B.; Rubel, F. World map of the Köppen-Geiger climate classification updated. *Meteorol. Z.* **2006**, *15*, 259–263. [[CrossRef](#)] [[PubMed](#)]
37. Comune di Abbiategrasso Piano di Governo del Territorio 2009, 0–33. Available online: <https://www.multiplan.servizirl.it/pgtwebn/#/public/dettaglio-piano/120662/documenti> (accessed on 29 May 2023).
38. IUSS Working Group WRB. *World Reference Base for Soil Resources 2014, Update 2015—International Soil Classification System for Naming Soils and Creating Legends for Soil Maps*; World Soil Resources Reports No. 106; FAO: Rome, Italy, 2015.
39. De Luca, D.A.; Destefanis, E.; Forno, M.G.; Lasagna, M.; Masciocco, L. The genesis and the hydrogeological features of the Turin Po Plain fontanili, typical lowland springs in Northern Italy. *Bull. Eng. Geol. Environ.* **2013**, *73*, 409–427. [[CrossRef](#)]
40. ERSAF. Ente Regionale per i Servizi alla Agricoltura e alle Foreste—Regione Lombardia Uso del suolo in Regione Lombardia. Atlante Descrittivo. 2019, p. 51. Available online: <https://www.ersaf.lombardia.it/pubblicazioni/uso-del-suolo-in-regione-lombardia-atlante-descrittivo/> (accessed on 29 May 2023).
41. Perego, A.; Sanna, M.; Giussani, A.; Chiodini, M.E.; Fumagalli, M.; Pilu, S.R.; Bindi, M.; Moriondo, M.; Acutis, M. Designing a high-yielding maize ideotype for a changing climate in Lombardy plain (northern Italy). *Sci. Total Environ.* **2014**, *499*, 497–509. [[CrossRef](#)]
42. Bove, M. *Il Riscoltore*; Ente Nazionale Risi: Milan, Italy, 2021; pp. 2–3.
43. Azar, R.; Villa, P.; Stroppiana, D.; Crema, A.; Boschetti, M.; Brivio, P.A. Assessing in-season crop classification performance using satellite data: A test case in Northern Italy. *Eur. J. Remote Sens.* **2016**, *49*, 361–380. [[CrossRef](#)]
44. Bux, C.; Lombardi, M.; Varese, E.; Amicarelli, V. Economic and Environmental Assessment of Conventional versus Organic Durum Wheat Production in Southern Italy. *Sustainability* **2022**, *14*, 9143. [[CrossRef](#)]
45. Douglas-Mankin, K.R.; Srinivasan, R.; Arnold, J.G. Soil and water assessment tool (SWAT) model: Current developments and applications. *Trans. ASABE* **2010**, *53*, 1423–1431. [[CrossRef](#)]
46. Deutsches Zentrum für Luft- und Raumfahrt (German Aerospace Center). Available online: https://www.dlr.de/EN/Home/home_node.html (accessed on 1 October 2020).
47. Regione Lombardia, 2013. Basi informative dei suoli. Geoportale della Lombardia. Available online: https://www.geoportale.regione.lombardia.it/metadati?p_p_id=detailSheetMetadata_WAR_gptmetadataportlet&p_p_lifecycle=0&p_p_state=normal&p_p_mode=view&_detailSheetMetadata_WAR_gptmetadataportlet_uuid=%257BA7138B8A-9025-4802-82BC-52267B60A3D7%257D# (accessed on 1 November 2020).
48. FORM RICHIESTA DATI. Available online: <https://www.arpalombardia.it/temi-ambientali/meteo-e-clima/form-richiesta-dati/> (accessed on 1 October 2020).
49. Uniyal, B.; Dietrich, J. Modifying Automatic Irrigation in SWAT for Plant Water Stress scheduling. *Agric. Water Manag.* **2019**, *223*, 105714. [[CrossRef](#)]
50. Arnold, J.G.; Kiniry, J.R.; Srinivasan, R.; Williams, J.R.; Haney, E.B.; Neitsch, S.L. *Input/Output Documentation Soil & Water Assessment Tool*; Texas Water Resources Institute: Thrall, TX, USA, 2012; pp. 1–650.
51. Abbaspour, K.C.; Rouholahnejad, E.; Vaghefi, S.; Srinivasan, R.; Yang, H.; Klöve, B. A continental-scale hydrology and water quality model for Europe: Calibration and uncertainty of a high-resolution large-scale SWAT model. *J. Hydrol.* **2015**, *524*, 733–752. [[CrossRef](#)]
52. Abbaspour, K.C.; Yang, J.; Maximov, I.; Siber, R.; Bogner, K.; Mieleitner, J.; Zobrist, J.; Srinivasan, R. Modelling hydrology and water quality in the pre-alpine/alpine Thur watershed using SWAT. *J. Hydrol.* **2007**, *333*, 413–430. [[CrossRef](#)]
53. Abbaspour, K.C.; Vajdani, M.; Haghghat, S. SWAT-CUP calibration and uncertainty programs for SWAT. In Proceedings of the MODSIM 2007 International Congress on Modelling and Simulation, Modelling and Simulation Society of Australia and New Zealand, Christchurch, New Zealand, 10–13 December 2007; pp. 1596–1602.
54. Abbaspour, K.C.; Vaghefi, S.A.; Yang, H.; Srinivasan, R. Global soil, landuse, evapotranspiration, historical and future weather databases for SWAT Applications. *Sci. Data* **2019**, *6*, 263. [[CrossRef](#)] [[PubMed](#)]
55. Kling, H.; Fuchs, M.; Paulin, M. Runoff conditions in the upper Danube basin under an ensemble of climate change scenarios. *J. Hydrol.* **2012**, *424–425*, 264–277. [[CrossRef](#)]
56. Henry, M. Nonparametric Tests Against Trend. *Econometrica* **1945**, *13*, 245–259.
57. Kendall, A.M.G. Further Contributions to the Theory of Paired Comparisons. *Biometrics* **1955**, *11*, 43–62. [[CrossRef](#)]
58. Aboelnour, M.; Gitau, M.W.; Engel, B.A. A comparison of streamflow and baseflow responses to land-use change and the variation in climate parameters using SWAT. *Water* **2020**, *12*, 191. [[CrossRef](#)]
59. Atta-ur-Rahman; Dawood, M. Spatio-statistical analysis of temperature fluctuation using Mann–Kendall and Sen’s slope approach. *Clim. Dyn.* **2017**, *48*, 783–797. [[CrossRef](#)]
60. Ahmad, I.; Tang, D.; Wang, T.; Wang, M.; Wagan, B. Precipitation trends over time using Mann-Kendall and spearman’s Rho tests in swat river basin, Pakistan. *Adv. Meteorol.* **2015**, *2015*, 431860. [[CrossRef](#)]
61. McLeod, A.I. Kendall Rank Correlation and Mann-Kendall Trend Test. R Package “Kendall”. Available online: <https://cran.r-project.org/web/packages/Kendall/> (accessed on 27 November 2023).

62. SNPA Cambiamento Climatico: In Lombardia, Oltre un Secolo di Dati Dall'osservatorio Milano Brera. Available online: <https://www.snepambiente.it/2019/03/13/cambiamento-climatico-in-lombardia-oltre-un-secolo-di-dati-a-milano-brera/> (accessed on 10 October 2023).
63. Abdullah, N.H.H.; Kuan, N.W.; Ibrahim, A.; Ismail, B.N.; Majid, M.R.A.; Ramli, R.; Mansor, N.S. Determination of soil water content using time domain reflectometer (TDR) for clayey soil. *AIP Conf. Proc.* **2018**, *2020*, 020016. [[CrossRef](#)]
64. Masseroni, D.; Ricart, S.; de Cartagena, F.R.; Monserrat, J.; Gonçalves, J.M.; de Lima, I.; Facchi, A.; Sali, G.; Gandolfi, C. Prospects for improving gravity-fed surface irrigation systems in mediterranean european contexts. *Water* **2017**, *9*, 20. [[CrossRef](#)]
65. Abiodun, O.O.; Guan, H.; Post, V.E.A.; Batelaan, O. Comparison of MODIS and SWAT evapotranspiration over a complex terrain at different spatial scales. *Hydrol. Earth Syst. Sci.* **2018**, *22*, 2775–2794. [[CrossRef](#)]
66. Qiao, L.; Will, R.; Wagner, K.; Zhang, T.; Zou, C. Improvement of evapotranspiration estimates for grasslands in the southern Great Plains: Comparing a biophysical model (SWAT) and remote sensing (MODIS). *J. Hydrol. Reg. Stud.* **2022**, *44*, 101275. [[CrossRef](#)]
67. Parajuli, P.B.; Risal, A.; Ouyang, Y.; Thompson, A. Comparison of SWAT and MODIS Evapotranspiration Data for Multiple Timescales. *Hydrology* **2022**, *9*, 103. [[CrossRef](#)]
68. Lindsey, R.; Dahlman, L. Climate Change: Global Temperature. Available online: <https://www.climate.gov/news-features/understanding-climate/climate-change-global-temperature> (accessed on 30 September 2023).
69. National Center for Environmental Information Annual 2022 Global Climate Report. Available online: <https://www.ncei.noaa.gov/access/monitoring/monthly-report/global/202213> (accessed on 10 October 2023).
70. SNPA. SNPA Presenta il Rapporto “GLI INDICATORI DEL CLIMA IN ITALIA NEL 2017”. 2018. Available online: <https://www.isprambiente.gov.it/it/evidenza/pubblicazioni/no-homepage/gli-indicatori-del-clima-in-italia-nel-2017> (accessed on 14 October 2023).
71. SNPA. *Il Clima in Italia Nel 2022*; Report SNPA n. 36/2023; SNPA: Rome, Italy, 2023; pp. 1–177.
72. Coldiretti. Siccità: 250mila Aziende a Rischio Crack. Available online: <https://www.coldiretti.it/economia/siccita-250mila-aziende-a-rischio-crack> (accessed on 14 October 2023).
73. Milly, P.C.D. Climate, soil water storage, and the average annual water balance. *Water Resour. Res.* **1994**, *30*, 2143–2156. [[CrossRef](#)]
74. Glenn, E.P.; Scott, R.L.; Nguyen, U.; Nagler, P.L. Wide-area ratios of evapotranspiration to precipitation in monsoon-dependent semiarid vegetation communities. *J. Arid Environ.* **2015**, *117*, 84–95. [[CrossRef](#)]
75. Faranda, D.; Pascale, S.; Bulut, B. Persistent anticyclonic conditions and climate change exacerbated the exceptional 2022 European-Mediterranean drought. *Environ. Res. Lett.* **2023**, *18*, 034030. [[CrossRef](#)]
76. Gao, X.; Wu, P.; Zhao, X.; Wang, J.; Shi, Y. Effects of land use on soil moisture variations in a semi-arid catchment: Implications for land and agricultural water management. *Land Degrad. Dev.* **2014**, *25*, 163–172. [[CrossRef](#)]
77. Mimeau, L.; Trambly, Y.; Brocca, L.; Massari, C.; Camici, S.; Finaud-Guyot, P. Modeling the response of soil moisture to climate variability in the Mediterranean region. *Hydrol. Earth Syst. Sci.* **2021**, *25*, 653–669. [[CrossRef](#)]
78. Zhou, T.; Han, C.; Qiao, L.; Ren, C.; Wen, T.; Zhao, C. Seasonal dynamics of soil water content in the typical vegetation and its response to precipitation in a semi-arid area of Chinese Loess Plateau. *J. Arid Land* **2021**, *13*, 1015–1025. [[CrossRef](#)]
79. Datta, S.; Taghvaeian, S.; Stivers, J. Understanding Soil Water Content and Thresholds for Irrigation Management Managing Irrigations Based on Soil Water Content Managing irrigations based on VWC data Managing Irrigations based on SMP data. *Okla. Coop. Ext. Serv.* **2017**, BAE-1537-1–BAE-1537-7. Available online: <https://extension.okstate.edu/fact-sheets/understanding-soil-water-content-and-thresholds-for-irrigation-management.html> (accessed on 1 October 2020).
80. Qi, J.; Zhang, X.; McCarty, G.W.; Sadeghi, A.M.; Cosh, M.H.; Zeng, X.; Gao, F.; Daughtry, C.S.T.; Huang, C.; Lang, M.W.; et al. Assessing the performance of a physically-based soil moisture module integrated within the Soil and Water Assessment Tool. *Environ. Model. Softw.* **2018**, *109*, 329–341. [[CrossRef](#)]
81. Ente Risi Riso Italiano. Available online: <https://www.risoitaliano.eu/ci-siamo-giocati-la-lombardia/> (accessed on 9 October 2023).
82. Giuliana, V.; Lucia, M.; Marco, R.; Simone, V. Environmental life cycle assessment of rice production in northern Italy: A case study from Vercelli. *Int. J. Life Cycle Assess.* **2022**, 1–18. [[CrossRef](#)]
83. Wu, D.; Cui, Y.; Xie, X.; Luo, Y. Improvement and testing of SWAT for multi-source irrigation systems with paddy rice. *J. Hydrol.* **2019**, *568*, 1031–1041. [[CrossRef](#)]
84. Tsuchiya, R.; Kato, T.; Jeong, J.; Arnold, J.G. Development of SWAT-paddy for simulating lowland paddy fields. *Sustainability* **2018**, *10*, 3246. [[CrossRef](#)]
85. Crespi, A.; Brunetti, M.; Ranzi, R.; Tomirotti, M.; Maugeri, M. A multi-century meteo-hydrological analysis for the Adda river basin (Central Alps). Part I: Gridded monthly precipitation (1800–2016) records. *Int. J. Climatol.* **2021**, *41*, 162–180. [[CrossRef](#)]

Disclaimer/Publisher’s Note: The statements, opinions and data contained in all publications are solely those of the individual author(s) and contributor(s) and not of MDPI and/or the editor(s). MDPI and/or the editor(s) disclaim responsibility for any injury to people or property resulting from any ideas, methods, instructions or products referred to in the content.

Acknowledgements

I want to express my gratitude to my family, particularly my mom and dad, for their support throughout my career, starting from the early days of kindergarten.

A heartfelt thank you goes out to all my colleagues at the University of Pavia, who have not only been academic colleagues but have also become friends and a second family. From the initial year of university to the end of my three-year PhD journey. Thanks to Camilla, Silvia, Fabiana, Ludovico, and everyone else (though I can't mention you all, you know who you are).

I am grateful to my long-time (old) friends and, in particular, lifelong friends Claudia, Marta, and Camilla, that have been there from the beginning.

I extend my thanks to my new colleagues from Est Sesia, who welcomed me warmly and made me feel at home immediately.

Finally, thanks to Prof. Michael Maerker and to our entire team: Alberto, Manuele, Odunayo, and Manuel.

To all those who have been a part of my life and have made these three years truly unforgettable, despite the challenges, we've shared something special, I love you all.